UNIVERSITAT POLITÈCNICA DE VALÈNCIA

DISEÑO, REALIZACIÓN Y EVALUACIÓN DE IMPLANTES INTRACORNEALES DIFRACTIVOS MULTIFOCALES

Memoria presentada por:
Diego Montagud Martínez

Directores:
Walter Daniel Furlan
Juan Antonio Monsoriu Serra

Julio, 2020

Dr. Walter Daniel Furlan, Catedrático de la Universitat de València del Departamento de Óptica y Optometría y Ciencias de la Visión y Dr. Juan Antonio Monsoriu Serra, Catedrático de la Universitat Politècnica de València del Departamento de Física Aplicada

CERTICAN que la presente memoria “Diseño, realización y evaluación de implantes intracorneales difractivos multifocales” resume el trabajo de investigación realizado, bajo su supervisión, por D. Diego Montagud Martínez y constituye su Tesis para optar al título de Doctor.

Y para que conste, en cumplimiento de la legislación vigente, firman el presente certificado en Valencia a 9 de Julio de 2020

Fdo.: Dr. Walter D. Furlan Fdo.: Dr. Juan A. Monsoriu Serra

Dedicado a:
mi madre y mi padre,
mis dos herman@s,
a Emma y Alexandra,
a mis cuñad@s,
a los que están por venir
y los que ya no están.

Agradecimientos y dedicatoria

Cuando alguien presenta una Tesis Doctoral, ésta lleva su nombre, sin embargo, es algo que me parece tremendamente injusto. Si algo he aprendido en estos 3-4 años de doctorado es que la investigación es como el fútbol, TRABAJO EN EQUIPO. Una vez te toca marcar los goles o llevarte la gloria (como lo del nombre de la Tesis), pero el goleador no es más que el que ha dado el pase o el que ha recuperado el balón. Detrás de ese gol o de esta Tesis hay un grupo de trabajo que, sin ellos, esta Tesis no sería ni de lejos lo que es. Por ello me gustaría dar las gracias a todos ellos.

En primer lugar, a mis dos directores de Tesis Walter y Juan, por dedicar su esfuerzo y sobre todo su tiempo en enseñarme todo lo que he aprendido durante estos años, además han sido comprensivos y pacientes.

En segundo lugar, y no por ello menos importante a Sento. Posiblemente a ti sea a quien más tenga que estarte agradecido, pues me has ayudado y explicado todos los diseños, entre otras cosas. Eres una gran persona y un buen amigo y creo que hacemos muy buen equipo, tu sabes de diseño de lentes y óptica-física y yo sé de ojos.

En tercer lugar, a Manu puesto que me explicó una cosa importante de ZEMAX que hizo que mi doctorado pasara por un punto de inflexión (“Grid Sag Surface”).

Os estaré eternamente agradecido por vuestro tiempo dedicado.

Ahora me gustaría dedicarles esta Tesis a unas cuantas personas. Es el trabajo de muchos años y la mejor recompensa además de obtener optar al título de Doctor es poder dedicárosla.

A mi madre Gloria y a mi padre Lisardo, por darme todo y ayudarme en todo, sé que a ti Mama te hará especial ilusión.

A mis dos hermanos, Lisardo y Gloria porque son de las personas que más quiero en el mundo.

A mis dos cuñados, Lucía y Carlos, también os quiero mucho.

A mis dos sobrinas Emma y Alexandra, sin lugar a dudas el motor de mi vida y lo que más quiero. También a los que están por llegar y a los que ya no están.

A mi tío Manolo, que quiere que sea catedrático sin ser doctor. Este es un paso adelante.

A todos mis amigos en especial a Quique, Cris, Carlos, Isadora, Esteban, Héctor, Miguel, Jano, Fer, Oscar y Pedro. También a Elia, Pepo y Celia.

A mis dos soles Nicolás y Arián, y también a Noemí.

A Héctor, Helena y Marc, unos nenes preciosos.

A mi primo Pablo, siempre te querré.

Y por supuesto a todos los que se lean esta Tesis, espero que os guste.

AMUNT!!!

Resumen

La presbicia es el error refractivo con mayor incidencia en la población debido al envejecimiento de la misma. Existen múltiples medidas para corregirla, desde lentes oftálmicas, lentes de contacto, lentes intraoculares etc… Actualmente, los implantes intracorneales (corneal inlays) se encuentran entre las soluciones más novedosas. Estos dispositivos se sitúan en el estroma corneal mediante una cirugía mínimamente invasiva. Existen tres implantes intracorneales comerciales cuyos mecanismos difieren entre sí. El más estudiado es el KAMRA inlay® y utiliza el efecto estenopeico para aumentar la profundad de foco. Por otra parte, Flexivue Microlens® se basa en una estructura multifocal donde el centro focaliza en lejos mientras que la periferia focaliza en cerca. Por último, Raindrop Near Vision® modifica la estructura de la córnea para aumentar el radio de curvatura de la parte central de ésta y permitir enfocar a distancias próximas. Todos ellos deben permitir el paso de nutrientes y oxígeno a través de la córnea, ya sea mediante aperturas o siendo permeables.

Existe un cuarto tipo de implante intracorneal no comercial desarrollado por el Diffractive Optics Group (DiOG), el cual distribuye los micro-agujeros, que permiten el paso de nutrientes y oxígeno, en las zonas transparentes de una placa zonal de Fresnel. Además, contiene un agujero central, que actúa como estenopeico. Este dispositivo tiene como nombre Diffractive Corneal Inlay (DCI).

Esta Tesis pretende modificar y optimizar los parámetros de diseño del DCI y comparar sus propiedades ópticas con otros implantes intracorneales comerciales.

Resum

La presbícia es l'error refractiu amb major incidència en la població degut a l'envelliment d'aquesta. Hi existeixen múltiples solucions per corregir-la, des de lents oftàlmiques, lents de contacte, lents intraoculars, etc... Actualment, els implants intracorneales comercials es troben entre les solucions mes noves. Aquests dispositius es situen a l'estroma corneal mitjançant uns cirurgia mínimament invasiva. Hi existeixen tres tipus d'implants intracorneals amb diferents mecanismes. El mes estudiat es el KAMRA inlay® i utilitza l'efecte estenopeic per augmentar la profunditat de focus. Per altra banda, Flexivue Microlens® es basa en una estructura multifocal on el centre de la lent focalitza en el focus llunyà mentre que la perifèria focalitza prop. Per últim Raindrop Near Vision® modifica l'estructura de la còrnia per augmentar el radi de curvatura de la part central d'aquesta i permetre enfocar a distàncies pròximes. Tots ells deuen permetre el pas de nutrients i oxigen a través de la còrnia, ja siga mitjançant obertures o sent permeables.

Existeix un quart tipus d'implant intracorneal no comercial desenvolupat pel Diffractive Optics Group (DiOG), el qual distribueix els micro-forats, que permeten el flux de nutrients i oxigen, en les zones transparents d'una placa zonal de Fresnel. A més, contenen un forat central, que actua com estenopeic. Aquest dispositiu rep el nom Diffractive Corneal Inlay (DCI).

Aquesta tesi pretén modificar i optimitzar els paràmetres de disseny del DCI i comparar les seues propietats òptiques amb altres implantes intracorneals comercials.

Abstract

Presbyopia is the refractive error with the highest incidence in the population due to the aging of the population. There are many solutions to correct it, from ophthalmic lenses, contact lenses, intraocular lenses, etc... Currently the corneal inlays are among the newest solutions. These devices are placed in the corneal stroma by means of minimally invasive surgery. There are three commercial corneal inlays whose mechanisms differ from each other. The most studied is KAMRA inlay® which uses the pinhole effect to increase the depth of focus. On the other hand, Flexivue Microlens® is based on a multi-focal structure where the center focuses at distance vision while the periphery focuses at near vision. Finally, Raindrop Near Vision® modifies the structure of the cornea to increase the radius of curvature of the central part of it and allow focusing at near vision. All of them must all allow pass through to the cornea nutrients and oxygen, either by holes or being permeable.

There is a fourth type of non-commercial corneal inlay developed by the Diffractive Optics Group (DiOG), which distributes micro-holes, allow the passage of nutrients and oxygen, in the transparent zones of a Fresnel zone plate. In addition, it contains a central hole, which acts as a pinhole. This device is called Diffractive Corneal Inlay (DCI).

This Thesis aims to modify and optimize the design parameters of the DCI and to compare its optical properties with other commercial corneal inlays.

Índice General

Capítulo 1
Introducción

En este apartado se revisa en primer lugar el estado del arte y los conceptos básicos en los cuales se fundamenta esta Tesis. En segundo lugar, se definen los objetivos a conseguir y por último se muestra la estructura general de la Tesis presentada en formato de compendio de publicaciones.

1.1. Antecedentes y objetivos de la investigación

Presbicia

La presbicia es uno de los errores refractivos más comunes debido al envejecimiento progresivo de la población y al aumento de la esperanza de vida. Se estima que alrededor de 2.000 millones de personas sufren "vista cansada" [Fricke18]. Consiste en la pérdida progresiva de la capacidad de acomodación del cristalino. Este problema visual normalmente aparece a partir de los 45 años de edad. La acomodación es la capacidad del cristalino de incrementar la curvatura de sus superficies y su espesor gracias a la contracción del músculo ciliar. De esta forma, aumenta su potencia como lente biconvexa, lo que nos permite enfocar objetos situados a distancias próximas. Con el envejecimiento ocular, esta capacidad para alterar su morfología se pierde debido en parte a una esclerosis de la estructura cristaliniana y también por una pérdida de función del músculo ciliar. Este proceso, presbicia, se acaba completando alrededor de los 65 años impidiendo a las personas enfocar a cualquier distancia.

Existen múltiples soluciones para el tratamiento de la presbicia:

Lentes oftálmicas: Históricamente fue la primera solución para la presbicia. En un principio se utilizaban lentes monofocales para ver de cerca, lupas. Posteriormente se usaron lentes bifocales. Estas lentes consistían en lentes monofocales para ver de lejos a las cuales se les añadía una pastilla en la parte inferior para aumentar su potencia y poder ver objetos cercanos. Actualmente las lentes oftálmicas han evolucionado hasta obtener un cambio gradual de la potencia de lejos a la de cerca. Dichas lentes se les denomina lentes progresivas, debido a la progresión de la potencia de la lente desde su parte superior (visión lejana) hasta su parte inferior (visión próxima). La principal desventaja de las lentes progresivas es que para que el paciente pueda mirar nítidamente, debe observar siempre por la parte central (pasillo) de la lente, puesto que en los extremos temporales y nasales la lente presenta un gran contenido de aberraciones. Además, requieren de un periodo de adaptación entre 1-6 meses.

Lentes de contacto multifocales: Las lentes de contacto multifocales permiten al portador ver a múltiples distancias gracias al diseño de la propia lente de contacto. Presentan una estructura radial alternando la potencia de lejos y de cerca [Garcia-Delpech18]. Fundamentalmente existen dos tipos de lentes, las

"centro lejos", cuyo centro es para visión de lejos y las "centro cerca", cuyo centro es para visión de cerca. El gran inconveniente de estas lentes de contacto es que tanto las imágenes de lejos como las de cerca aparecen en la retina (una enfocada y otra desenfocada) reduciendo el contraste y la calidad visual. Otra de las desventajas es que son pupilodependientes debido a su diseño radial. También requieren de una neuroadaptación para permitir al cerebro desechar las imágenes desenfocadas.

Monovisión con lentes de contacto: Consiste en corregir el ojo dominante con una lente de contacto monofocal para visión lejana, mientras que el ojo no dominante se corrige para visión de cerca. También se pueden emplear lentes de contacto multifocales de baja adición para cubrir la visión intermedia con ambos ojos. La mayor desventaja que presentan la pérdida de la visión de profundidad o estereopsis.

Cirugía refractiva: Existen múltiples soluciones quirúrgicas para tratar la presbicia. A continuación, se enumeran cada una de ellas en función del mecanismo de acción y por último se desarrolla la solución adoptada en la presente Tesis:

1. **Monovisión quirúrgica:** Se trata quirúrgicamente la córnea del ojo no dominante para miopizarla, por tanto, el ojo dominante actúa en visión lejana mientras que el no dominante focaliza los objetos situados a una distancia cercana. Entre las grandes desventajas de esta técnica encontramos que se reduce la estereopsis, es una técnica irreversible y se pierden las distancias intermedias.
2. **Lentes intraoculares:** Las lentes intraoculares (IOLs del inglés Intraocular Lenses) se utilizan en cirugía de catarata para extraer el cristalino opacificado y sustituirlo por una lente que puede ser monofocal, bifocal o trifocal [Wang18]. Es una técnica ampliamente utilizada y permite al sujeto ver con ambos ojos tanto en lejos como en cerca y en visión intermedia si se utilizan lentes trifocales. Entre sus desventajas presenta que se pierde la acomodación residual que pudiera tener el paciente y que es una técnica irreversible. Además, se han de operar ambos ojos y en función de la IOL que se emplee en la cirugía se pueden perder las distancias intermedias. Actualmente las IOLs de foco extendido denominadas EDOF [Wang18] son las que se encuentran en mayor auge.
3. **Implantes intracorneales:** Debido a que la Tesis trata sobre el diseño de nuevos implantes intracorneales (CIs del inglés Corneal Inlays), se va a dedicar un apartado a continuación.

Implantes intracorneales

Estos dispositivos ópticos son la técnica más novedosa para la corrección de la presbicia. Consisten en unos implantes que se introducen en el estroma corneal permitiendo corregir la presbicia. Al añadirse tejido en lugar de extraerse, como

es el caso de la cirugía de IOLs o monovisión quirúrgica, se considera una técnica mínimamente invasiva y reversible [Lindstrom13]. Todos los implantes comerciales se introducen en el ojo no dominante, dejando el dominante para visión de lejos [Charman14]. Además, deben de permitir el paso de nutrientes y oxígeno a través del estroma corneal. Existen fundamentalmente tres tipos de mecanismos de acción en los que se basan los implantes corneales comerciales:

Extensión de profundidad de foco: El mecanismo de acción consiste en aumentar la profundidad de foco utilizando un estenopeico y permitiendo ver a distancias intermedias. El ejemplo más conocido de CI que utiliza este mecanismo es el KAMRA inlay® (Acufocus, Inc., Irvine, CA, USA) (Fig. 1A), el cual es el más implantado y estudiado [Lindstrom13, Vilupuru15, Wang18]. Consiste en un estenopeico de material fluoruro de polivinilideno de 1.6 mm de diámetro interno y 3.8 mm de diámetro externo. Al aumentar la profundidad de foco, permite ver en distancia lejana y en intermedia pero no en visión cercana.

Implantes refractivos: Están divididos en dos zonas refractivas, una para visión de lejos y otra para visión de cerca. Flexivue Microlens® (Presbia Cooperatief, UA, Irvine, CA, USA) se basa en este principio de funcionamiento (Fig. 1B). Está fabricado a partir de un copolimero de hidroxietil metacrilato y metil metacrilato. Presenta un diseño bifocal con una zona central para visión de lejos de potencia nula y una zona periférica de potencia positiva para la visión de cerca. Además, en la zona central contiene un agujero para permitir el paso de nutrientes y oxígeno [Vukich18, Wang18, Waring11].

Cambio de la curvatura corneal: Este implante se sitúa en el estroma de la córnea y modifica la estructura de la cara anterior de la misma incrementando el radio de curvatura de la parte central y aumentando la potencia de la superficie corneal en el centro. Raindrop Near Vision Inlay® (ReVision Optics, Lake Forest, CA, USA) es un CI comercial que utiliza este mecanismo de acción y consiste en una lente de hidrogel de silicona, material permeable a los nutrientes y oxígeno, mejorando la visión de cerca (Fig. 1C). La dificultad de este implante radica en que la curvatura corneal modificada por el mismo no es igual para todos los pacientes y por tanto la variación intrasujeto es alta [Arlt15, Moarefi17, Wang18].

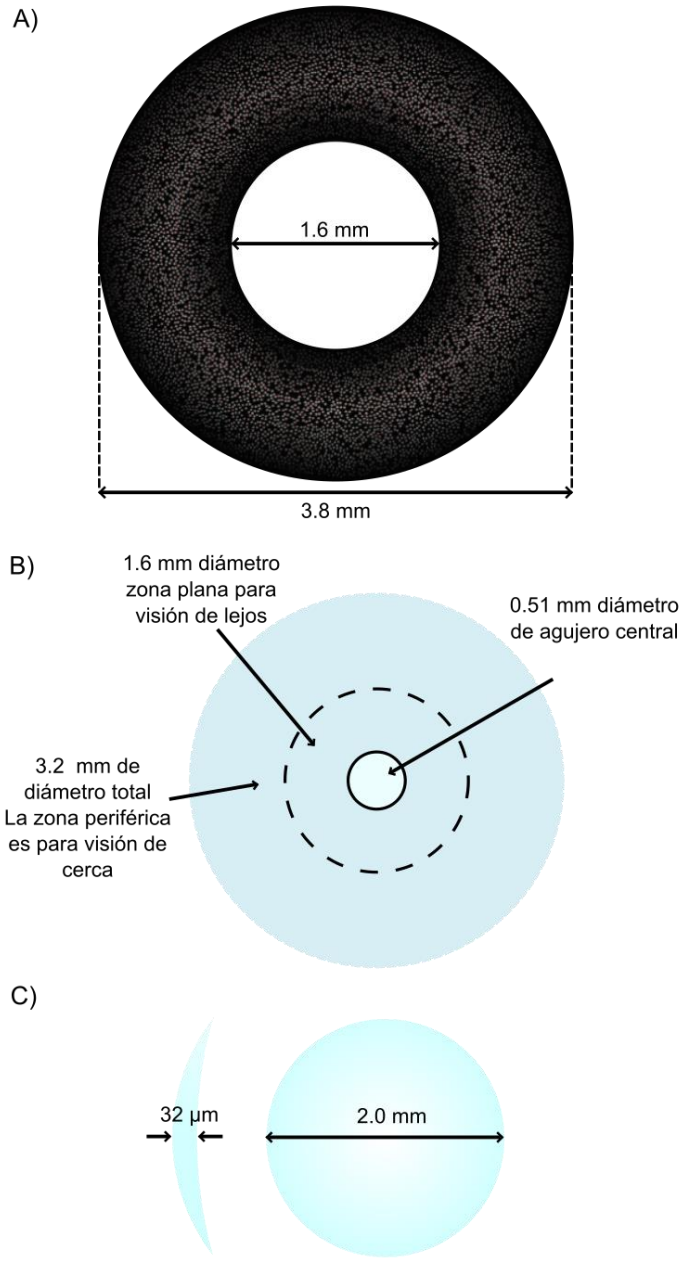

Figura 1: Estructuras y medidas de los tres CIs comerciales más utilizados: A) Kamra Inlay, B) Flexivue Microlens y C) Raindrop Near Vision. Las figuras mantienen la misma escala proporcional entre sí.

Diffractive Corneal Inlay

Además de los tres implantes comerciales mencionados en el apartado anterior, existe un cuarto mecanismo de acción, el cual ha sido descrito y publicado por los miembros del Diffractive Optics Group (DiOG) [Furlan17]. La presente Tesis se basa en dicho mecanismo y por ello se describe a continuación su principio de funcionamiento.

Este nuevo CI llamado Diffractive Corneal Inlay (DCI) se apoya en el fenómeno de la difracción, por el cual se produce una desviación de los rayos luminosos cuando pasan por una abertura de diámetro del orden de la longitud de onda, para generar uno o más focos y dotar al CI de multifocalidad.

El DCI consta de un disco con una pequeña apertura central y una serie de micro-agujeros no solapados distribuidos en lo que serían las zonas transparentes de una placa zonal de Fresnel (Fig. 2ª). Su mecanismo de acción consiste en explotar la difracción intrínseca producida por los micro-agujeros permeables a los nutrientes para crear una lente difractiva.

Un concepto similar, llamado “photon sieve”, fue propuesto anteriormente por Kipp y colaboradores [Kipp01] para enfocar los rayos X. Un “photon sieve” es una variación de la placa de la zona de Fresnel, que, en lugar de alternar anillos transparentes y opacos de igual área, está formado por un disco opaco con agujeros estenopeicos no superpuestos distribuidos en las correspondientes zonas transparentes de Fresnel. Se han realizado estudios indicando que los “photon sieve” pueden lograr un enfoque más nítido suprimiendo los efectos de difracción de orden superior en comparación con la placa zonal de Fresnel correspondiente [Andersen10, Giménez06, Kipp01, Menon05].

En concordancia con lo expuesto anteriormente, el DCI es un único dispositivo microestructurado (con cualquier sustrato) que combina los conceptos de agujero estenopeico y “photon sieve”. Por lo tanto, los efectos de los altos órdenes de difracción en las imágenes lejanas y cercanas se minimizan, debido a las interferencias destructivas producidas por la distribución espacial de los micro-agujeros [Andersen10, Giménez06, Kipp01, Menon05]. Además, la distribución espacial y el diámetro de los micro-agujeros en cada zona también puede ser modificados para obtener una intensidad relativa optimizada entre los focos de visión cercana y lejana, y/o para corregir las aberraciones oculares de alto orden. Adicionalmente, los micro-agujeros permiten el paso de nutrientes y oxígeno por el estroma corneal. Este hecho es esencial para la biocompatibilidad de los CIs en el ojo.

En la Figura 2 se observa la estructura de la placa zonal de Fresnel y su DCI equivalente. Por un lado, el agujero central del disco permite generar el orden cero de difracción, el cual produce una extensión del foco de visión lejana,

mientras que la luz difractada a través de los micro-agujeros genera el foco de cerca.

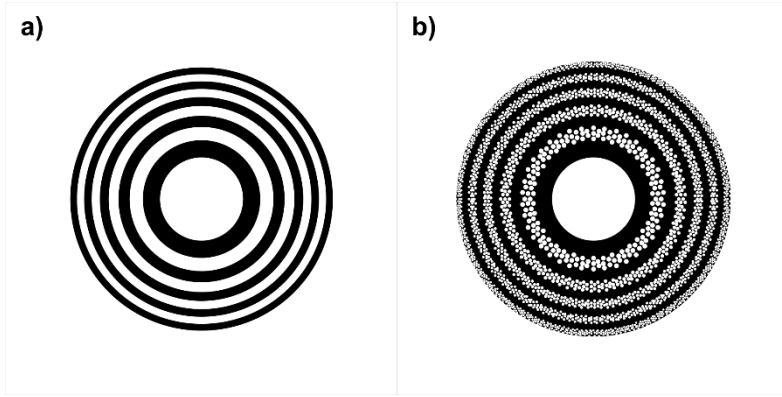

Figura 2: a) Placa zonal de Fresnel y b) DCI equivalente. Las zonas blancas permiten el paso de luz mientras que las zonas negras son opacas.

En la Figura 3, se muestran los resultados experimentales del diseño original de la DCI.

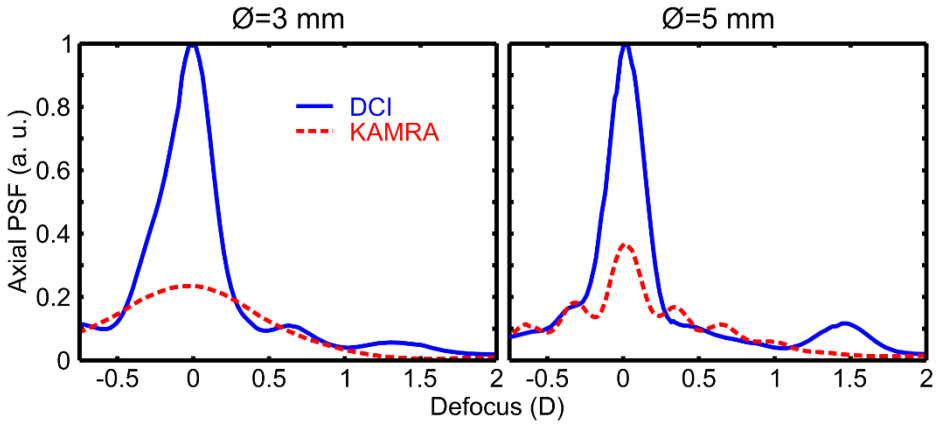

Figura 3: Resultados experimentales del diseño de partida de la DCI (azul) comparados con el KAMRA Inlay (rojo punteado) en banco óptico para apertura de 3.0 mm (izquierda) y 5.0 mm (derecha).

Esta Tesis pretende optimizar y modificar los diferentes parámetros del DCI original para mejorar las características del dispositivo difractivo y obtener nuevas propiedades ópticas y compararlas con otros CIs comerciales mediante simulación numérica en diferentes modelos de ojos teóricos.

Con estas premisas, los objetivos concretos de la Tesis son los siguientes:

1. Selección, comparación y evaluación de un dispositivo óptico en diferentes modelos de ojo teórico.
2. Optimizar los parámetros del DCI original de amplitud y medir las propiedades ópticas del implante dentro de modelos de ojo teórico.
3. Comparar las propiedades ópticas y características clínicas entre el diseño optimizado del DCI y un CI comercial.
4. Modificar los parámetros de diseño del DCI para mejorar las propiedades ópticas en visión cercana.
5. Obtener un nuevo diseño con perfil trifocal y compararlo con un CI comercial de características similares.

1.2. Estructura de la Tesis

El trabajo científico que se muestra a continuación es una Tesis por compendio de publicaciones científicas. Cada uno de los artículos que se presentan en el siguiente capítulo puede ser leído independientemente de los otros pues consta de una introducción teórica, metodología, resultados y conclusiones. Sin embargo, todos ellos juntos conforman un trabajo completo sobre el diseño y optimización de implantes intracorneales difractivos para la corrección de la presbicia. La Tesis está compuesta por cinco capítulos:

1. Introducción.
   1.1. Antecedentes y objetivos de la investigación.
   1.2. Estructura de la Tesis.
   1.3. Resumen de las publicaciones.
2. Publicaciones.
   2.1. Influence on the theoretical model eye on the numerical evaluation of fractal intraocular lenses.
   2.2. Optical evaluation of new designs of multifocal diffractive corneal inlays.
   2.3. Diffractive corneal inlays: a new concept for correction of presbyopia.
   2.4. Imaging performance of a diffractive corneal inlay for presbyopia in a model eye.
   2.5. Proposal of a new diffractive corneal inlay to improve near vision in a presbyopic eye.
   2.6. A new trifocal corneal inlay for presbyopia.
3. Discusión de los resultados obtenidos.
4. Conclusiones.
   4.1. Cumplimiento de objetivos.

4.2. Aportaciones realizadas.
4.3. Futuras líneas de investigación.
5. Bibliografía general.

1.3. Resumen de las publicaciones

El **Capítulo 1** de la introducción consta de un breve repaso sobre el estado del arte con los tres puntos clave de la Tesis: presbicia y soluciones más comunes, implantes intracorneales comerciales más utilizados y el diseño original del Diffractive Corneal Inlay [Furlan17]. Además, se recoge los objetivos a alcanzar y se muestra la estructura la Tesis en los diferentes capítulos.

Las publicaciones que componen la Tesis se incluyen y se explican detalladamente en el **Capítulo 2**. A continuación, se va a realizar un resumen sobre cada uno de estas publicaciones.

La **primera publicación** se titula "*Influence on the theoretical model eye on the numerical evaluation of fractal intraocular lenses*" [Montagud-Martínez19d] y ha sido aceptado en la Revista Mexicana de Física. Actualmente se encuentra en edición para su inminente publicación. Esta revista tiene un factor de impacto de 0.766 en el JCR de 2018 y se ubica en el cuartil Q4 (68/81) en la categoría PHYSICS, MULTIDISCIPLINARY. Aunque su factor de impacto no es muy elevado, es una de las mejores revistas científicas publicadas en Latinoamérica. Además, se presentó como poster en el Encuentro Iberoamericano de Óptica (RIAO) de 2019 [Montagud-Martínez19e]. En este trabajo se pretende evaluar numéricamente las propiedades ópticas de tres modelos de ojo teórico contrastados [Atchison06, Escudero-Sanz99, Liou97] utilizando una IOL de diseño propio y evaluar la influencia de la aberración esférica (SA) en cada modelo.

La **segunda publicación** "*Optical Evaluation of New Designs of Multifocal Diffractive Corneal Inlays*" [Montagud-Martínez19c] ha sido publicada en la revista Journal of Ophthalmology. Esta revista tiene un factor de impacto de 1.580 en el JCR de 2018 y se ubica en el cuartil Q3 (41/60) en la categoría OPHTHALMOLOGY. En este artículo se compara dos diseños optimizados de DCI con un CI comercial, KAMRA Inlay. Los nuevos diseños presentan un perfil bifocal en comparación con la extensión de foco que produce el KAMRA Inlay.

La **tercera publicación** pertenece al capítulo del libro "*Visual Impairment and Blindness - What We Know and What We Have to Know*" y se titula "*Diffractive Corneal Inlays: A New Concept for Correction of Presbyopia*" [Montagud-Martínez19a]. Este libro publicado en abierto se encuentra en fase de indexación en el Book Citation Index y otras bases de datos científicas. En este capítulo de libro se seleccionan los mismos diseños de la publicación anterior y se vuelven

a comparar con el KAMRA Inlay, pero en dos modelos de ojo diferentes. También se realizan simulaciones de imágenes para todos los implantes en ambos modelos de ojo y se seleccionan diferentes parámetros para las métricas mostradas.

"*Imaging Performance of a Diffractive Corneal Inlay for Presbyopia in a Model Eye*" [Montagud-Martínez19b] es el título de la **cuarta publicación** de la Tesis. Fue publicada en la revista IEEE ACCES en el año 2019. Esta revista tiene un factor de impacto de 4.098 en el JCR de 2018 y se ubica en el cuartil Q1 (52/266) en la categoría ENGINEERING, ELETRICAL & ELECTRONIC. En este trabajo se presenta un diseño optimizado del DCI y se compara con el KAMRA Inlay en el ojo modelo de Liou-Brennan [Liou97], el más utilizado en la literatura clínica. Además de medir las propiedades ópticas de ambos implantes, se comparó la sensibilidad al descentramiento de los CI, una propiedad clínicamente determinante.

La **quinta publicación** "*Proposal of a new diffractive corneal inlay to improve near vision in a presbyopic eye*" [Montagud-Martínez20] se publicó en la revista Applied Optics en 2020. Esta revista tiene un factor de impacto de 1.973 en el JCR de 2018 y se ubica en el cuartil Q2 (47/95) en la categoría OPTICS. El objetivo del trabajo fue modificar el diseño del DCI para mejorar el foco de cerca. Para ello se transformó parte central del diseño de amplitud (micro-agujeros y opaco) en un perfil que introducía un desfase de π (transparente con un grosor determinado) convirtiéndola en un diseño híbrido de amplitud-fase. Se comparó el nuevo modelo llamado HDCI con el mejor modelo de DCI.

La última y **sexta publicación** "*A new trifocal corneal inlay for presbyopia*" [Furlan20] se encuentra en proceso de revisión en una revista de alto prestigio internacional en el ámbito de la óptica. El DCI que se presenta en este trabajo tiene un diseño puramente de fase. La evaluación numérica de este implante se comparó con uno comercial de propiedades similares, Flexivue Microlens. El nuevo diseño de DCI llamado PDCI presentó un perfil trifocal, siendo el único implante intracorneal existente con tres focos y además mostró una mejor tolerancia al descentramiento comparado con el implante comercial.

.

Capítulo 2
Publicaciones

2.1. Influence of the theoretical model eye on the numerical evaluation of fractal intraocular lenses

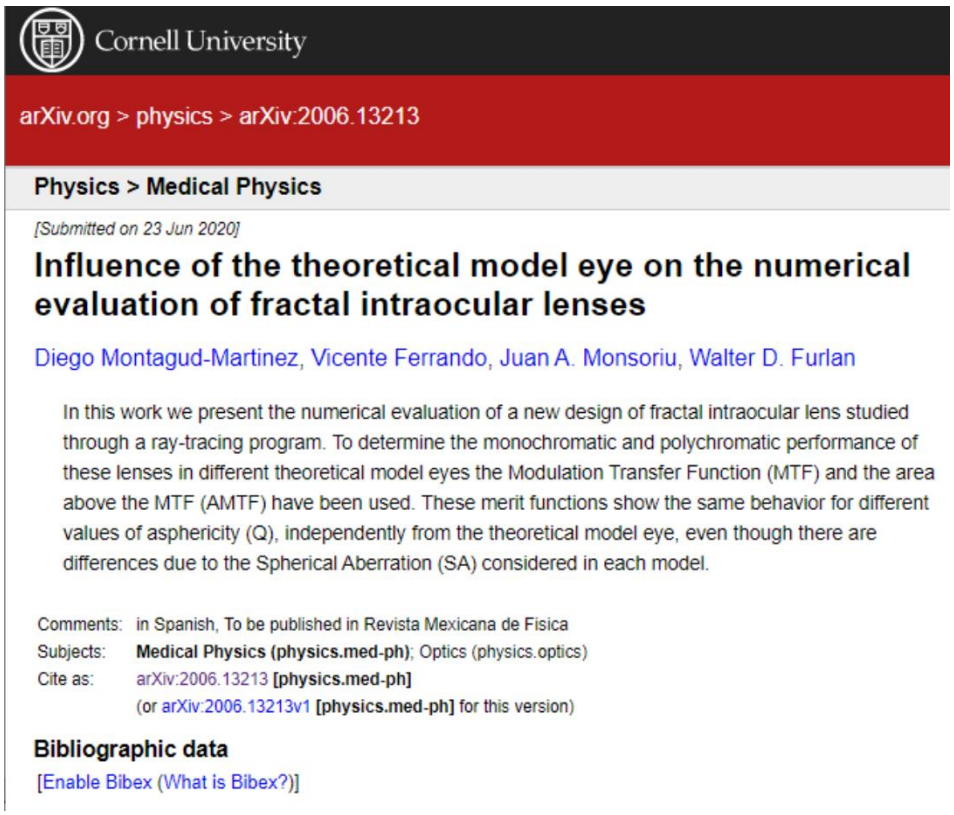

Cornell University

arXiv.org > physics > arXiv:2006.13213

Physics > Medical Physics

[Submitted on 23 Jun 2020]

Influence of the theoretical model eye on the numerical evaluation of fractal intraocular lenses

Diego Montagud-Martinez, Vicente Ferrando, Juan A. Monsoriu, Walter D. Furlan

In this work we present the numerical evaluation of a new design of fractal intraocular lens studied through a ray-tracing program. To determine the monochromatic and polychromatic performance of these lenses in different theoretical model eyes the Modulation Transfer Function (MTF) and the area above the MTF (AMTF) have been used. These merit functions show the same behavior for different values of asphericity (Q), independently from the theoretical model eye, even though there are differences due to the Spherical Aberration (SA) considered in each model.

Comments: in Spanish, To be published in Revista Mexicana de Fisica
Subjects: **Medical Physics (physics.med-ph)**; Optics (physics.optics)
Cite as: arXiv:2006.13213 **[physics.med-ph]**
(or arXiv:2006.13213v1 **[physics.med-ph]** for this version)

Bibliographic data

[Enable Bibex (What is Bibex?)]

2.1. Influence of the theoretical model eye on the numerical evaluation of fractal intraocular lenses

Diego Montagud-Martínez[1]*, Vicente Ferrando[1], Juan A. Monsoriu[1] y Walter D. Furlan[2]

[1] Centro de Tecnologías Físicas, Universitat Politècnica de València, 46022 Valencia, Spain.

[2] Departamento de Óptica y Optometría y Ciencias de la Visión, Universitat de València, 46100 Burjassot, Spain.

*diemonma@upvnet.upv.es

Abstract

In this work we present the numerical evaluation of a new design of fractal intraocular lens studied through a ray-tracing program. To determine the monochromatic and polychromatic performance of these lenses in different theoretical model eyes the Modulation Transfer Function (MTF) and the area above the MTF (AMTF) have been used. These merit functions show the same behavior for different values of asphericity (Q), independently from the theoretical model eye, even though there are differences due to the Spherical Aberration (SA) considered in each model.

Keywords: Intraocular Lens; Fractal; Optics.

Introducción

Una lente intraocular (IOL) es una lente que se inserta en el ojo sustituyendo al cristalino que se ha opacificado perdiendo su transparencia e impidiendo al ojo enfocar a diferentes distancias [Charman14]. A este proceso quirúrgico, que es uno de los más empleados, se le denomina operación de cataratas. Además, debido al incremento de la esperanza de vida de las personas, este proceso de envejecimiento del cristalino va progresivamente en aumento [Charman14]. Existen múltiples diseños de IOLs en el mercado. Dependiendo de la cantidad de focos que presenten tenemos: lentes monofocales, con un foco para visión de lejos, bifocales, para visión de lejos y cerca, o trifocales con un foco adicional en distancia intermedia [Hayasi09]. También existen lentes multifocales que además presentan una extensión de la profundidad de foco utilizando como mecanismo la SA. Este tipo de lentes se les conoce como lentes de foco extendido (EDOF) [Liu19].

A la hora de diseñar una nueva IOL es imprescindible, en primer lugar, realizar simulaciones numéricas con el modelo de la nueva lente (con programas de

trazado de rayos). Posteriormente y una vez fabricada, se mide experimentalmente las propiedades ópticas de la IOL en el banco óptico y finalmente se realizan ensayos clínicos con pacientes. Para las simulaciones numéricas se utilizan programas de trazado de rayos que permiten evaluar la calidad óptica de cualquier elemento óptico, en este caso de una IOL. Dependiendo de la complejidad de la simulación se pueden obtener resultados más reales utilizando modelos de ojo teóricos propuestos previamente en la bibliografía [Atchison17]. Existen múltiples modelos de ojos teóricos y cada uno de ellos tiene sus ventajas y desventajas. Entre los más destacados encontramos los modelos de Atchison [Atchison06] y Liou-Brennan [Liou97], cuyos parámetros oculares están basados en datos biométricos de pacientes con una edad media de 45 años, o el de Navarro [Escudero-Sanz99]. Estos tres modelos presentan dos superficies corneales, una pupila y cristalinos de diferente índole. Sin embargo, los parámetros oculares para los distintos modelos discrepan y las mayores diferencias se encuentran en las Q corneales que afectan directamente a la SA del modelo de ojo, así como el ángulo de incidencia de la luz y el índice de refracción del cristalino.

El objetivo de este trabajo es evaluar numéricamente mediante el programa de trazado de rayos ZEMAX™ OpticStudio (EE versión 18.7, ZEMAX Development Corporation, Bellevue, Washington, USA) tres modelos de ojos teóricos en los que se ha extraído el cristalino y se ha introducido una nueva IOL bifocal EDOF de diseño propio basada en estructuras fractales [Remón18].

Métodos

Nuevo diseño de lente intraocular fractal

La lente estudiada en este trabajo consiste en un diseño híbrido refractivo-difractivo [Liu19], el cual proporciona una extensión de foco y una baja aberración cromática. Está inspirada en la placa zonal fractal de Cantor [Saavedra03]. En la Figura 1 se puede observar como a partir del conjunto triádico de Cantor de orden 2, definido a lo largo de la coordenada radial cuadrática, se obtiene el perfil fractal de la lente propuesta. La IOL resultante presenta una distribución fractal de zonas anulares de diferente potencia (radio de curvatura) generando un diseño refractivo-difractivo con dos focos principales uno, para visión de lejos y otro para visión de cerca. En el software de trazado de rayos se introdujo la nueva lente intraocular fractal (FIOL) como una lente de dos superficies (r_{ant}= 21.4 mm y r_{post}= -17.0 mm) con un espesor de 0.7 mm y un índice de refracción (n=1.55) similar al de las IOL comerciales. El perfil fractal se introdujo en ZEMAX en la cara anterior como una superficie “grid sag”, en la cual se introducen las sagitas de la superficie fractal, mientras que la cara posterior de la FIOL presentaba un diseño esférico (Q=0) o asférico (Q=-10).

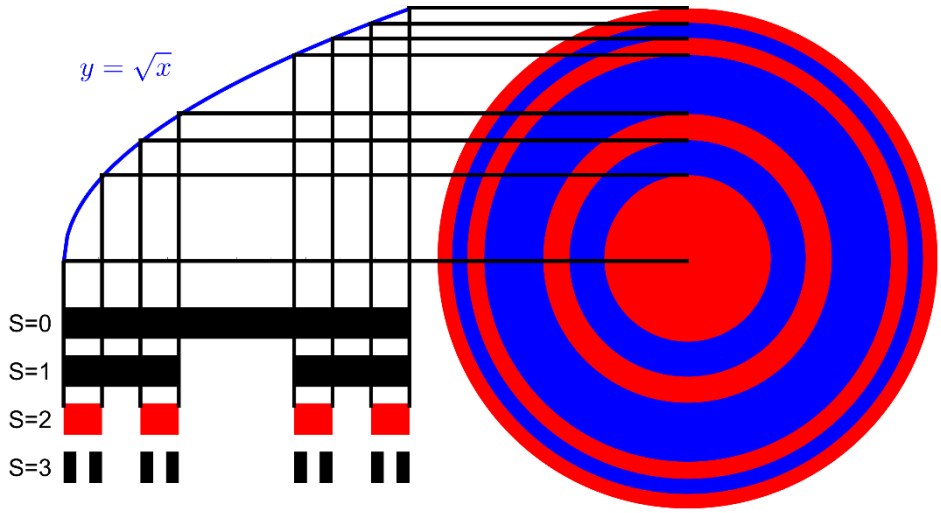

Figura 1: Obtención del perfil fractal de la lente a partir del conjunto triádico de Cantor.

Modelos de ojos teóricos

Para este estudio se utilizaron tres ojos teóricos ampliamente utilizados: Atchison [Atchison06], Liou-Brennan [Liou97] y Navarro [Escudero-Sanz99]. En la tabla 1 se muestran los parámetros oculares de cada modelo. No se muestran los datos del cristalino ya que en este estudio se sustituyeron por la FIOL. El valor de Q para la cara anterior y posterior de la córnea en cada modelo de ojo afecta al valor global de la SA de dicho modelo. Esto unido a la FIOL esférica (Q=0) o asférica (Q=-10) generará diferencias entre los modelos de ojo.

	Parámetros	Atchison	Liou-Brennan	Navarro
Córnea Anterior	Radio curvatura (mm)	7.77	7.77	7.72
	Q	-0.15	-0.18	-0.26
	n	1.376	1.376	1.3771
	Espesor (mm)	0.55	0.55	0.55
Córnea Posterior	Radio curvatura (mm)	6.40	6.40	6.5
	Q	-0.275	-0.60	0
	n	1.3374	1.336	1.3374
	Espesor (mm)		3.16	3.05
FIOL anterior (perfil fractal)	Radio curvatura (mm)	21.40		
	Q	0		
	n	1.55		
	Espesor (mm)	0.70		
FIOL posterior	Radio curvatura (mm)	-17.00		
	Q	0 o -10		
	n	1.336	1.336	1.336
	Espesor (mm)	Ajustado		

Tabla 1: Parámetros oculares de los tres modelos utilizados.

Registro de medidas

Después de ajustar la longitud axial de cada modelo de ojo se procedieron a medir las MTFs de los tres modelos con la IOL sin el perfil fractal (monofocal), con la FIOL esférica y con la FIOL asférica en las vergencias comprendidas entre +0.50 D y -3.50 D en pasos de 0.25 D. La luz utilizada para la obtención de las MTFs fue monocromática (λ=555 nm) y policromática siguiendo la distribución V(λ) dada por el propio software (λ_1=470 nm, λ_2=510 nm, λ_3=555 nm, λ_4=610 nm, λ_5=650 nm con sus respectivos pesos de 0.091, 0.503, 1, 0.503 y 0.107). Las pupilas que se utilizaron en las simulaciones fueron de 3.0 mm y 4.5 mm. El iris se situó en el mismo plano de la cara anterior de la IOL para los tres modelos. Utilizando un código propio de Matlab (versión R2018b, Mathworks Inc, Natick, Massachusetts, USA) se calcularon por el método de los trapecios el área bajo la curva de cada MTF (AMTF) entre las frecuencias de 9.49 ciclos/grado y 59.86 ciclos/grado para cada uno de los modelos en las condiciones antes descritas. Dichas frecuencias equivalen a agudezas visuales de 0.32 y 2.00 en escala decimal. Nótese que esta métrica, AMTF, se correlaciona muy bien con la AV correspondiente [Alarcon16].

2.1. Influence of the theoretical model eye on the numerical evaluation of fractal intraocular lenses

Resultados y discusión

En la Figura 2 se muestran las MTFs de los focos de lejos para pupilas de 3.0 mm (a) y 4.5 mm (b), respectivamente. Como puede observarse para los tres modelos de ojos no existen muchas diferencias entre la luz monocromática y la luz policromática. Por tanto, la aberración cromática de los modelos para ambas condiciones lumínicas es despreciable. También se observa que en el modelo de Atchison y Navarro las MTFs son más altas, tanto la monofocal como las FIOLs. En el caso del modelo de Liou-Brennan las MTFs son menores pero la diferencia entre la monofocal y las FIOLs en proporción es menor que para los otros dos modelos. El comportamiento de las lentes es más similar en los modelos de Atchison y Navarro que en el modelo de Liou-Brennan debido a la discrepancia y complejidad de este último con respecto a los dos anteriores. Además, la diferencia entre la FIOL esférica y la FIOL asférica aumenta al aumentar la pupila debido a que la influencia de la Q y la SA global del ojo es mayor cuanto mayores son las distancias de los rayos no paraxiales con respecto al eje visual.

En la Figura 3 se observan las MTFs de los focos de cerca para pupilas de 3.0 mm (a) y 4.5 mm (b). Nótese como las MTFs en estas figuras están en escala logarítmica para poder observar mejor las gráficas. Al igual que ocurre con el foco de lejos, los modelos de Atchison y Navarro predicen valores de MTFs más similares que en el caso del de Liou-Brennan. Además, también se confirma que al aumentar la pupila las diferencias entre la FIOL esférica y asférica aumentan. Al incrementar el tamaño pupilar la luz más alejada del eje visual no atraviesa el perfil fractal y por tanto focaliza en lejos. Por eso, las MTFs en 3.0 mm son mejores que en 4.5 mm sobre todo para las altas frecuencias.

A pesar de que las MTFs muestran buenos resultados, las AMTFs a través de foco permiten observar el comportamiento de la lente en diferentes vergencias tal y como se muestra en la Figura 4 para pupilas de 3.0 mm (a) y 4.5 mm (b), respectivamente. En la Figura 4a se muestra claramente el perfil bifocal de la FIOL y como no existen diferencias significativas entre las medidas con luz monocromática y luz policromática. Esto último puede comprobarse también en la Figura 4b. Centrándonos en la pupila de 3.0 mm observamos como para los tres modelos de ojo el efecto de añadir una superficie asférica al perfil fractal es el mismo, es decir, desplaza los focos hacia vergencias positivas, si bien este desplazamiento es ligeramente mayor para el foco de cerca. Además, en los tres casos las alturas de las AMTFs en lejos son mejores para la FIOL asférica que la esférica.

Si nos fijamos en la Figura 4b podemos observar como las AMTFs caen de manera significativa debido a las aberraciones de los modelos. Es decir, al aumentar el tamaño pupilar a 4.5 mm los rayos que llegan a la retina dejan de ser paraxiales provocando peores AMTFs tanto para la monofocal como para

ambas FIOLs. Además, se produce una extensión del foco de cerca como consecuencia de la estructura fractal del diseño. También se puede observar como la inclusión de una superficie asférica a la FIOL mejora el foco de lejos y de cerca en los tres modelos de ojo teórico.

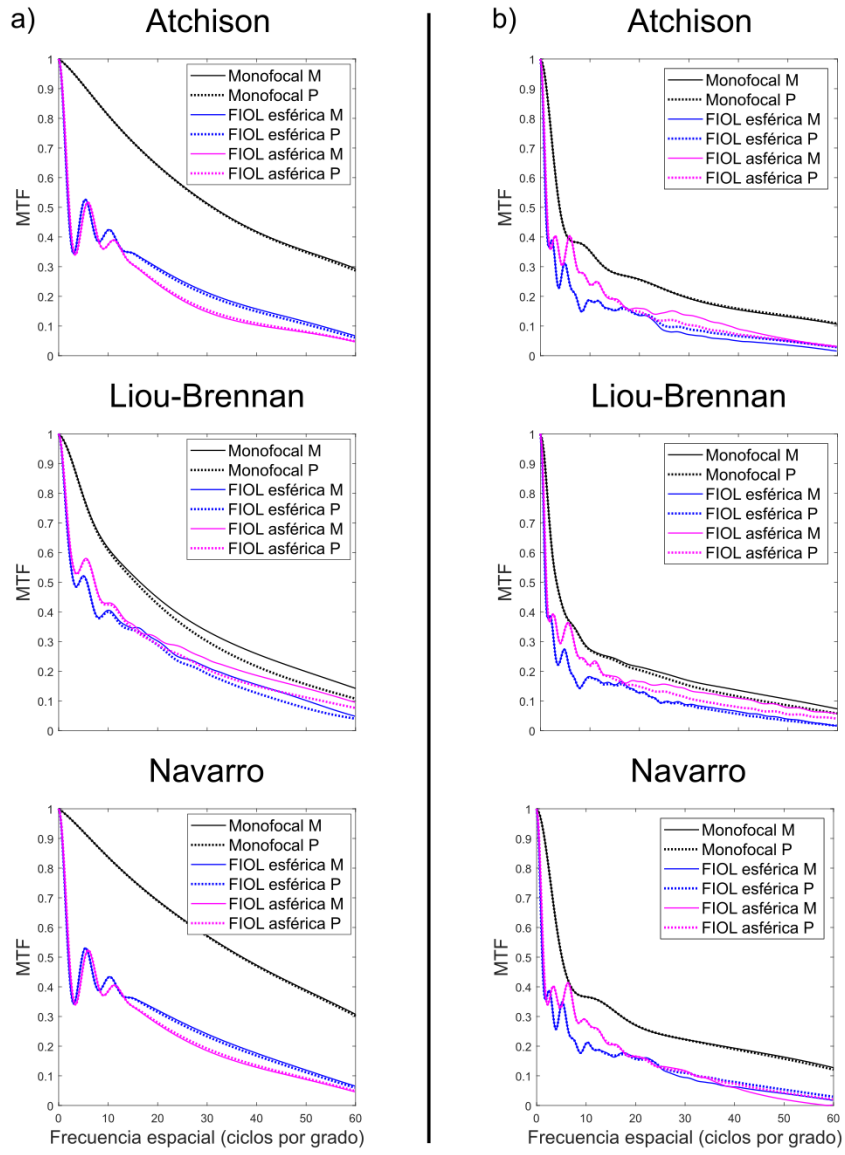

Figura 2: MTFs en el foco de lejos para pupila de 3.0 mm (a), MTFs en el foco de lejos para pupila de 4.5 mm (b). Las líneas continuas representan luz monocromática y las líneas discontinuas luz policromática.

2.1. Influence of the theoretical model eye on the numerical evaluation of fractal intraocular lenses

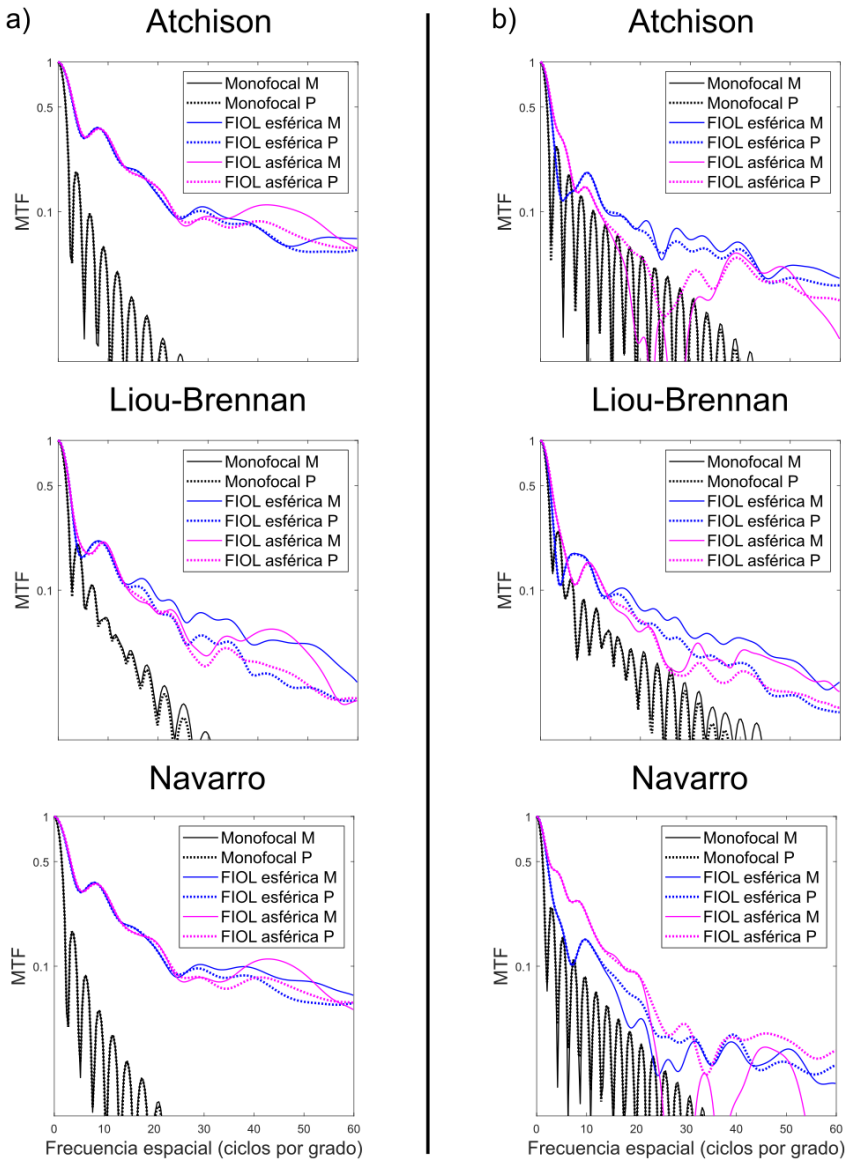

Figura 3: MTFs en el foco de cerca para pupila de 3.0 mm (a), MTFs en el foco de cerca para pupila de 4.5 mm (b). Las líneas continuas representan luz monocromática y las líneas discontinuas luz policromática.

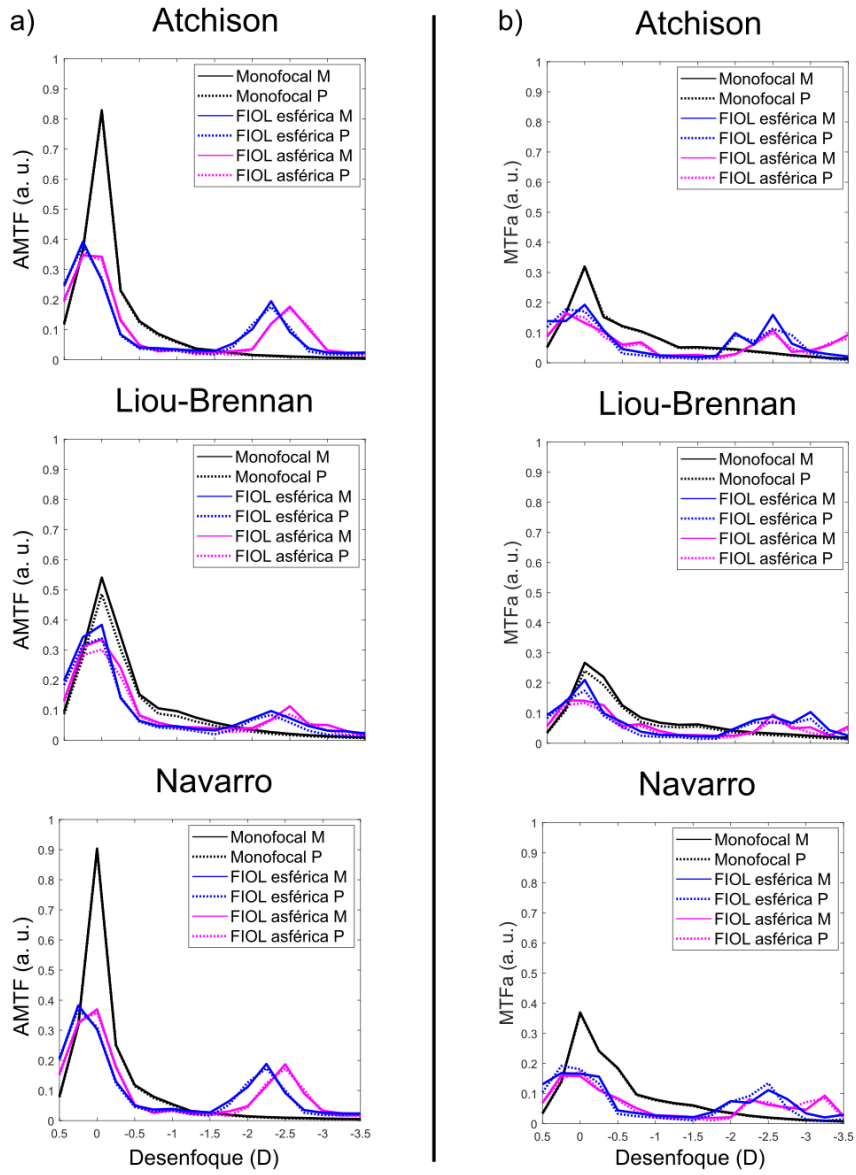

Figura 4: AMTFs para pupila de 3.0 mm (a), AMTFs para pupila de 4.5 mm (b). Las líneas continuas representan luz monocromática y las líneas discontinuas luz policromática.

Conclusiones

Los programas de trazado de rayos constituyen una herramienta esencial para la validación numérica de nuevos diseños de elementos ópticos. Estos programas permiten determinar la calidad óptica de estos elementos mediante

funciones de mérito como son la MTF y la AMTF, e incluso simular imágenes. En este trabajo se ha caracterizado una lente con perfil fractal y con dos asfericidades diferentes para tres modelos de ojos teóricos. Los resultados muestran que, aunque los modelos de ojos teórico presentan resultados diferentes, la tendencia es similar para los tres. La FIOL propuesta presenta un perfil bifocal con foco extendido en cerca para todos los modelos de ojo que mejora al añadir una superficie asférica.

Agradecimientos

Este trabajo ha sido financiado por el Ministerio de Economía y Competitividad (Proyecto DPI-2015-71256-R) y por la Generalitat Valenciana (Proyecto PROMETEO/2019/048), España. D. Montagud-Martínez y V. Ferrando agradecen la financiación por parte de la Universitat Politècnica de València, España (FPI-2016 y PAID-10-18, respectivamente).

Bibliografía

[Alarcon16] Alarcon A, Canovas C, Rosen R, Weeber H, Tsai L, Hileman K, et al. Preclinical metrics to predict through-focus visual acuity for pseudophakic patients. Biomed Opt Express, BOE. 2016;7(5):1877–88.

[Atchison06] Atchison DA. Optical models for human myopic eyes. Vision Research. 2006;46(14):2236–50.

[Atchison17] Atchison DA, Schematic eyes, 1st ed. Taylor & Francis, Boca Raton, 2017.

[Charman14] Charman WN. Developments in the correction of presbyopia II: surgical approaches. Ophthalmic Physiol Opt. 2014;34(4):397–426.

[Escudero-Sanz99] Escudero-Sanz I, Navarro R. Off-axis aberrations of a wide-angle schematic eye model. J Opt Soc Am A, JOSAA. 1999;16(8):1881–91.

[Hayasi09] Hayashi K, Manabe S, Hayashi H. Visual acuity from far to near and contrast sensitivity in eyes with a diffractive multifocal intraocular lens with a low addition power. Journal of Cataract & Refractive Surgery. 2009;35(12):2070–6.

[Liou97] Liou H-L, Brennan NA. Anatomically accurate, finite model eye for optical modeling. J Opt Soc Am A, JOSAA. 1997;14(8):1684–95.

[Liu19] Liu J, Dong Y, Wang Y. Efficacy and safety of extended depth of focus intraocular lenses in cataract surgery: a systematic review and meta-analysis. BMC Ophthalmol. 2019;19(1):198.

[Remón18] Remón L, García-Delpech S, Udaondo P, Ferrando V, Monsoriu JA, Furlan WD. Fractal-structured multifocal intraocular lens. PLoS ONE. 2018;13(7):e0200197.

[Saavedra03] Saavedra G, Furlan WD, Monsoriu JA. Fractal zone plates. Opt Lett, OL. 2003;28(12):971–3.

2.2. Optical Evaluation of New Designs of Multifocal Diffractive Corneal Inlays

Special Issue

Personalized Optical Designs and Manipulating Optics: Applications on the Anterior Segment of the Eye

View this Special Issue

Research Article | Open Access
Volume 2019 | Article ID 9382467 | 6 pages | https://doi.org/10.1155/2019/9382467

Optical Evaluation of New Designs of Multifocal Diffractive Corneal Inlays

Diego Montagud-Martínez,[1] Vicente Ferrando,[1] Juan A. Monsoriu,[1] and **Walter D. Furlan**[2]

Show more

Academic Editor: Pablo Pérez-Merino

Received	Accepted	Published
19 Jun 2019	09 Sep 2019	11 Nov 2019

Abstract

Purpose. To assess the imaging properties of two different designs of a new concept of corneal inlays whose working principle is based on diffraction. *Methods.* The quality of the retinal images provided by Diffractive Corneal Inlays (DCIs) was evaluated theoretically in comparison with Small Aperture Corneal Inlay (SACI). ZEMAX OpticStudio software was employed for the simulations in an eye model with different pupil diameters (3.0 mm and 4.5 mm). The employed merit functions in the analysis were the Modulation Transfer Function (MTF), the area under the MTF (MTFa), and the Point Spread Function (PSF). Comparison was made with the SACI at different defocus conditions. *Results.* The bifocal nature of the DCIs was demonstrated in a model eye for the first time. It was shown that the intensity of the near focus depends on the radius of the central zone. Retinal image quality of the DCI was equal to or exceeded the SACI in the majority of visual conditions as was demonstrated with simulated images. *Conclusions.* A new customizable type of corneal inlays has been evaluated using objective numerical simulations. Improvements in imaging of near objects and in light throughput compared with the popular small aperture inlays were demonstrated. These findings open a new technical branch of minimally invasive surgical solutions for the treatment of presbyopia.

2.2. Optical Evaluation of New Designs of Multifocal Diffractive Corneal Inlays

Diego Montagud-Martínez[1], Vicente Ferrando[1], Juan A. Monsoriu[1] y Walter D. Furlan[2*]

[1] Centro de Tecnologías Físicas, Universitat Politècnica de València, 46022 Valencia, Spain.

[2] Departamento de Óptica y Optometría y Ciencias de la Visión, Universitat de València, 46100 Burjassot, Spain.

*walter.furlan@uv.es

Abstract

Purpose. To assess the imaging properties of two different designs of a new concept of corneal inlays whose working principle is based on diffraction.

Methods. The quality of the retinal images provided by Diffractive Corneal Inlays (DCIs) were evaluated theoretically in comparison with Small Aperture Corneal Inlay (SACI). ZEMAX OpticStudio software was employed for the simulations in an eye model with different pupil diameters (3.0 mm and 4.5 mm). The employed merit functions in the analysis were the Modulation Transfer Function (MTF), the Area under the MTF (AMTF), and the Point Spread Function (PSF). Comparison was made with the SACI at different defocus conditions.

Results. The bifocal nature of the DCIs was demonstrated in a model eye for the first time. It was shown that the intensity of the near focus depends on the radius of the central zone. Retinal image quality of the DCI was equal to or exceeded the SACI in the majority visual conditions as was demonstrated with simulated images.

Conclusions. A new customizable type of corneal inlays has been evaluated using objective numerical simulations. Improvements in imaging of near objects and in light throughput compared with the popular small aperture inlays were demonstrated. These findings open a new technical branch of minimally invasive surgical solutions for the treatment of presbyopia.

Introduction

Presbyopia affects almost all adults over 45 years old and it has been estimated that globally there are more than 1.8 billion people with presbyopia, 820 million of whom had near visual impairment because they had no, or inadequate, vision correction [Fricke18].

At present, the minimum invasive surgical option for presbyopes who don't want glasses or contact lenses is to implant a corneal inlay. By means of a femtosecond laser, the surgeon creates a pocket inside the corneal stroma where the inlay is inserted rendering the surgical procedure fast, simple, and importantly: reversible.

Based on working principle, different options have been launched in the market in the last years: corneal reshaping device, refractive corneal device, and small aperture corneal inlay (SACI) [Charman14]. The last one: commercially known as Kamra® inlay (AcuFocus, Inc., Irvine, California, USA) is undoubtedly the most popular due to the reported good clinical outcomes [Yilmaz11, Seyeddain13]. This device is an opaque disk of a biocompatible material (polyvinylidene fluoride) with a central aperture that produces an extended depth of focus. In addition, to facilitate the flow of nutrients to cells of the corneal stroma, the disk has a reduced external diameter, and has more than 8,000 micro-pores, in a size range of 5–11 μm diameter. Unfortunately, although SACI implantation can result in improved intermediate and near vision, it has several important intrinsic drawbacks. First, only about twenty percent of the incident light passes through the disc's central aperture. Secondly, as much as five percent of incident light is diffracted by the disc's microholes. Thirdly, as the SACI is implanted monocularly, the interocular asymmetry induced by anisocoria combined with monovision deteriorate binocular summation [Castro16] and stereoacuity [Castro18].

In an effort to avoid these drawbacks our group recently proposed a new concept of corneal inlays that take profit of the diffraction phenomena originated in the micro-pores of the SACI [Furlan17]. The result (DCI), is a device that, by exploiting the photon sieve concept [Kipp01], creates a diffractive focus for near vision in the implanted eye, on a personalized basis. In fact, an additional and important benefit of the DCI is that its optical characteristics (addition, intensity ratio between the near and far foci, etc…) can be modified by varying the size of the pinholes and the pattern of their distribution indicating that DCIs could be customized for a variety of specific patient's needs.

Materials and Methods

Model Eye.

The assessment of the imaging properties of two different DCI was investigated by implementing a schematic-eye in the Zemax OpticStudio optical design software (http://www.zemax.com/os/opticstudio). The phakic model eye employed in the simulations was the Eye Retinal Image.zmx included in the Zemax software (see Table I), in which the polychromatic receptor photopic spectral sensitivity is simulated using 470, 510, 555, 610, and 650 nm wavelengths, with relative weights i.e.: of 0.091, 0.503, 1.0, 0.503, and 0.107, respectively.

Corneal Inlays

Two DCIs models with an external diameter of 4.15 mm were evaluated in this study, both designed to provide a near focus corresponding to a typical addition of +2.50 D. Model DCI #1 was designed a central hole of 1.00 mm diameter surrounded by 8 rings conformed by a total of 6394 holes. DCI #2 was designed with a central hole of 1.6 mm diameter surrounded by 8 rings with a total of 5989 holes. These two models have been considered to show the versatility in the DCI design and to study the influence on the resulting image performance of the central hole diameter. The external diameter corresponds to the original design [Furlan17]. A completely opaque SACI with the dimensions of the Kamra® has been evaluated in parallel as a reference. The inlays were located in the model eye at 0.20 mm from the anterior corneal surface as "User Defined Aperture" (uda) in ZEMAX, with the same radius of curvature and an asphericity of the anterior cornea surface (see Table I). The inlays thickness was assumed as 5 μm, Diagrams of the evaluated DCIs and SACI are shown in Fig.1.

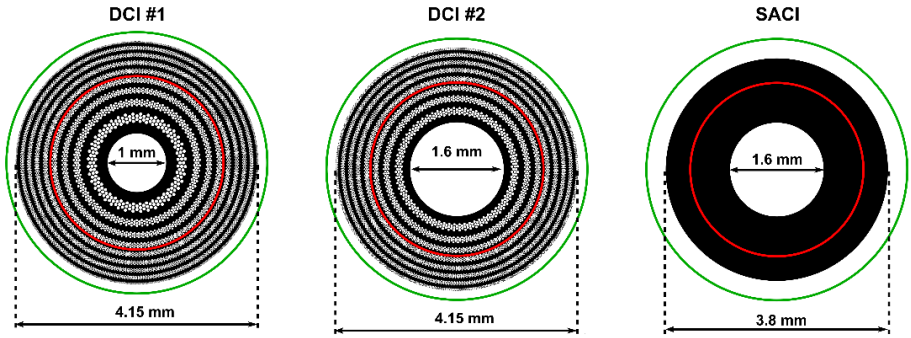

Figure 1: Diagrams of the corneal inlays evaluated in this study. The red and green circles represent 3.0 mm and 4.5 mm pupil diameters respectively.

Metrics

The image quality provided by the corneal inlays in this study was assessed using different merit functions. First, the MTFs were computed for different object vergences in the range +0.5 D to −3.5 D in steps of 0.1 D. The best focus position of the retina remained the same for all MTF calculations. In each case, the AMTF was calculated as the numerical integral (using the trapezoid rule) for MTFs in a frequency range from 0 cpd to 59.9 cpd. This last spatial frequency corresponds to a visual acuity of -0.2 logMAR.

Additionally, simulated images of a visual acuity test chart were obtained from the PSF provided by ZEMAX by means of the numerical convolution using a Matlab (Mathworks, Inc. R2018b) code. The simulations were performed with polychromatic light using 5 wavelengths as previously mentioned.

Surface	Radius (mm)	Asphericity	Thickness (mm)	Refractive index
Anterior Cornea	7.80	-0.50	0.20	1.377
Anterior CI	7.80	-0.50	0.005	1.377
Posterior CI	7.80	-0.50	0.315	1.377
Posterior Cornea	6.70	-0.30	3.1	1.337
Iris	-	-	0.1	1.337
Anterior Lens	10	0	3.7	1.42
Posterior Lens	-6	-3.25	16.58	1.336

Table 1: Phakic model eye with corneal inlay (CI).

Results and Discussion

Figure 2 shows the MTFs of provided by the three corneal inlays at far and near foci for 3.0 mm and 4.5 mm pupil diameters simulating the eye response to photopic and mesopic lighting conditions, respectively. In order to enhance the differences, the MTFs in the near focus was represented on a logarithmic scale in the range 0.03 to 1.

Note that, except for the distance focus and 3.0 mm pupil diameters, the performance of both models of DCI is superior to the SACI, even though the diffractive effects of the SACI (nocive for the image quality, in this case) have not been considered in the simulations. A better MTF curve was achieved by DCI #2 at far for both pupils but with minimum differences. On the other hand, DCI #1 provides a better near focus than DCI #2. These results can be also verified in terms of area under MTF. Figure 3 shows AMTF computed for 3.0 mm 4.5 mm pupils in the range of frequencies that are important in terms of visual acuity.

For 3.0 mm pupil diameter, bigger differences can be observed between the three designs. DCI #1 has the lower values for the far focus, but the higher values for the near focus. These differences are attenuated for 4.5 mm pupil. In this case, all the three inlays have a comparable performance at far, but both DCIs maintain an effective near focus.

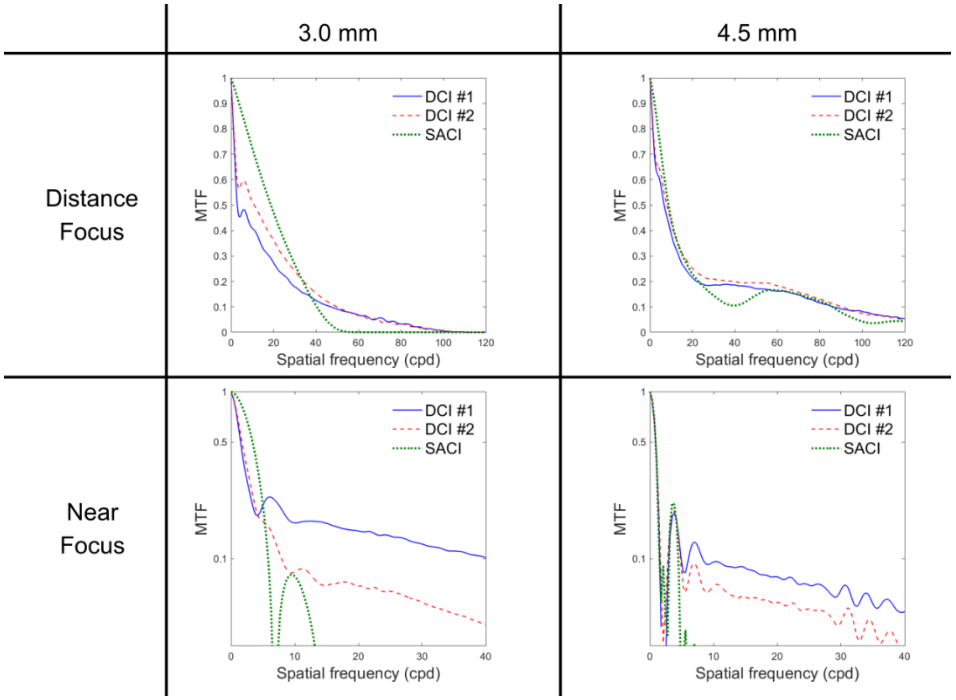

Figure 2: MTFs at far and near foci provided by the three corneal inlays considered in this study.

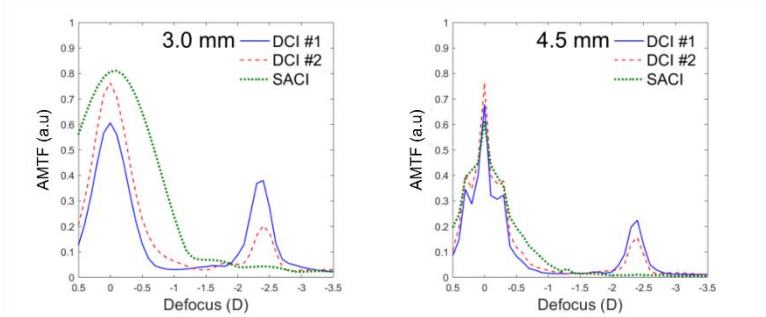

Figure 3: Comparative AMTF, in arbitrary units (a.u.), for 3.0 and 4.5 mm pupil diameters.

Figures 2 and 3 reveal the image quality of the studied corneal inlays; however, the main difference between the DCIs and SACI performance relies in the light throughput, which is more explicit in the comparison between the images obtained from the corresponding PSFs.

Figures 4 and 5 show the PFSs provided by the model eye with two pupil diameters, virtually implanted with the different inlays, for point objects at far and near distances. Note that the scales of the PSFs are different, indicating the different intensities achieved with each inlay model. In these figures the

corresponding simulated images of three Snellen “E’s”, with sizes corresponding to 0.4, 0.2 and 0 logMAR visual acuities are shown next to the corresponding PSF.

These images have been obtained as the convolution of the corresponding PSF with the test object. In this way, the relative intensity of the images and the spatial extension of the PSFs can be directly compared, except for the SACI at near, in this case, the image intensity has been multiplied by a factor of 4 because otherwise this image would be almost black. Note that in Fig. 5 the area of the PSF window has been extended to cover the spread of the PSF of the SACI at near.

The image quality and the relative image intensity between them can be clearly observed in figures 4 and 5. As can be seen, the image obtained with SACI is attenuated significantly. This is a very important fact because it was demonstrated that although the *binocular* distance visual acuity with a monocularly implanted SACI induces a *binocular* summation, the visual acuity for near distance seems to be close to the near distance acuity of the eye with SACI [Tabernero11].

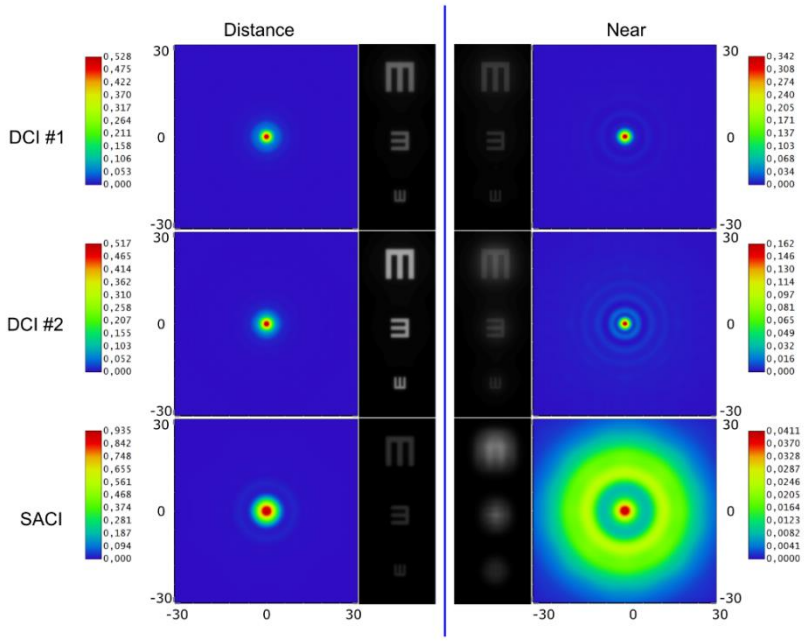

Figure 4: PSFs and the corresponding simulated images of the three inlays for distance and near objects Zemax model eye with pupil diameter 3.0 mm.

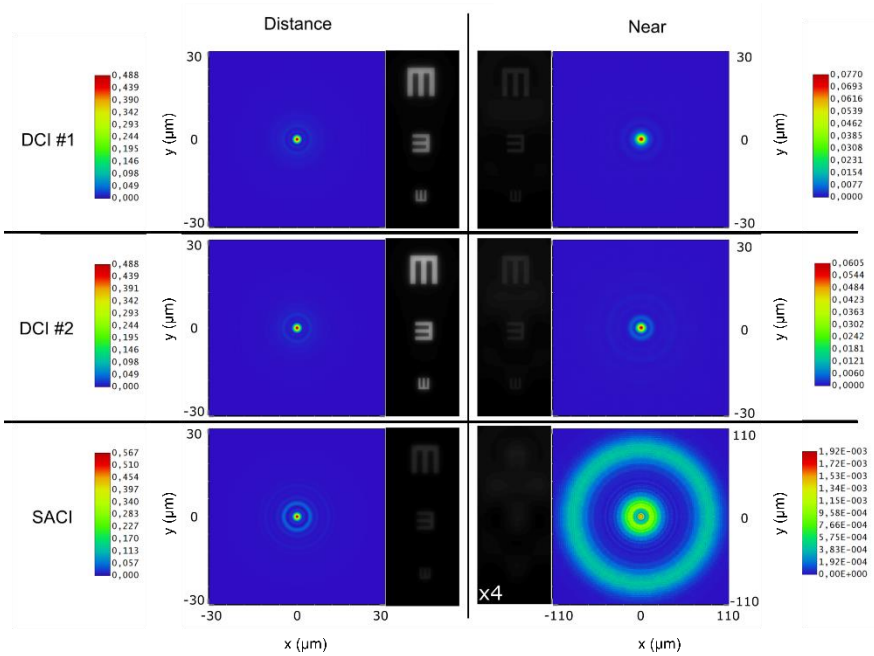

Figure 5: PSFs and the corresponding simulated images of the three inlays for distance and near objects Zemax model eye win pupil diameter 4.5 mm).

Conclusions

In conclusion, we performed an optical simulation on a new customizable treatment option for correcting presbyopia, the DCI. We found that the larger transmission of DCI compared with the SACI, makes the proposed inlay highly luminous efficient, and its diffractive structure provides a near focus. Moreover, by using different models of the DCI, we have shown that the intensity ratio between the far and near foci can be controlled by adjusting the diffractive structure, which seems to be clinically relevant taking into account the particular patient's visual needs. In fact, in this study, we studied two different designs and demonstrated that the intensity of the DCIs foci depends on the radius of the central zone, being more intense the near focus for the DCI #1 than for the DCI #2, but the opposite happens for the far focus. The PSFs and the simulated images show the improved performance of the DCI in comparison with the SACI, especially in near vision.

Data Availability

The data supporting the results of the current article are available from the corresponding author upon request.

Conflicts of Interest

The authors declare that there is no conflict of interest regarding the publication of this paper.

Funding Statement

This work was supported in part by the Ministerio de Economía y Competitividad, Spain, [Grant DPI2015-71256-R].

Acknowledgments

D. Montagud-Martinez and V. Ferrando acknowledge the financial support from the Universitat Politècnica de València, Spain (fellowships FPI-2016 and PAID-10-18, respectively).

References

[Castro16] Castro JJ, Soler M, Ortiz C, Jiménez JR, Anera RG. Binocular summation and visual function with induced anisocoria and monovision. Biomed Opt Express. 2016;7(10):4250–62.

[Castro18] Castro JJ, Ortiz C, Jiménez JR, Ortiz-Peregrina S, Casares-López M. Stereopsis Simulating Small-Aperture Corneal Inlay and Monovision Conditions. J Refract Surg. 2018;34(7):482–8.

[Charman14] Charman WN. Developments in the correction of presbyopia II: surgical approaches. Ophthalmic Physiol Opt. 2014;34(4):397–426.

[Fricke18] Fricke TR, Tahhan N, Resnikoff S, Papas E, Burnett A, Ho SM, et al. Global Prevalence of Presbyopia and Vision Impairment from Uncorrected Presbyopia: Systematic Review, Meta-analysis, and Modelling. Ophthalmology. 2018;125(10):1492–9.

[Furlan17] Furlan WD, García-Delpech S, Udaondo P, Remón L, Ferrando V, Monsoriu JA. Diffractive corneal inlay for presbyopia. J Biophotonics. 2017;10(9):1110–4.

[Kipp01] Kipp L, Skibowski M, Johnson RL, Berndt R, Adelung R, Harm S, et al. Sharper images by focusing soft X-rays with photon sieves. Nature. 2001;414(6860):184–8.

[Seyeddain13] Seyeddain O, Bachernegg A, Riha W, Rückl T, Reitsamer H, Grabner G, et al. Femtosecond laser-assisted small-aperture corneal inlay implantation for corneal compensation of presbyopia: two-year follow-up. J Cataract Refract Surg. 2013;39(2):234–41.

[Tabernero11] Tabernero J, Schwarz C, Fernández EJ, Artal P. Binocular Visual Simulation of a Corneal Inlay to Increase Depth of Focus. Invest Ophthalmol Vis Sci. 2011;52(8):5273–7.

[Yilmaz11] Yılmaz OF, Alagöz N, Pekel G, Azman E, Aksoy EF, Cakır H, et al. Intracorneal inlay to correct presbyopia: Long-term results. J Cataract Refract Surg. 2011;37(7):1275–81.

2.3. Diffractive corneal inlays: A new concept for correction of presbyopia

Open access peer-reviewed chapter - ONLINE FIRST

Diffractive Corneal Inlays: A New Concept for Correction of Presbyopia

By Diego Montagud-Martínez, Vicente Ferrando, Salvador Garcia-Delpech, Juan A. Monsoriu and Walter D. Furlan

Submitted: June 4th 2019 Reviewed: August 20th 2019 Published: September 20th 2019
DOI: 10.5772/intechopen.89265

Abstract

A new class of corneal inlays for treatment of presbyopia is described, which uses diffraction as the working principle. The inlay consists of an opaque disk with a small central aperture surrounded by an array of micro-holes that are distributed following the order of a given Fresnel zone plate having N zones. In this way, the central hole of the disk produces an extension of the depth of focus of the eye for distance vision and contributes to the zero order of diffraction, and the light diffracted by the micro-holes in the periphery produces a real focus for near vision. In our general design, the number of zones and the diameter of the central hole are free parameters that can be used to design customized devices with different addition power and near-focus intensity. Two different designs are analyzed to show this property. In the analysis, we employed a ray tracing software to study the performance of the new inlays in the two different model eyes. The results are compared with those obtained with a model of the small-aperture inlay that is currently in the market. The different merit functions used in the comparison and the image simulations performed with the inlays in the model eyes show the excellent performance of our proposal.

2.3. Diffractive corneal inlays: A new concept for correction of presbyopia

Diego Montagud-Martínez[1*], Vicente Ferrando[1], Salvador Garcia-Delpech[2], Juan A. Monsoriu[1] y Walter D. Furlan[3]

1 Centro de Tecnologías Físicas, Universitat Politècnica de València, 46022 Valencia, Spain.

[2] Hospital Universitari i Politècnic La Fe, Valencia, Spain

3 Departamento de Óptica y Optometría y Ciencias de la Visión, Universitat de València, 46100 Burjassot, Spain.

*diemonma@upvnet.upv.es

Abstract

A new class of corneal inlays for treatment of presbyopia is described which working principle is diffraction. The inlay consists on opaque disc with a small central aperture surrounded by an array of micro-holes which are distributed following the order of a given Fresnel zone plate having N zones. In this way, the central hole of the disc produces an extension of the depth of focus of the eye for distance vision and contributes to the zero order of diffraction and, the light diffracted by the micro-holes in the periphery produce a real focus for near vision. In our general design, the number of zones and the diameter of the central hole are free parameters that can be used to design customized devices with different addition power and near focus intensity. Two different designs are analyzed to show this property. In the analysis we employed a ray tracing software to study the performance of the new inlays in two different model eyes. The results are compared with those obtained with a model of the small aperture inlay that is currently in the market. The different merit functions used in the comparison and the image simulations performed with the inlays in the model eyes show the excellent performance of our proposal

Keywords: *presbyopia, corneal inlay, diffractive optics, refractive surgery, cornea.*

Introduction

Affecting approximately 2 billion people worldwide, presbyopia is the most common refractive defect in the population, disturbing the quality of life of people over 45 years. It is expected that this situation will grow to reach 2,100 million in 2020 [Arlt15]. In fact, presbyopia is a natural condition of the human being due to aging and it is caused by the loss of ability of the crystalline lens to accommodate.

The treatment of presbyopia has historically been addresses from multiple perspectives: spectacles (reading glasses, bifocals and progressive), multifocal contact lenses, and refractive surgery. Within this area, the most recent surgical approach is in the use of corneal inlays (CI) [Arlt15, Charman14]. These implants consist of lenticles of a biocompatible synthetic material that, as the name implies, are placed into the corneal stroma. The main advantage of CI over other surgical therapies, like intraocular lenses, is that it is a minimally invasive and reversible surgery [Lindstrom13]; in addition, CI are stable, and do not require maintenance.

Currently, all CIs are implanted monocularly in the non-dominant eye producing a modified variant of the monovision system, which consists in using the dominant eye for distance vision and the non-dominant one for intermediate-near vision. Commercial examples of CIs are: the Flexivue microlens® (Presbia Cooperatief, UA, Irvine, CA, USA) [Arlt15, Limnopoulou13, Moarefi17], the Raindrop® (ReVision Optics, Lake Forest, CA, USA) [Arlt15, Moarefi17, Garza13] and the Small Aperture Corneal Inlay (SACI) whose trade name is KAMRA® inlay (Acufocus, Inc, Irvine, CA, USA) [Arlt15, Moarefi17, Internet19a, Yilmaz08, Waring11, Vilupuru15]. The principle of operation of each model is different. The Flexivue inlay is a bifocal device of the center-far type, since it has a central hole for the passage of nutrients that allows the vision of far and a peripheral area for the near vision that contains the power of addition. The Raindrop inlay uses a different refractive principle, which consists of introducing a lencticle of permeable material in the center of the corneal stroma to create a hyperprolate cornea. Therefore, the cornea becomes itself a center-near bifocal lens. Finally, the SACI uses the pinhole effect to extend the depth of focus of the eye in far vision. Indeed, it consists of an opaque ring of 1.6 mm internal diameter and 3.6 mm external diameter, constructed with carbon-doped polyvinylidene fluoride. It has about 8400 micro-holes with diameters between 5-10 µm, distributed randomly to allow the passage of nutrients through the stroma, which gives it around 5% transmittance [Vilupuru15]. Surgically, it is introduced at a depth of 200 µm. The SACI is the most successful commercial CI and has been widely studied both clinically and theoretically [Arlt15, Moarefi17, Internet19a, Yilmaz08, Waring11, Vilupuru15]. However, it has certain drawbacks. As it is an opaque ring, the amount of light that reaches the retina of each eye is different causing a degradation of binocular distance visual acuity [Vukich18], and a potential detrimental effect on the binocular summation ratio [Gilchrist87]. Moreover, SACI produces marked interocular differences in visual latency and a Pulfrich effect, [Plainis13]. Other visual function that is compromised by the SACI is a deterioration in stereoacuity with respect to natural conditions, especially for near and intermediate distances [Castro18].

In this chapter we describe a new concept of CI developed by our research group that is based on the concept of diffraction. It consists of a variation of an amplitude Fresnel zone plate [Machado17] in which micro holes conform the clear zones of the zone plate in a similar way as was proposed to construct the so-called photon

sieves [Kipp01]. Photon sieves were conceived for its use in X-ray microscopy, but have also found numerous applications in various scientific and technological areas [Menon05, Andersen05, Giménez06]. Inspired by this concept, we conceived the first Diffractive Corneal Inlay (DCI) in which the distribution of holes in an opaque ring has been ordered to achieve a bifocal intrastromal lens. In this way, the light diffracted by the inlay (an unwanted effect in the SACI commercial design) generates a focus, which would allow presbyopic patients to see close objects clearly. To demonstrate its properties, in the following sections theoretical and numerical results are compared with the SACI, using two different theoretical eye models implemented in the ZEMAX ™ OpticStudio software (EE version 18.7, ZEMAX Development Corporation, Bellevue, Washington, USA). To evaluate the optical quality of ICs, the Modulation Transfer Function (MTF), which defines the visibility of a given optical system for all spatial frequencies [Artal17], the area under the MTF curve (AMTF), computed for different object vergences, and the Point Spread Function (PSF) [Artal17]. that describes the response of an optical system to a point source have been used. In addition, the numerically calculated PSFs have been used to obtain simulated images of an optotype test chart.

Diffractive Corneal Inlay (DCI)

The starting point of the DCI design is an amplitude Fresnel zone plate, which has been devised with the optical power necessary to generate the addition. In it, instead of fully transparent zones, micro-holes are made to allow the passage of light and the nutrients. forming a single structure without any substrate. The DCI [Furlan17], in addition to presenting the aforementioned micro-hole structure, has a central hole that acts as a pinhole of variable diameter, thus the DCI presents different diffractive orders. The zero order focuses the light for distant vision, while the +1 order forms the near focus. By varying the number of rings, the number and size of the micro holes, as well as the internal diameter of the central hole, the diffraction efficiency of the far and near foci can be modified.

Here we evaluated two DCIs models in comparison with a SACI with the dimensions of the Kamra® (see Figure 1). Both DCIs were designed to provide a near focus corresponding to an addition of +2.50 D, and both have an external diameter of 4.15 mm. DCI 1.0 has a central hole of 1.00 mm diameter surrounded by 8 rings with a total of 6394 holes. DCI 1.6 was designed with a central hole of 1.6 mm diameter surrounded by 7 rings conformed by a total of 5989 holes. A completely opaque with the dimensions of the SACI, as shown in Figure 1, was evaluated in parallel for comparison.

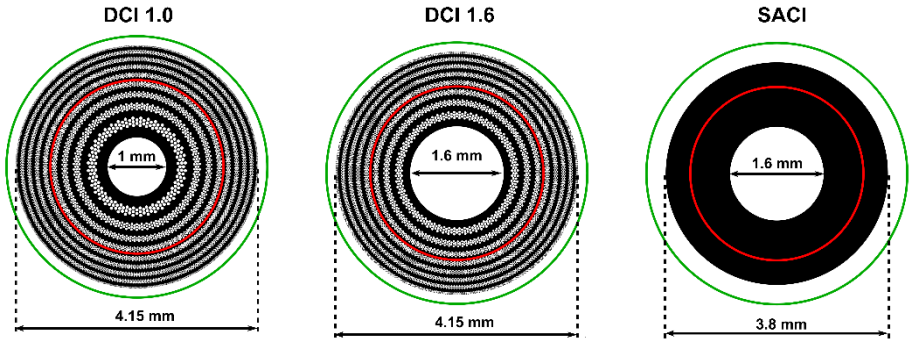

Figure 2: Design of the analyzed DCIs and the SACI

Focusing properties. Axial Irradiance

To evaluate the focusing properties of the DCIs, we first computed the axial irradiances provided by them in air under monochromatic illumination for a wavelength of 555 nm using the Fresnel approximation [10]. Figure 2 shows the results, computed for CIs with external pupils of 3.0 mm and 4.5 mm diameter (see the red and green circles in Fig. 1). As can be seen, the profile of the DCIs is clearly bifocal while that of the SACI is, as expected, of a typical extended focus one. Note also that both DCIs have a more intense focus than the SACI in distant vision (zero defocus).

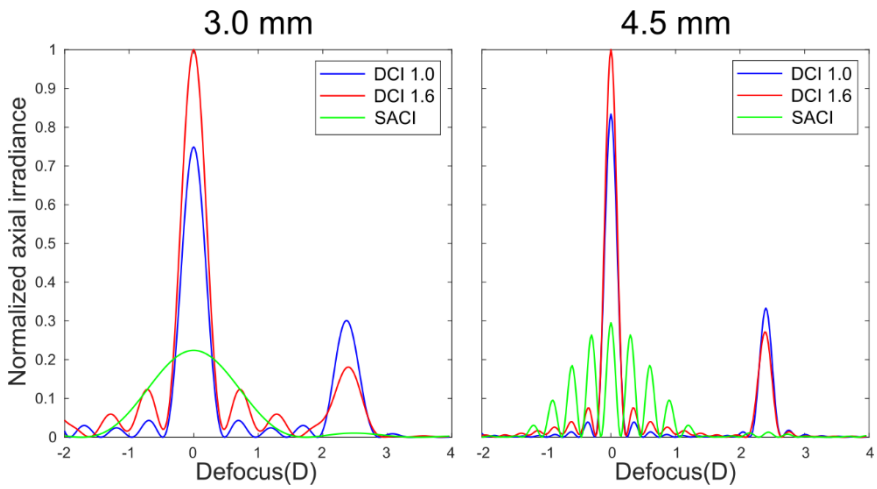

Figure 3: Normalized axial irradiances of the three CIs for pupil diameters of 3.0 mm (left) and 4.5 mm (right).

MTFs y AMTFs

The MTFs and AMTFs of the inlays have been calculated using the ZEMAX ™ OpticStudio software, in which two theoretical eye models have been

implemented: the Liou-Brennan Model Eye (LBME) [Liou97] and the Zemax Model Eye (ZME) [Internet19b].

The ZME is an eye model included in the software package. Table 1 shows the data sheet used for the simulations with the ZME.

Surface	Radius (mm)	Asphericity	Thickness (mm)	Refractive index
Anterior Cornea	7.80	-0.50	0.200	1.377
Anterior CI	7.80	-0.50	0.005	1.377
Posterior CI	7.80	-0.50	0.315	1.377
Posterior Cornea	6.70	-0.30	3.100	1.337
Iris	-	-	0.100	1.337
Anterior Lens	10.00	0.00	3,700	1,420
Posterior Lens	-6.00	-3,25	16.580	1.336

Table 1: Parameters of ZME

The LBME is one of the most popular theoretical models because it has the most realistic biometrical data obtained from 45 years old people (young presbyopes). It takes into account the alpha angle [Liou97] (the angle between the visual axis and the optical axis), the 0.5 mm nasal displacement of the pupil, and the gradient refractive index of the crystalline lens. Its optical parameters, are shown in Table 2. The major difference between both models relies in the corneal asphericities (Q) that induces different values for the spherical aberration (SA) in each eye.

In these models eyes, both DCIs and the SACI, have been inserted virtually at a distance of 200 µm from the anterior surface of the cornea, simulating the surgical procedure of the SACI [Moarefi17]. In the simulation in Zemax, the inlays have been introduced as *uda* (user defined aperture) files. To simulate a thickness of 5 µm for the CIs, two CI surfaces were introduced into each eye model, as can be seen in Tables 1 and 2. The CIs were centered on the visual axis of each model eye.

Surface	Radius (mm)	Asphericity	Thickness (mm)	Refractive index
Anterior Cornea	7.77	-0.18	0.200	1.376
Anterior CI	7.77	-0.18	0.005	1.376
Posterior CI	7.77	-0.18	0.295	1.376
Posterior Cornea	6.40	-0.60	3.16	1.336
Iris	-	-	0.00	-
Anterior Lens	12.4	-0.94	1.59	$1.368 + 0.049057\ z - 0.015427\ z^2 - 0.001978\ r^2$
Posterior Lens	Infinity	-	2.43	$1.407 - 0.006605\ z^2 - 0.001978\ r^2$

Table 2: Parameters of LBME, the pupil is decentered 0.5 mm nasally and the incidental beams have an angle of entry of 5°

The MTFs have been calculated for the far and near foci, and also for different vergences between +0.50 D and -3.50 D in steps of 0.10 D, in order to calculate the AMTF. The AMTFs have been obtained integrating the MTF values for a frequency range from 9.49 to 59.86 cycles per degree (cpd), corresponding to visual acuities (VA) between 0.5 logMAR and -0.2 logMAR respectively. All calculations were obtained with a wavelength of 555 nm.

Figure 3 shows the MTFs at the far and near foci for 3.0 mm pupils. As can be seen, both model eyes predict a similar behavior for the three CIs in both far and near foci. It should be mentioned that for the LBME the represented MTFs in Figure 3 are computed as the mean values between the sagittal and the tangential MTF curves. In addition, as explained in previous sections, the higher internal diameter of the DCI 1.6 causes that a higher amount of light focuses on the far distance image with respect to the DCI 1.0. For this reason, the MTF at the far focus of the DCI 1.6 is the better one. The opposite is true for the near focus, while SACI theoretically presents an extended focus, as can be seen in the AMTF, it does not have a defined focus for near vision. In contrast, the diffractive profile of the DCIs generates the near focus that can be seen in the Figure 3c. The MTF for the near vision focus of DCI 1.0 is better than for DCI 1.6 because the total area of the inlay is higher. On the other hand, differences between both eye models are hardly observed, because for a 3.0 mm pupil the influence of the LBME asymmetry and the SA are both minimal.

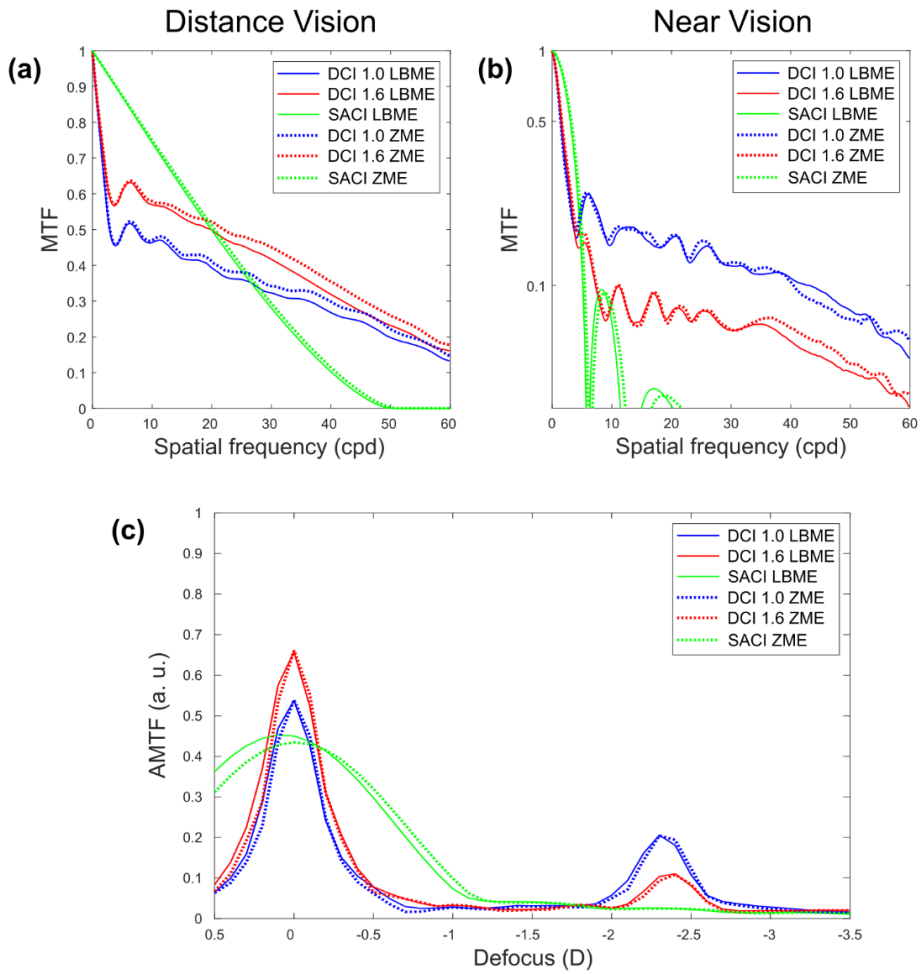

Figure 4: 3.0 mm pupil: (a) MTF distance vision, (b) MTF near vision, and (c) AMTF for different defocus conditions of the three CIs: DCI 1.0 (blue), DCI 1.6 (red) and SACI (green) for LBME (continuous lines) and ZME (dashed lines)

Figure 4 shows the same merit functions as in Figure 3, but calculated for 4.5 mm pupils. The influence of the SA on the eye models can be seen in Figure 4c. While the AMTFs of the three CIs in the ZME maintain their focus of vision at distance (zero defocus), in the LBME the AMTFs peaks of the far focus are shifted 0.1 D due to the influence of the SA; however, in the near focus this effect is not so obvious. It is important to note the effect of the pupil size on the depth of focus of the inlays. As can be seen in the comparison between Figure 3c and 4c, the AMTF of both ICDs is less affected than the AMTF of the SACI, since for the latter the depth of focus is severely reduced.

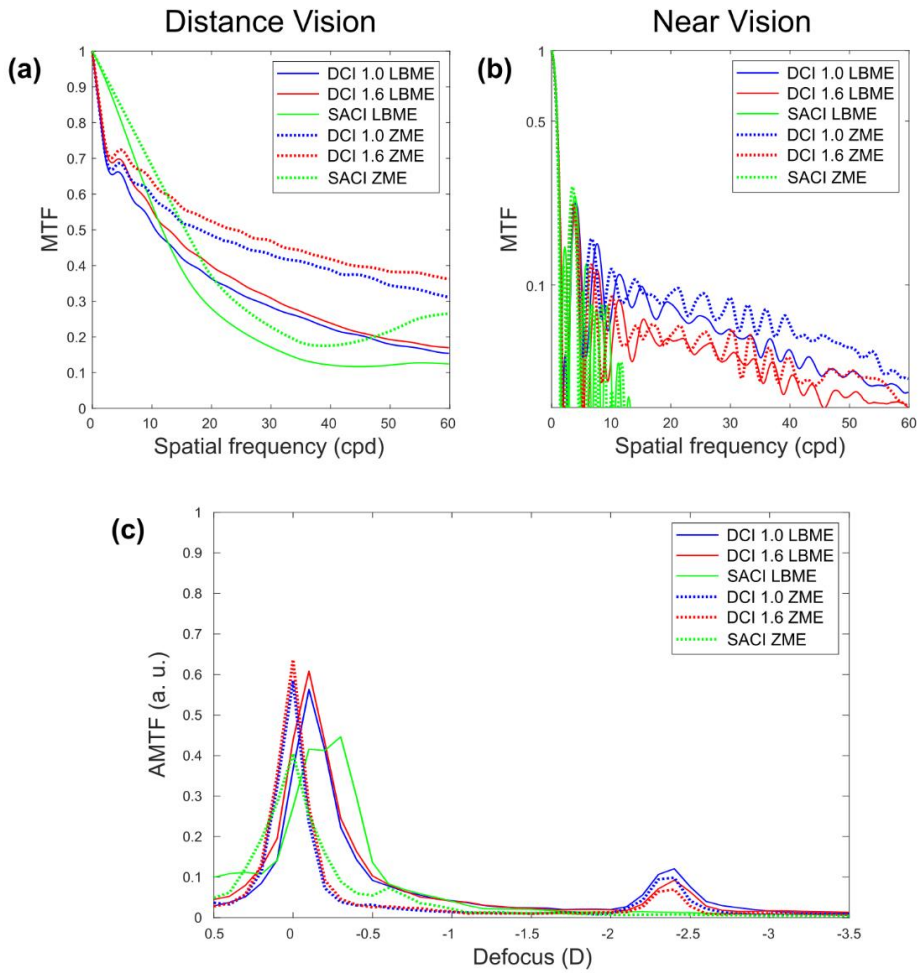

Figure 5: 4.5 mm pupil: a) MTF distance vision, (b) MTF near vision, and (c) AMTF for different defocus conditions of the three CIs: DCI 1.0 (blue), DCI 1.6 (red) and SACI (green) for LBME (continuous lines) and ZME (dashed lines)

PSF and image simulation.

As stated above, the PSF describes the ability of an optical system (in our case an eye model with a CI) to form a good image of a point source. An ideal PSF corresponds to a diffraction-limited system and is known as the Airy disk, with a high intensity central peak, which is more or less concentrated depending on the pupil size. For real systems the PSF spreads out, as more extended is the PSF, the system is worse.

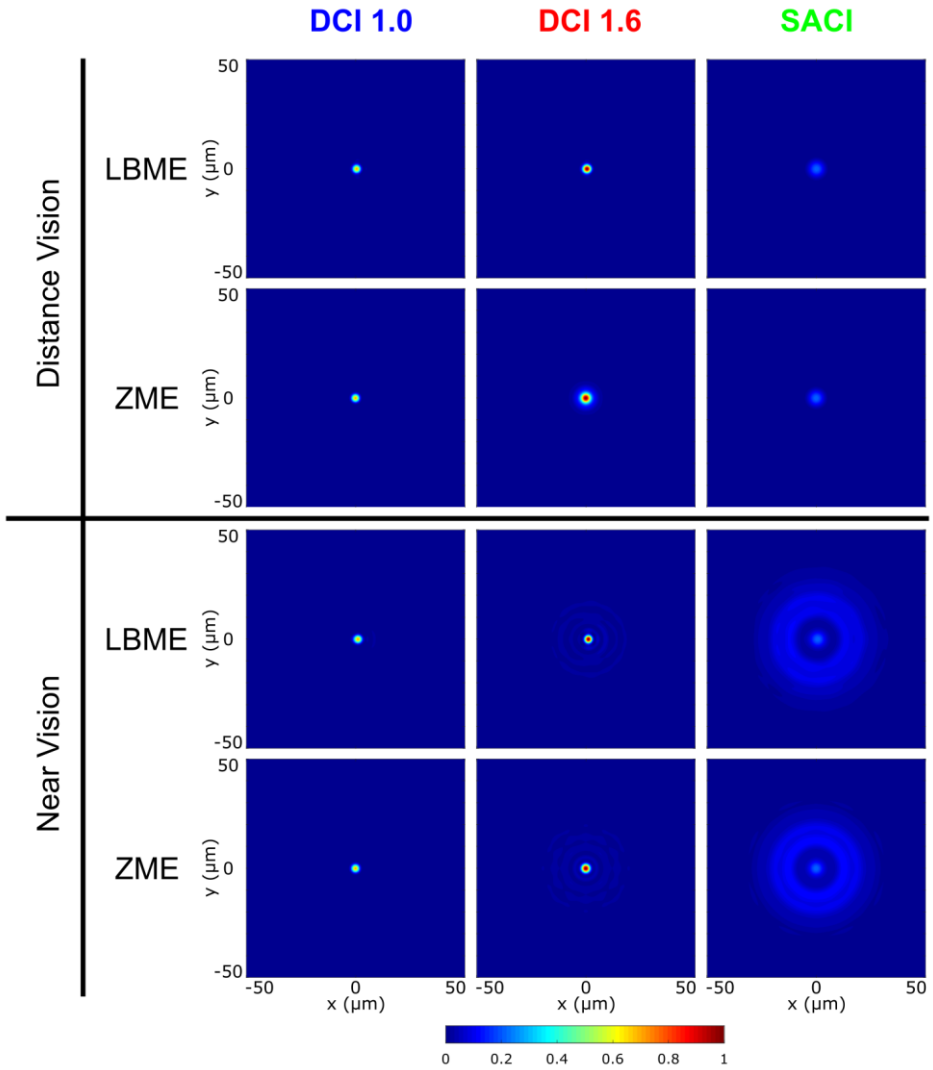

Figure 6: PSFs normalized to the maximum of each triplet of CIs for pupil of 3.0 mm in distance vision (top) and near vision (bottom).

Figures 5 and 6 show the PSFs obtained for the 3.0 mm and 4.5 mm pupils respectively of the three ICs in both eye models. PSFs calculated with ZEMAX were weighted according to the axial irradiances calculated in section 3 for each CI. Considering that foci in distance and in near vision have different range intensities, different normalizations were performed in order to compare them. In this way, the PSFs at the far and near foci are normalized to the maximum of value of the DCI 1.6 PSF in the ZME, and the PSFs of the near vision focus are normalized to the maximum of the PSF of the near focus DCI 1.6 of the ZME in each focus respectively. This means that in Figures 5 and 6 can be only

compared the eye models of the three CIs in each focus, but far and near PSFs have different normalizations.

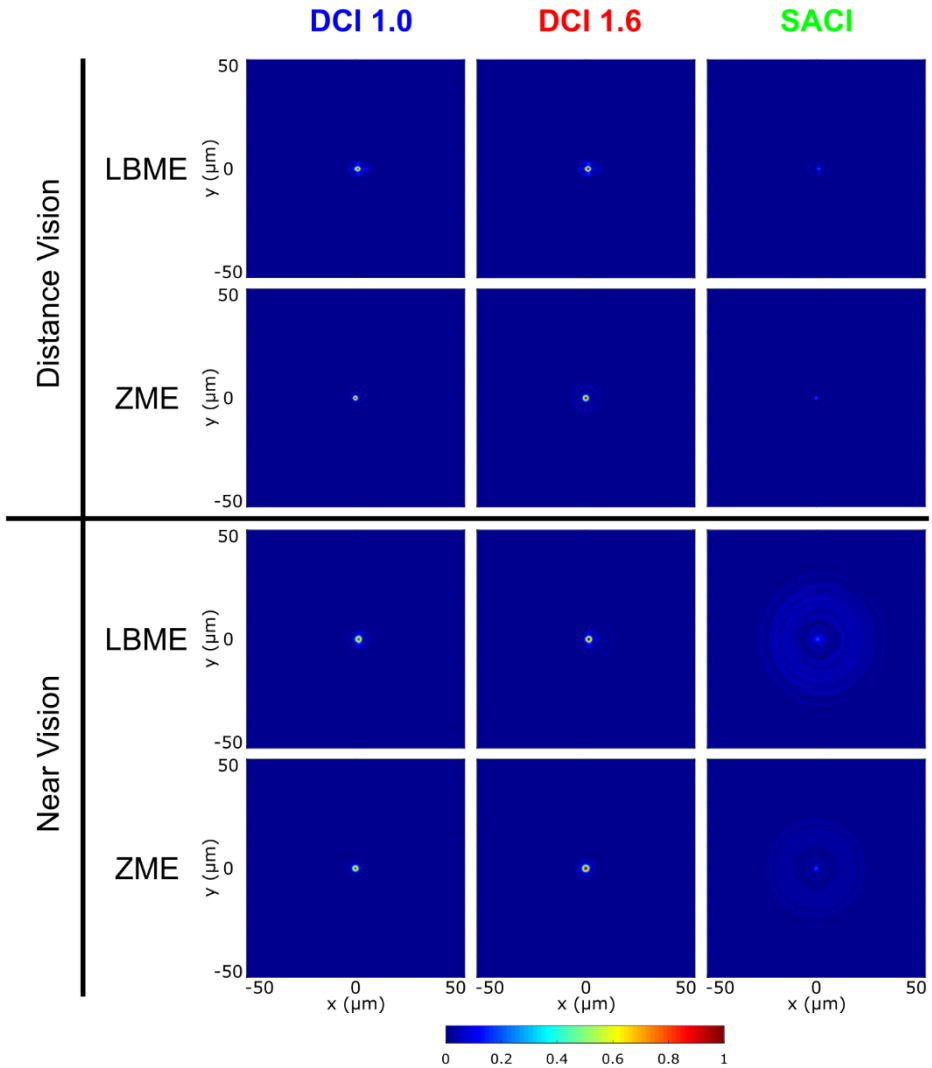

Figure 7: PSFs normalized to the maximum of each triplet of CIs for pupil of 4.5 mm in distance vision (top) and near vision (bottom).

Figure 5 shows that, for both the LBME and the ZME in distance vision, DCI 1.6 has a more intense focus than the other two CIs, but it has a slightly wider peak than DCI 1.0. In near vision the same trend is shown, the maximum of the DCI 1.6 is higher than that of the other two CIs, but its surrounding halo is also more extended. Note that the SACI has an even greater halo. For 3.0 mm pupil at near vision the first impression is that the PSF for DCI 1.6 is better than the one for DCI 1.0; however, it should be borne in mind that while the maximum value of the

first one is the unity, the energy is very dispersed (the halo). In DCI 1.0 although the maximum is less than 0.802, the energy is more concentrated and therefore the PSF is better. The explanation of why the PSF of DCI 1.6 is globally better is simple: the diffraction efficiency of DCI 1.6 is better, focusing more light on the near vision focus. On the other hand, as expected, for 3.0 mm pupil diameter the CIs performance is similar in both eye models.

Figure 6 shows the same composition as Figure 5 but with the 4.5 mm pupil. As we explained before, by increasing the pupil diameter the influence of SA is higher on each eye model. On the one hand, a focal shift is produced, as already shown in Figure 3c, and on the other hand, the shape and height of the PSF is also affected. The comparison of the performance of both eye models for 4.5 mm pupil diameter shows more noticeable differences than those observed with the small pupil. In all cases, the LBME has more extended and asymmetrical halos than ZME. This is due to the influence of the SA, and also, to the asymmetry of the LBME.

Finally, after the quantitatively comparison of the merit functions for the three CIs, images of an optotype chart have been simulated. To this end, the PSFs obtained from ZEMAX were normalized to their respective maximum values, and then, weighed by the axial irradiances of each IC calculated in section 3. These normalized and weighted PSFs, were convolved with Landolt C optotypes corresponding to three different values of VA: 0.4 logMAR, 0.2 logMAR and 0.0 logMAR.

Figures 7 and 8 show simulated images for 3.0 mm and 4.5 mm pupil diameters, respectively. For 3.0 mm pupil, it can be seen that while the DCIs have a greater contrast than the SACI, the resolution of the three ICs is similar because the extension of the corresponding PSFs are almost the same (see Fig.5). At the near focus it is observed that there is no focus on SACI, but in DCI 1.0 although the contrast is lower, the resolution is higher and the halo is smaller than for DCI 1.6. When comparing the performance of the eye models, as already mentioned, there are no significant differences because when using a small pupil, the influence of high-order aberrations is minimal.

The simulated images for 4.5 mm pupil are shown in Figure 8. It can be seen that the differences between the eye models are most noticeable, mainly in the halos in near vision. The halos of the ZME are symmetrical while those of the LBME are not. Despite these differences, the behavior of the three CIs maintains the same trend. The images at the foci for both DCIs are comparable in contrast and definition. The reason that they resemble for distance vision is because with a large pupil part of the light that passes outside the inlays (external diameter of 4.15 mm), goes to the far focus. Therefore, the intensities ratio between the far and near foci increases and are similar for both DCIs.

By comparing both pupils, the best foci in the distance are for the DCIs with 4.5 mm pupil. The best focus for near vision is the DCI 1.0 since it presents more diffractive rings contributing to the near focus.

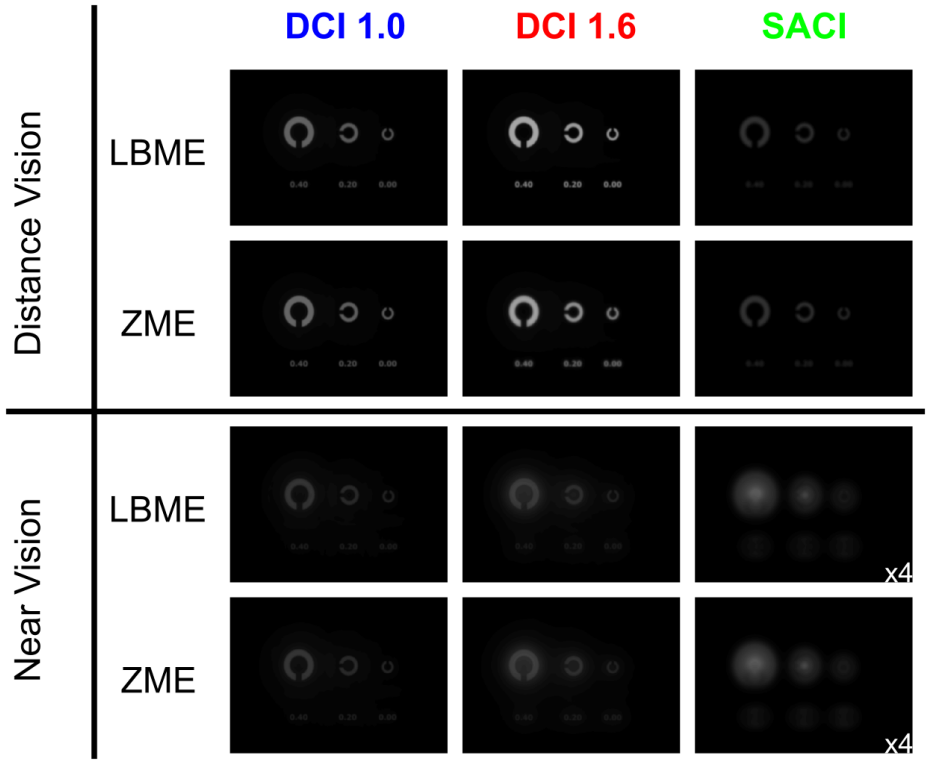

Figure 8: Image simulation for 3.0 mm of pupil in distance vision (top) and near vision (bottom) for the three CIs in the two model eyes. The intensity of the image simulation of SACI in near vision has been multiplied x4.

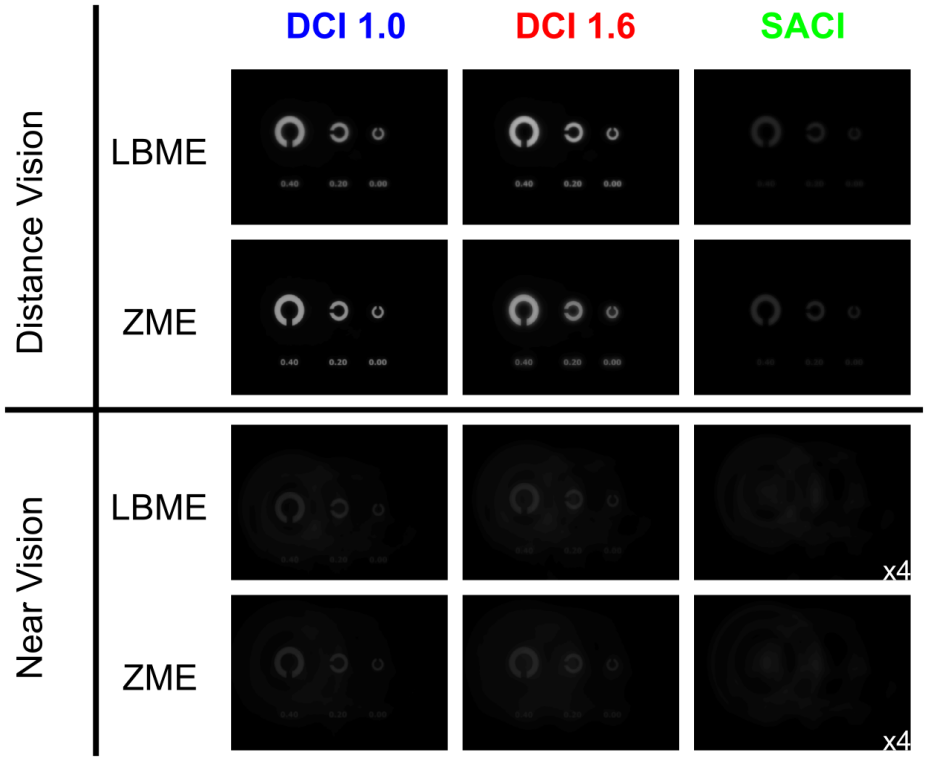

Figure 9: Image simulation for 4.5 mm of pupil in distance vision (top) and near vision (bottom) for the three CIs in the two model eyes. The intensity of the image simulation of SACI in near vision has been multiplied x4.

Conclusions

We have demonstrated that both DCIs designs have a clearly bifocal profile due to their diffractive nature. Moreover, they also have a better MTFs and AMTFs than the SACI, (see Figures 3 and 4). The results presented in this chapter confirm the versatility of the DCI design because, opposite at what happens for the SACI which only presents a fixed depth focus, the distribution of the holes in the DCI can be modified (customized) to alter the relationship between the far and near vision foci. It is also verified that while for the 3.0 mm pupil, the three CIs have a similar behavior in both eye models, for 4.5 mm the differences are more due to the high order aberrations of each model.

The PSFs show the differences between each CI for each situation, on the one hand, the DCIs generally show higher peaks and a high energy concentration, less extension of the PSF, but higher than SACI. These results can be clearly appreciated in the simulated images shown in Figures 7 and 8.

In summary, the DCI is a diffractive CI that combines the principle of operation of the small aperture inlay, for the central hole, with the diffraction generated by the micro-holes in the ring to generate a focus in near vision. The micro holes allow the construction of a single-piece inlay able to be inserted into the corneal stroma allowing nutrients to pass through it. The results show the higher light throughput of the DCI as compared with the SACI, in addition to better PSFs and simulated images. In addition, we have demonstrated the differences that can be obtained in results (light distribution between the foci) depending on the design of a DCI allowing to customize the CI for each patient based on their visual needs.

However, since it is a numerical simulation work with a ray tracing program, studies in an optical bench and clinical trials with contact lenses, that include the structure of the DCIs, should be carried out in a future.

Acknowledgments

Funding: Ministerio de Economía y Competitividad (DPI2015-71256-R); Generalitat Valenciana (PROMETEO/2019/048).

D. Montagud-Martínez and V. Ferrando acknowledge the financial support from the Universitat Politècnica de València, Spain (fellowships FPI-2016 and PAID-10-18, respectively).

Conflicts of Interest

The authors declare that there is no conflict of interest regarding the publication of this paper

References

[Andersen05] Andersen G. Large optical photon sieve. Opt Lett, OL. 2005;30(22):2976–8.

[Arlt15] Arlt E, Krall E, Moussa S, Grabner G, Dexl A. Implantable inlay devices for presbyopia: the evidence to date. Clin Ophthalmol. 2015;9:129–37.

[Artal17] Artal P. Handbook of Visual Optics, Two-Volume Set. CRC Press; 2017. 856 p.

[Castro18] Castro JJ, Ortiz C, Jiménez JR, Ortiz-Peregrina S, Casares-López M. Stereopsis Simulating Small-Aperture Corneal Inlay and Monovision Conditions. J Refract Surg. 2018;34(7):482–8.

[Charman14] Charman WN. Developments in the correction of presbyopia II: surgical approaches. Ophthalmic Physiol Opt. 2014;34(4):397–426.

[Furlan17] Furlan WD, García-Delpech S, Udaondo P, Remón L, Ferrando V, Monsoriu JA. Diffractive corneal inlay for presbyopia. J Biophotonics. 2017;10(9):1110–4.

[Garza13] Garza EB, Gomez S, Chayet A, Dishler J. One-year safety and efficacy results of a hydrogel inlay to improve near vision in patients with emmetropic presbyopia. J Refract Surg. 2013;29(3):166–72.

[Gilchrist87] Gilchrist J, Pardhan S. Binocular Contrast Detection with Unequal Monocular Illuminance*. Ophthalmic and Physiological Optics. 1987;7(4):373–7.

[Giménez06] Giménez F, Monsoriu JA, Furlan WD, Pons A. Fractal photon sieve. Opt Express, OE. 2006;14(25):11958–63.

[Internet19a] KAMRA Inlay Restores Reading Vision [Internet]. [cited 2019 Aug 14]. Available from: https://kamra.com/

[Internet 19b] Zemax OpticStudio Knowledgebase—Zemax [Internet]. [cited 2019 Aug 14]. Available from: https://customers.zemax.com/os/resources/learn/knowledgebase/zemax-models-of-the-human-eye.

[Kipp01] Kipp L, Skibowski M, Johnson RL, Berndt R, Adelung R, Harm S, et al. Sharper images by focusing soft X-rays with photon sieves. Nature. 2001;414(6860):184–8.

[Limnopoulou13] Limnopoulou AN, Bouzoukis DI, Kymionis GD, Panagopoulou SI, Plainis S, Pallikaris AI, et al. Visual outcomes and safety of a refractive corneal inlay for presbyopia using femtosecond laser. J Refract Surg. 2013;29(1):12–8.

[Lindstrom13] Lindstrom RL, Macrae SM, Pepose JS, Hoopes PC. Corneal inlays for presbyopia correction. Curr Opin Ophthalmol. 2013;24(4):281–7.

[Liou97] Liou H-L, Brennan NA. Anatomically accurate, finite model eye for optical modeling. J Opt Soc Am A, JOSAA. 1997;14(8):1684–95.

[Machado17] Machado FJ, Monsoriu JA, Furlan WD. Fractal light vortices. In: Chapter from the Book Vortex Dynamics and Optical Vortices. 1st ed. Intech; 2017. 257 p.

[Menon05] Menon R, Gil D, Barbastathis G, Smith HI. Photon-sieve lithography. J Opt Soc Am A, JOSAA. 2005;22(2):342–5.

[Moarefi17] Moarefi MA, Bafna S, Wiley W. A Review of Presbyopia Treatment with Corneal Inlays. Ophthalmol Ther. 2017;6(1):55–65.

[Plainis13] Plainis S, Petratou D, Giannakopoulou T, Radhakrishnan H, Pallikaris IG, Charman WN. Small-aperture monovision and the Pulfrich experience: absence of neural adaptation effects. PLoS ONE. 2013;8(10):e75987.

[Vilupuru15] Vilupuru S, Lin L, Pepose JS. Comparison of Contrast Sensitivity and Through Focus in Small-Aperture Inlay, Accommodating Intraocular Lens, or Multifocal Intraocular Lens Subjects. Am J Ophthalmol. 2015;160(1):150-162.e1.

[Vukich18] Vukich JA, Durrie DS, Pepose JS, Thompson V, van de Pol C, Lin L. Evaluation of the small-aperture intracorneal inlay: Three-year results from the cohort of the U.S. Food and Drug Administration clinical trial. J Cataract Refract Surg. 2018;44(5):541–56.

[Waring11] Waring GO. Correction of presbyopia with a small aperture corneal inlay. J Refract Surg. 2011;27(11):842–5.

[Yilmaz08] Yilmaz OF, Bayraktar S, Agca A, Yilmaz B, McDonald MB, van de Pol C. Intracorneal inlay for the surgical correction of presbyopia. J Cataract Refract Surg. 2008;34(11):1921–7.

2.4. Imaging performance of a diffractive lens implanted in the human cornea

Journals & Magazines > IEEE Access > Volume: 7

Imaging Performance of a Diffractive Corneal Inlay for Presbyopia in a Model Eye

Publisher: IEEE | Cite This | PDF

5 Author(s) Diego Montagud-Martínez ; Vicente Ferrando ; Federico Machado ; Juan A. Monsoriu ; Walter D. Furlan All Authors

73 Full Text Views

Open Access Comment(s)

Under a Creative Commons License

Abstract

Document Sections

I. Introduction

II. Methods

III. Results

IV. Discussion and Conclusion

Authors

Figures

References

Abstract:
In this work we evaluated the imaging properties of the Diffractive Corneal Inlay (DCI), a novel type of corneal implant working by diffraction that we proposed for the treatment of presbyopia. ZEMAX OpticStudio software was employed for the numerical assessment, with simulations performed in a human-based eye model. In the ray tracing analysis, we used the Modulation Transfer Function (MTF), the Area under the MTF (AMTF), and the Point Spread Function (PSF). The theoretical performance of the DCI under different situations was evaluated in comparison with a commercially available pinhole based corneal inlay. Finally, real images were obtained experimentally in vitro in a model eye with inlays prototypes. The obtained results allow to state that the DCI exhibits a very high light throughput, improved imaging capabilities for far and near objects, and robustness against decentrations.

Topic: Advanced Optical Imaging for Extreme Environments

Published in: IEEE Access (Volume: 7)

Page(s): 163933 - 163938 **INSPEC Accession Number:** 19144258

2.4. Imaging performance of a diffractive lens implanted in the human cornea

Diego Montagud-Martínez[1], Vicente Ferrando[1], Federico Machado[1], Juan A. Monsoriu[1] y Walter D. Furlan[2*]

1 Centro de Tecnologías Físicas, Universitat Politècnica de València, 46022 Valencia, Spain.

2 Departamento de Óptica y Optometría y Ciencias de la Visión, Universitat de València, 46100 Burjassot, Spain.

* walter.furlan@uv.es

Abstract

In this work we evaluated the imaging properties of the Diffractive Corneal Inlay (DCI), a novel type of corneal implant for the treatment of presbyopia, which based on the diffraction phenomena. ZEMAX OpticStudio software was employed for the numerical assessment, with simulations performed in a human-based complex eye model. In the ray tracing analysis, we used the Modulation Transfer Function (MTF), the Area under the MTF (AMTF), and the Point Spread Function (PSF). The theoretical performance of the DCI under different situations was evaluated in comparison with a commercially available pin-hole based corneal inlay. Finally, real images were obtained experimentally in vitro in a model eye with inlays prototypes. The obtained results allow to state that the DCI exhibits a very high light throughput, improved imaging capabilities for far and near objects, and robustness against decentrations.

Keywords: corneal inlays, diffractive lenses.

Introduction

The human eye is often considered as an optical instrument composed of two positive lenses made of transparent living tissue: the cornea and the crystalline lens. Opposite to many artificial optical systems, in which lenses are centered on the optical axis and separated by air, the eye is not a centered optical system since the ocular surfaces are not perfectly aligned. In addition, several tissues and fluids with different refractive indexes and internal structure are present in the way of light from the outside world to the retina. The light reaching the eye is first refracted by tear film and the cornea (a transparent compound tissue with several layers). Behind the cornea is the anterior chamber, filled with the aqueous humor. Next, the iris acts as a diaphragm with a pupil that limits the amount of light passing into the eye. The pupil size is variable, between 2 mm to 8 mm, depending mainly on the ambient light. The crystalline lens is located immediately behind the iris. It is a gradient-index lens, that can change its shape to modify its

optical power allowing the eye to focus on objects placed at different distances. This property (called accommodation) declines continuously with age until reaching presbyopia, a condition that makes harder to focus clearly on near objects. Finally, the space between the crystalline and the retina is filled with a transparent gel-like substance: the vitreous body.

Taking into account the above-mentioned brief description, the imaging process in the human eye is far from being considered as “conventional” by an optical engineer because of the complex environment in which this process takes place. In particular, a challenging problem for an optical engineer is the design of an optical device for the treatment of presbyopia. In conjunction with multifocal intraocular lenses, corneal inlays are one of the most recent advances in this field. These devices are implanted inside the cornea with a surgical procedure that includes the creation of ‘pockets’ by precise femtosecond lasers within the corneal stroma.

Based on their physical principles, corneal inlays can be classified into different categories: refractive inlays, small aperture inlays, and diffractive inlays. Refractive corneal inlays act locally at central part of the cornea either, by modifiying its curvature (Raindrop Near Vision inlay, ReVision Optics), or by altering the refractive index (Presbia Flexivue Microlens, Presbia Cooperatief) [Charman14, Arlt15]. A recent review of the corneal inlays currently used for the correction of presbyopia [Lindstrom13], concluded that refractive inlays are very limited, most likely because induce high order aberrations that result in decreased contrast sensitivity.

On the other hand, Small Aperture Corneal Inlays (SACIs) with the commercial name Kamra® (Acufocus, Inc.) are often used today owing to the positive outcomes achieved in improved uncorrected near and intermediate vision [Lindstrom13, Vilupuru15]. This device is simply an opaque disc made of a biocompatible material (polyvinylidene fluoride impregnated with carbon nanoparticles) with a central hole acting as pinhole-like aperture that produces an extended depth of focus. To facilitate the flow of nutrients to cells of the corneal stroma, it has a reduced external diameter, and more than 8,000 micro-pores, in a size range of 5–11 μm diameter. However, its reduced light throughput, forces its implantation only in the non-dominant eye creating a “modified monovision” situation [Charman14]; this added to the light randomly diffracted by the micro-holes across the implant, produce some drawbacks, including compromised distance visual acuity [Vukich18], a potential detrimental effect on the binocular summation ratio [Gilchrist87]. a marked interocular differences in visual latency and a Pulfrich effect. [Plainis13]. Other visual function compromised by this inlay is stereoacuity, which could suffer a deterioration with respect to natural conditions, especially for near and intermediate distances [Castro18].

In a recent paper [Furlan17], we have demonstrated that the diffraction intrinsically originated by the pores in the SACI can be harnessed to provide a

focus for near distance vision, in a similar fashion as a photon sieve [Kipp01, Giménez06] does. In practice, we have combined the photon sieve and the SACI pinhole-effect concepts to develop a novel class of corneal implants: the diffractive corneal inlays (DCIs). In this way, we were able to turn the negative diffractive effects of SACI from a disadvantage into a significant advantage, because the micro-holes in the DCI would not just permit the flow of nutrients, but also create a diffractive focus for near vision. Moreover, we announced that by optimizing the size and spatial distribution of the holes, different designs would be able to vary the addition and the relative intensity between near and far foci. In this way, this new type of prosthesis could allow doctors to customize the treatment of presbyopia. In that previous work, the focusing properties of the DCI were investigated, like a conventional diffractive optical element, analyzing its diffraction pattern in air by computing the Point Spread Function (PSF) along the optical axis in air using the Fresnel approximation. Experimental results of the axial PSF in free space propagation were also provided with a DCI simulated in a liquid crystal SLM. These preliminary results demonstrated that the DCI has a better performance than the SACI [Furlan17]. With these promising findings, the next step is to investigate the potential benefits in image formation by DCIs by means of merit functions that evaluate the eye's quality of vision in a more realistic environment. Therefore, the purpose of this study is to assess the image quality provided by an optimized version of the DCI, in comparison with the SACI in an accurate model eye. This model is especially suitable for this study for two main reasons: First, it reflects average biometrical data from a large group of individuals, incorporating a realistic amount of spherical aberration and a grin based model crystalline lens [Liou97, Bakaraju08]. Second, it takes into consideration the angle kappa, the angle between the line of sight and the pupillary axis, which is fundamental to explore the robustness of our proposal against decentrations for different pupil diameters. In fact, for the SACI it was demonstrated that the centration of the inlay is critical to achieve good vision [Tabernero12]. Finally, in order to confirm our theoretical predictions, experimental results were also obtained with a model eye mounted in an optical bench in accordance with the ISO 11979-9 Standard.

Methods

Corneal inlays

The DCI model evaluated in this study consisted in a disk of 4.15 mm diameter with a central hole of 1.00 mm diameter surrounded by 8 rings conformed by a total of 6395 holes of different size, being the smallest ones of 11 μm diameter. It was designed to provide a near diffractive focus corresponding to a nominal addition of +2.50 D. For comparison, a completely opaque SACI with the dimensions of the Kamra® has been evaluated in parallel with ZEMAX. Sketches of the evaluated DCI and SACI are shown in Fig. 1. The thickness of both inlays were assumed as 5 μm.

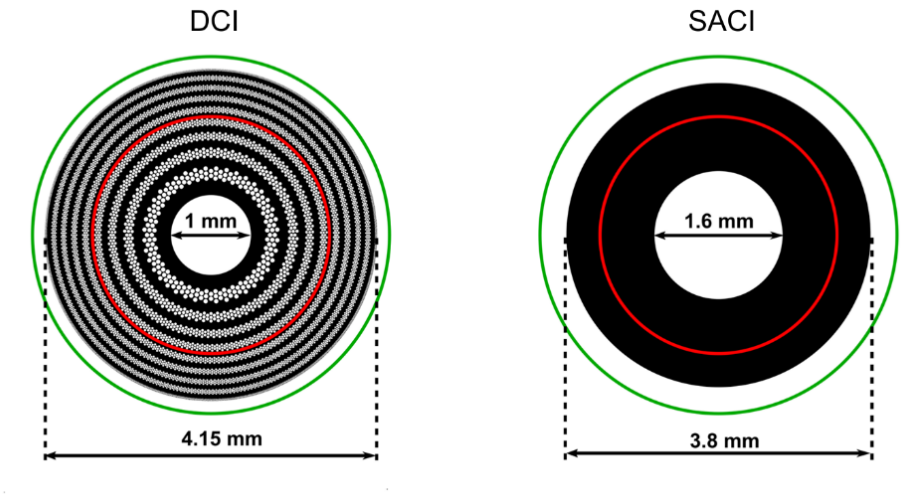

Figure 1: Diagrams of the corneal inlays evaluated in this study. The red and green circles represent 3.0 mm and 4.5 mm pupil diameters respectively.

Numerical Methods

Zemax OpticStudio design software (version 18.7, LLC, Kirkland, WA, USA) was employed to simulate the effects of both inlays in the Liou-Brennan model eye. This model eye is characterized by aspheric corneal elements; a gradient index crystalline lens; a decentered iris pupil (0.50 mm in the nasal direction); and a tilted visual axis, (5 degrees relative to the optical axis) [Liou97]. The model data is shown in Table 1. The inlays were located in the model eye at 0.25 mm from the anterior corneal surface as “User Defined Apertures” (uda file). In the simulations, the same values for the radius of curvature and for the asphericity of the anterior corneal surface were considered for both inlays. The original version of the Liou–Brennan model eye did not have a value for the retinal curvature. However, considering that the curvature of the retina may have an impact on image quality with inlay decentration, in this work we have included the retina with a -12 mm radius. Two different pupils (iris) diameters were evaluated: 3.0 mm and 4.5 mm (emulating photopic and mesopic conditions). To better appreciate the sensitivity of the inlays to decentration, we assumed monochromatic spatially incoherent light with a wavelength of 555 nm, corresponding to the highest sensitivity of the human eye in photopic vision [Gross08].

Surface	Radius (mm)	Asphericity	Thickness (mm)	Refractive index
Anterior Cornea	7.77	-0.18	0.200	1.376
Anterior CI	7.77	-0.18	0.005	1.376
Posterior CI	7.77	-0.18	0.295	1.376
Posterior Cornea	6.40	-0.60	3.16	1.336
Iris	-	-	0.100	1.337
Anterior Lens	12.4	-0.94	1.59	1.368 + 0.049057 z − 0.015427 z2 − 0.001978 r2
Posterior Lens	Infinity	-	2.43	1.407 − 0.006605 z2 − 0.001978 r2
Retina	-8.10	0.96	16.26	1.336

Table 1: Liou-brennan model eye Zemax data sheet (r and z are radial and axial coordinates in the crystalline lens)

In fact, two conditions were considered: first, the inlays were centered on the visual axis (line of sight) [Schwiegerling13] at the inlay plane, and, second, the inlays were decentered of 0.8 mm towards the temporal direction. The MTF feature of the Zemax OpticStudio was employed to calculate the MTF at the retina for different object vergences. Due to the asymmetry of the model eye, the MTFs in tangential and sagittal directions were different; thus, to obtain a simple measure for the image quality, the arithmetic mean between the tangential and sagittal MTFs was considered. The position of the retina remained the same for all MTF calculations.

Experimental Procedure

The optical performance of the DCI was experimentally tested in vitro with a custom made image forming system using an ISO eye model [ISO14]. To this end, the inlays, were printed on graphic films (standard polyester films) using a photoplotter with 5080 lpi resolution. In the optical setup, whose description and performance have been described in detail elsewhere [Calatayud13], the illumination system consisted of a white LED with a band-pass filter (wavelength 560 ±10 nm) placed behind it to obtain monochromatic images. The test object (1951 USAF resolution test chart) was located in front of an achromatic lens of focal length 160 mm, acting as Badal lens to simulate distance and near vergences. The artificial presbyopic eye was constructed with an achromatic doublet acting as artificial cornea and a wet cell in which a monofocal 10 D intraocular lens (AIALA model F551250; AJL Ophthalmic SA; Álava, Spain) [Furlan16], was located. Two different lens holders with diameters 3.0 mm and

4.5 mm were employed as artificial pupils. In the experiment, the printed inlays were located just in front of the cornea lens. An 8-bit CMOS camera (EO-5012C; Edmund Optics, Illinois, USA); attached to an X5 microscope (focused on the far focal plane of the intraocular lens) was used to capture the image of object for two different vergences.

Results

The results of the MTFs computed for the DCI and SACI inlays are shown in Figure 2. The MTFs for distance focus show that in the range of spatial frequencies from 30 cpd to 60 cpd, which correspond to high rates of visual acuity, the MTF values for the DCI are higher than the SACI for both, centered and decentered conditions. On the other hand, for the near focus, the MTF for the SACI drops to zero. In this case, the MTFs was represented in logarithmic scale from 0.03 to 1 to enhance differences between centered and decentered conditions for the DCI. At this point it is important to note that the harmful diffraction effects produced by the microholes in the SACI were not taken into account. In fact, diffracted light by the pores (5% of the total) would worsen even more the results for the SACI MTFs. [Charman19]. As can be seen, the DCI is more robust against decentrations than SACI. Note that for the distance focus the curve for the SACI drops with the decentration for 3 mm pupil but grows for 4.5 mm pupil. This effect is due to the light that reach the retina coming from the outer part of the annulus. However, in this case the depth of focus is highly reduced [Atchison16]. This result can be better appreciated in the AMTF shown in Fig.3.

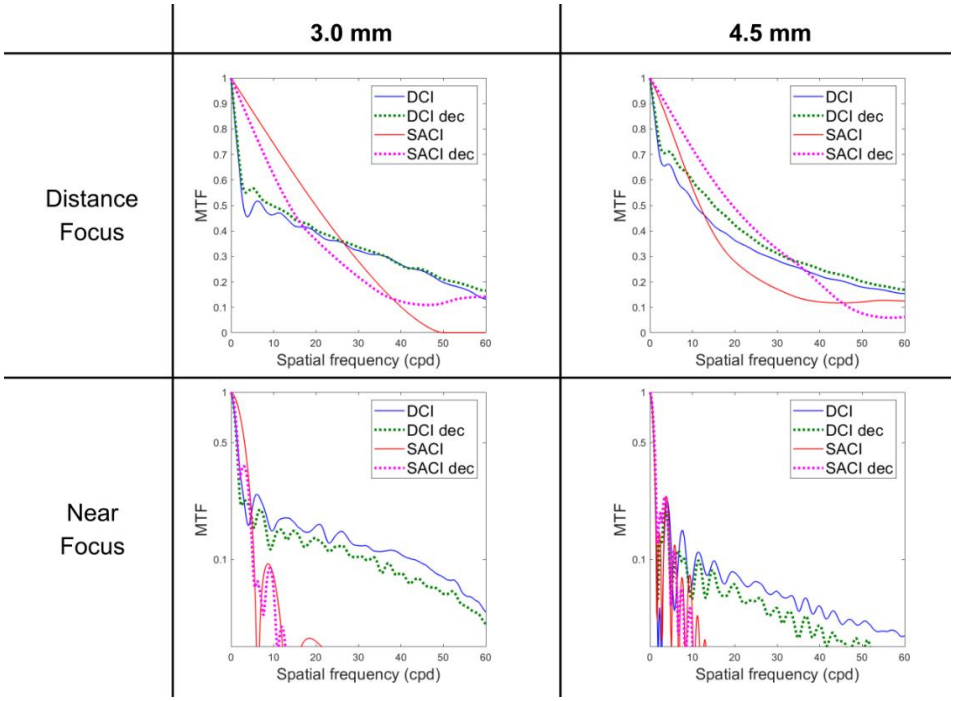

Figure 2: MTFs for distance and near objects. DCI and SACI curves correspond to the inlays centered on the visual axis. "DCI dec" and "SACI dec" correspond to the inlays decentered 0.8 mm towards the temporal direction.

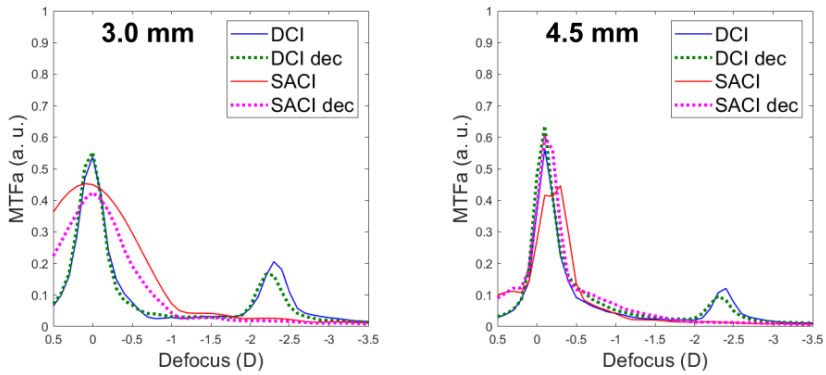

Figure 3: Through the focus AMTFs. DCI and SACI curves correspond to the inlay centered on the visual axis. "DCI dec" and "SACI dec" correspond to the inlays decentered 0.8 mm towards the temporal direction.

The AMTF was computed for different object vergences between +0.5 to −3.5 D (in 0.1D steps), and for spatial frequencies in the range: 9.5 cpd to 59.9 cpd. These frequencies correspond, approximately, to visual acuities between 0.5 logMAR and -0.2 logMAR (assuming that a logMAR of 0 is equivalent to a retinal spatial frequency of 30 cpd and that scale invariance holds). Note that, as

expected [Tabernero12], the depth of focus of the SACI is very sensitive to both, decentration and pupil diameter. On the contrary, the DCI globally maintains the typical bifocal shape with a little drop at the near focus for 4.5 mm pupil. However, as we will see next, this effect is partially compensated by the increase in the light throughput with this pupil diameter. Another useful metric we employed for the comparison of both inlays was the PSF. Moreover, from the PSF provided by ZEMAX, we obtained simulated images of a high contrast visual acuity test chart, by means of the numerical convolution, using a custom Matlab code (Mathworks, Inc. R2018b). Figures 4 and 5 show the PFSs provided by the model eye virtually implanted with both inlays for point objects at far and near distances with two pupil diameters. In these figures, the corresponding simulated images of a high contrast tumbling E chart, with letter sizes corresponding to 0.4 logMAR, 0.2 logMAR and 0 logMAR visual acuities are shown next to the corresponding PSF. The simulated images were obtained as the convolution of the PSF (normalized to the maximum value for each pupil diameter) with the optotype. To obtain the images, after the normalization we imposed the condition of image energy conservation by setting to 1 the sum value of each PSF frame. Then each PSF was weighted by its theoretical relative intensity [Furlan17]. In this way, the relative intensity of the images can be directly compared. Figure 4 shows the results for both inlays centered. As can be seen, the PSF for the DCI is better than the PSF for the SACI in all situations. Note also the different contrast in the images of optotypes, which is a consequence of the relative light throughput of the inlays. With a 3 mm pupil diameter the SACI acts as a circular aperture, but as the pupil diameter increases, additional light enters through the iris aperture producing the halo that is clearly appreciated in the PSFs. Note that in the plots of the PSF at near the scale was extended to 200 microns to show the extension of the halos. In the image of the SACI at near the intensity was multiplied by a factor of 4, because otherwise this (defocused) image would not be noticeable. It can be verified that for near objects, the eye with the SACI does not resolves the letters of 0.4 logMAR. For 3.0 mm pupil there is a kind of contrast inversion in the image that could help the patient to identify the letters, but for a large pupil the visual acuity decreases, and this would no longer possible.

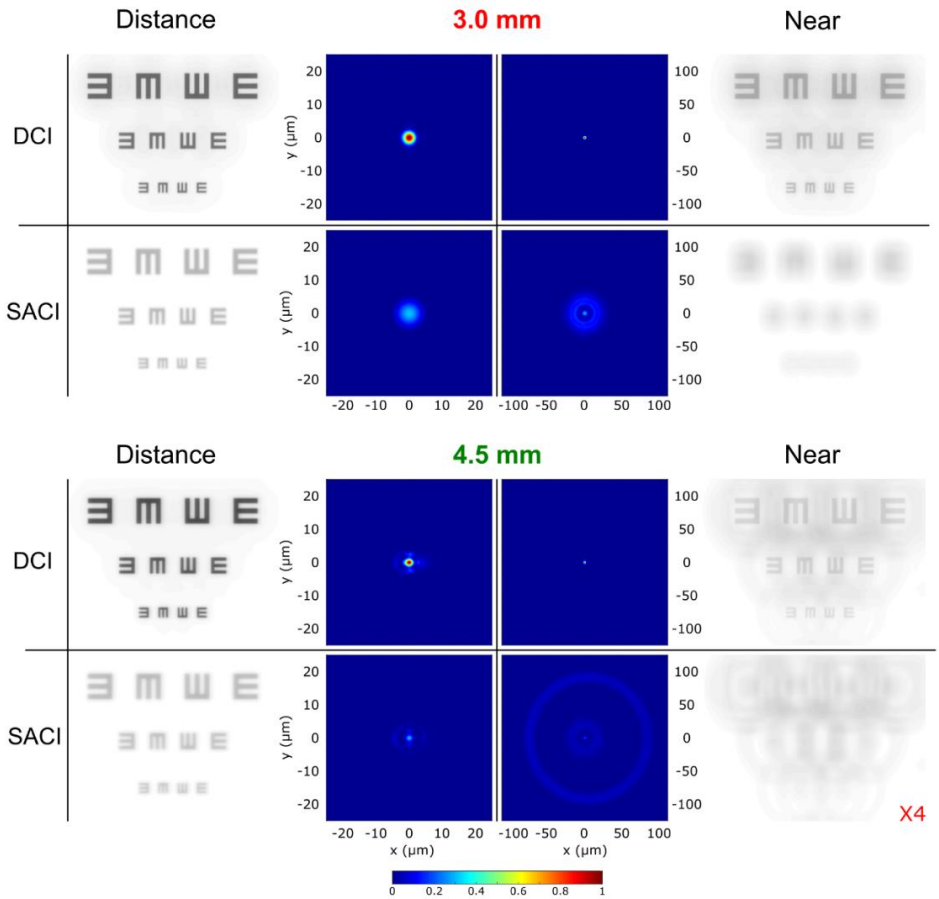

Figure 4: PSFs at the far and near foci provided by the DCI and SACI inlays. The corresponding simulated images are shown side by side. For SACI at near the image intensity was enhanced 4 times.

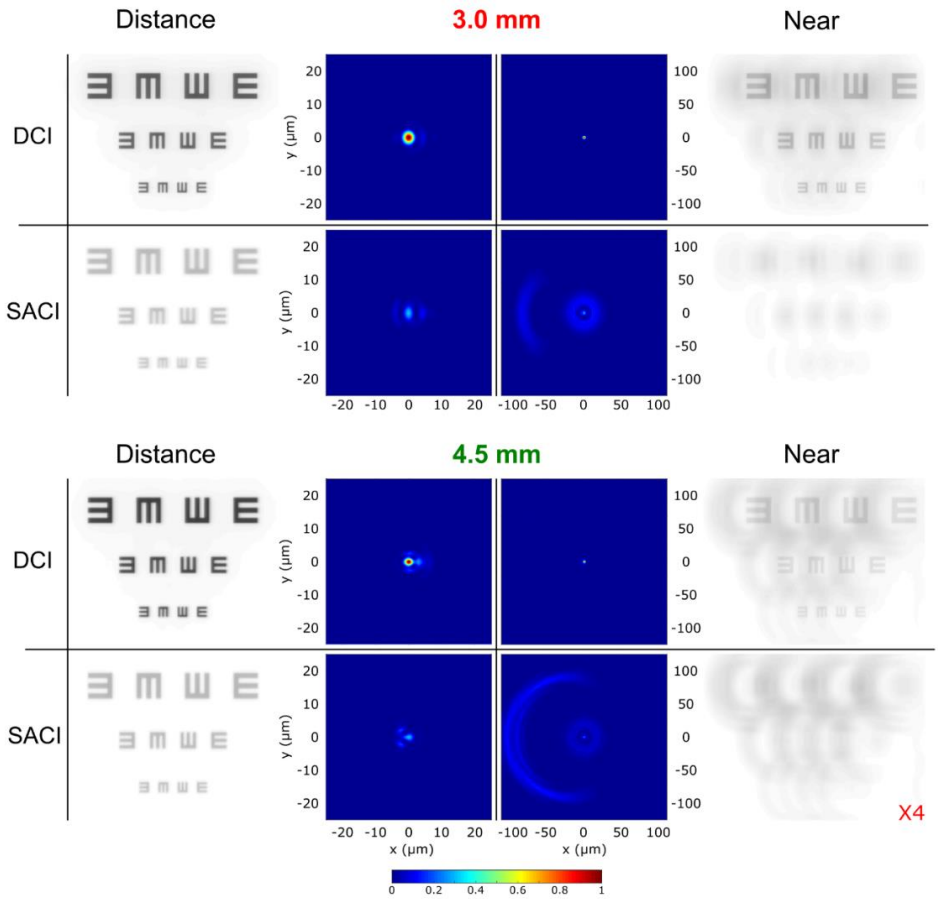

Figure 5: Idem Fig. 4, but with the inlays decentered 0.8 mm in the temporal direction.

We want to emphasize that these results for the SACI coincide with those obtained by Schwarz et al. [Schwarz14] in real eyes with the same optotype, but using a visual simulator based on adaptive optics. Figure 5 is equivalent to Figure 4 but with the inlays decentered 0.8 mm in the temporal direction. By comparing Fig. 4 and Fig. 5, it is clear that the tolerance of the DCI to decentration is much higher than the SACI, because the closer resemblance of the corresponding PSFs at near and distance, for both pupil diameters. Finally, the images obtained experimentally with the physical inlays in front of model eye cornea are shown in Fig. 6. These images, achieved for the same pupil diameters used in the numerical simulations, demonstrate the light throughput difference between the DCI and the conventional SACI predicted in Fig. 4.

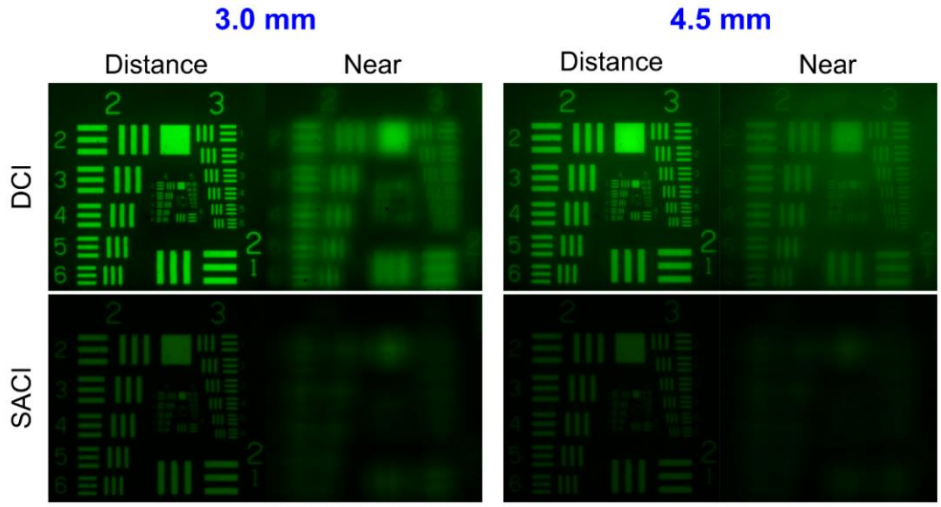

Figure 6: Experimental images obtained for an artificial presbyopic model eye (ISO 11979-9 Standard) with the DCI and SACI located in just front of the artificial cornea.

Discussion and conclusions

In this work we have provided evidence of the good performance of the DCI as image forming device in comparison with the commercially available pin-hole based corneal inlay. Both devices were virtually implanted in the Liou–Brennan model eye considering that, in addition to be one of the most physiologically realistic models, its optical parameters are based on measurements of early presbyopes, which are likely the best candidates for corneal inlay surgery. In fact, a similar model eye has been already applied for investigating the effect of the SACI on the peripheral visual field [Atchison16]. Additionally, we reported experimental results, obtained in vitro according to the ISO 11979-9 Standard, which also gave a favorable verification for the performance of the DCI in image formation. Specifically, we demonstrated that, compared with the SACI our proposal provides images with high intensity levels. This is important because, current inlays need to be implanted monocularly in the non-dominant eye, with the risk of significant decline in the patient's binocular visual performance, compromising stereoacuity [Castro18], and also binocular visual acuity because binocular summation is less effective as the interocular differences in retinal image increase. In fact, Tabernero and coworkers [Tabernero11] found that, the binocular far-distance visual acuity achieved with one eye implanted with SACI comply binocular summation; but, in contrast, the visual acuity for near distance seems to match to the near distance acuity of the eye with SACI. Therefore, according to our results, can assume that even adopting the same criterion of monocular implantation, the binocular performance of the DCI at near could be better than the SACI, but this is an assumption that should be confirmed in future studies. On the other hand, considering that the clinical outcomes demonstrated

that SACI is very sensitive to centration (even requiring recentration in some cases) [Tabernero12], another relevant result of this work is that in a realistic model eye, the DCI is more robust against decentration than SACI, as can be seen in Fig. 2 and 3. Moreover, the AMTFs represented in Fig. 3 reveal that the DCI is also less pupil dependent than the SACI. The drop of the depth of focus obtained for the SACI for 4.5 mm pupil, in comparison with the result for 3.0 mm pupil diameter, evident in this figure, can be attributed to the light that passes through the outer part of the inlay, which counteracts the pinhole effect. This effect was not previously found in other studies of the SACI in which the external diameter of the inlay was ignored. In spite of this, the better results obtained for the inlays centered on the visual axis agree with those reported Tabernero and Artal [Tabernero12]. A limitation of this work is that the eye model, despite of being anatomically accurate, it is still a model, that obviously does not reproduce the effect of image processing by the brain. Therefore, as was done for the SACI in the recent years, more theoretical, and above all, clinical work is needed to assess the visual performance in real human eyes. The use of visual simulators could be the first step in this process. In addition, since the intensity ratio of the far and near focal spots can be controlled by adjusting the proportion of the area of the DCI central hole and the surrounding structure, visual simulators could confirm whether this unique feature would allow the construction of customizable corneal implants. Another significant consequence of the improved light throughput of the DCI could be its bilateral implantation. Summarizing: Bifocality, high transmission efficiency, and robustness against decentration are benefits of the DCI not previously achieved simultaneously by any other corneal inlay.

Acknowledgments

D. Montagud-Martínez and V. Ferrando acknowledge the financial support from the Universitat Politècnica de València, Spain (fellowships FPI-2016 and PAID-10-18, respectively).

References

[Arlt15] Arlt E, Krall E, Moussa S, Grabner G, Dexl A. Implantable inlay devices for presbyopia: the evidence to date. Clin Ophthalmol. 2015;9:129–37.

[Atchison16] Atchison DA, Blazaki S, Suheimat M, Plainis S, Charman WN. Do small-aperture presbyopic corrections influence the visual field? Ophthalmic Physiol Opt. 2016;36(1):51–9.

[Bakaraju08] Bakaraju RC, Ehrmann K, Papas E, Ho A. Finite schematic eye models and their accuracy to in-vivo data. Vision Res. 2008;48(16):1681–94.

[Calatayud13] Calatayud A, Remón L, Martos J, Furlan WD, Monsoriu JA. Imaging quality of multifocal intraocular lenses: automated assessment setup. Ophthalmic and Physiological Optics. 2013;33(4):420–6.

[Castro18] Castro JJ, Ortiz C, Jiménez JR, Ortiz-Peregrina S, Casares-López M. Stereopsis Simulating Small-Aperture Corneal Inlay and Monovision Conditions. J Refract Surg. 2018;34(7):482–8.

[Charman14] Charman WN. Developments in the correction of presbyopia II: surgical approaches. Ophthalmic Physiol Opt. 2014;34(4):397–426.

[Charman19] Charman WN, Liu Y, Atchison DA. Small-aperture optics for the presbyope: do comparable designs of corneal inlays and intraocular lenses provide similar transmittances to the retina? J Opt Soc Am A Opt Image Sci Vis. 2019;36(4):B7–14.

[Furlan16] Furlan WD, Remón L, Llorens C, Rodriguez-Vallejo M, Monsoriu JA. Comparison of two different devices to assess intraocular lenses. Optik. 2016;127(20):10108–14.

[Furlan17] Furlan WD, García-Delpech S, Udaondo P, Remón L, Ferrando V, Monsoriu JA. Diffractive corneal inlay for presbyopia. J Biophotonics. 2017;10(9):1110–4.

[Gilchrist87] Gilchrist J, Pardhan S. Binocular Contrast Detection with Unequal Monocular Illuminance*. Ophthalmic and Physiological Optics. 1987;7(4):373–7.

[Giménez06] Giménez F, Monsoriu JA, Furlan WD, Pons A. Fractal photon sieve. Opt Express, OE. 2006;14(25):11958–63.

[Gross08] Gross H, Blechinger F, Achtner B, Handbook of Optical Systems. Vol. 4, Survey of Optical Instruments, 2015, 1092 p.

[ISO14] ISO 11979-2:2014. Ophthalmic implants — Intraocular lenses — Part 2: Optical properties and test methods.

[Kipp01] Kipp L, Skibowski M, Johnson RL, Berndt R, Adelung R, Harm S, et al. Sharper images by focusing soft X-rays with photon sieves. Nature. 2001;414(6860):184–8.

[Lindstrom13] Lindstrom RL, Macrae SM, Pepose JS, Hoopes PC. Corneal inlays for presbyopia correction. Curr Opin Ophthalmol. 2013;24(4):281–7.

[Liou97] Liou H-L, Brennan NA. Anatomically accurate, finite model eye for optical modeling. J Opt Soc Am A, JOSAA. 1997;14(8):1684–95.

[Plainis13] Plainis S, Petratou D, Giannakopoulou T, Radhakrishnan H, Pallikaris IG, Charman WN. Small-aperture monovision and the Pulfrich experience: absence of neural adaptation effects. PLoS ONE. 2013;8(10):e75987.

[Schwarz14] Schwarz C, Manzanera S, Prieto PM, Fernández EJ, Artal P. Comparison of binocular through-focus visual acuity with monovision and a small aperture inlay. Biomed Opt Express. 2014;5(10):3355–66.

[Schwiegerling13] Schwiegerling JT. Eye Axes and Their Relevance to Alignment of Corneal Refractive Procedures. J Refract Surg. 2013;29(8):515–6.

[Tabernero11] Tabernero J, Schwarz C, Fernández EJ, Artal P. Binocular Visual Simulation of a Corneal Inlay to Increase Depth of Focus. Invest Ophthalmol Vis Sci. 2011;52(8):5273–7.

[Tabernero12] Tabernero J, Artal P. Optical modeling of a corneal inlay in real eyes to increase depth of focus: optimum centration and residual defocus. J Cataract Refract Surg. 2012;38(2):270–7.

[Vilupuru15] Vilupuru S, Lin L, Pepose JS. Comparison of Contrast Sensitivity and Through Focus in Small-Aperture Inlay, Accommodating Intraocular Lens, or Multifocal Intraocular Lens Subjects. Am J Ophthalmol. 2015;160(1):150-162.e1.

[Vukich18] Vukich JA, Durrie DS, Pepose JS, Thompson V, van de Pol C, Lin L. Evaluation of the small-aperture intracorneal inlay: Three-year results from the cohort of the U.S. Food and Drug Administration clinical trial. J Cataract Refract Surg. 2018;44(5):541–56.

2.5. Proposal of a new diffractive corneal inlay to improve near vision in a presbyopic eye

Proposal of a new diffractive corneal inlay to improve near vision in a presbyopic eye

Diego Montagud-Martínez, Vicente Ferrando, Juan A. Monsoriu, and Walter D. Furlan

Author Information · Find other works by these authors

Applied Optics Vol. 59, Issue 13, pp. D54-D58 (2020) · https://doi.org/10.1364/AO.383581

Abstract

A new class of diffraction-based corneal inlays for treatment of presbyopia is described. The inlay is intended to achieve an improvement of the near focus quality over previous designs. Our proposal is a two-zone hybrid device with separated amplitude and phase areas having a central aperture and no refractive power. An array of micro-holes is distributed on the surface of the inlay conforming a binary photon sieve. In this way, the central hole of the disk contributes to the zero order of diffraction, and the light diffracted by the micro-holes in the peripheral photon sieve produces a real focus for near vision. We employed ray-tracing software to study the performance of the new inlay in the Liou–Brennan model eye. The modulation transfer functions (MTFs) at the distance and near foci, and the area under the MTFs for different object vergences, were the merit functions used in the evaluation. The results were compared with those obtained with previous pure amplitude designs. Additionally, image simulations were performed with the inlays in the model eye to show the good performance of our proposal in improving the quality of the near vision.

Related Topics

Optics & Photonics Topics
Diffraction efficiency
Eye models
Fresnel zones

2.5. Proposal of a new diffractive corneal inlay to improve near vision in a presbyopic eye

Diego Montagud-Martínez[1], Vicente Ferrando[1], Juan A. Monsoriu[1] y Walter D. Furlan[2*]

1 Centro de Tecnologías Físicas, Universitat Politècnica de València, 46022 Valencia, Spain.

2 Departamento de Óptica y Optometría y Ciencias de la Visión, Universitat de València, 46100 Burjassot, Spain.

* walter.furlan@uv.es

Abstract

A new class of diffraction-based corneal inlays for treatment of presbyopia is described. The inlay is intended to get an improvement of the near focus quality over previous designs. Our proposal is a two zone hybrid device with separated amplitude and phase areas having a central aperture and no refractive power. An array of micro-holes is distributed on the surface of the inlay conforming a binary photon sieve. In this way, the central hole of the disk contributes to the zero order of diffraction, and the light diffracted by the micro-holes in the peripheral photon sieve produces a real focus for near vision. We employed a ray tracing software to study the performance of the new inlay in the Liou-Brennan model eye. The MTFs at the distance and near foci, and the area under the MTFs for different object vergences, were the merit functions used in the evaluation and the results were compared with those obtained with previous pure amplitude designs. Additionally, image simulations were performed with the inlays in the model eye to show the good performance of our proposal in improving the quality of the near vision.

Introduction

Corneal inlays are optical devices employed by ophthalmologists to provide good near and intermediate vision of presbyopic people between the ages of 45 and 60 years old. As their name suggest, corneal inlays are surgically implanted within the corneal stroma (the thicker middle layer of the cornea) into a small pocket created with a femtosecond laser. The pocket seals itself, and the entire procedure typically takes only few minutes. Actually, corneal inlay surgery is less invasive than other procedures, which involve implanting intraocular lenses inside the eye, either directly in front or behind of the iris. Moreover, corneal inlay surgery is usually combined with LASIK surgery to correct both presbyopia and refractive defects [Lindstrom13, Charman14, Arlt15].

Considering their physical operating principles, corneal inlays can be classified into different categories: refractive inlays, small aperture inlays and diffractive inlays [Charman14, Furlan17], being the last category the most recent development in this field. In fact, in Ref [Furlan17] our team reported the first Amplitude Diffractive Corneal Inlay (ADCI) as the result of the combination of two concepts: the pin-hole effect [Trindade15] (used in the above mentioned small aperture inlays) and the photon sieve [Kipp11, Giménez06] (a photon sieve is essentially an amplitude Fresnel zone plate in which the transparent rings have been replaced by a set of non-overlapping holes distributed within the corresponding area).

Recently we have studied different designs of ADCI in comparison with small aperture corneal inlay, both, numerically in different model eyes [Montagud-Martínez19b, Montagud-Martínez19c], and also experimentally in vitro with ADCI prototypes [Montagud-Martínez19c]. Those studies revealed that ADCI exhibit a higher light throughput, and improvements in imaging of near objects. In an effort to further improve the near vision of presbyopic people, here we present a new class of diffraction-based corneal inlays. The fundamental difference with the previous ADCI models is that it is a hybrid device with two concentric ring areas: the inner one having a pure phase transmittance and the outer one having a pure amplitude transmittance. Thus, the new model, called Hybrid Diffractive Corneal Inlay (HDCI) is a solid ring in which these two differentiated parts, are drilled with an array of micro-holes distributed on the surface of the inlay conforming a binary photon sieve. In this way, the central hole of the disk contributes to the zero order of diffraction, and the light diffracted by the micro-holes in the peripheral photon sieve produces a real focus for near vision. We employed Zemax Optic Studio software to study the performance of the new inlay in the Liou-Brennan model eye. The merit functions we used in the evaluation of the HDCI were: the Modulation Transfer Function (MTF) at the distance and near foci, and the area under the MTFs (AMTFs) for different object vergences. Results were compared with those obtained with an equivalent ADCI. Additionally, the Point Spread Functions (PSFs) were computed and image simulations were performed with the inlays in the model eye to evaluate the performance of our proposal.

Diffractive Corneal Inlays

To describe the HDCI design, let us recall that previous designs of ADCI were considered [Montagud-Martínez19b] in which the radius of the central hole, and the area covered by the surrounding photon sieve structure was varied to obtain different ratios of energy between the near and far foci. The higher values of the axial irradiance at the near focus were obtained with the design shown in Fig. 1a), where the black region represents the opaque surface (with zero transmittance), while the white regions are holes drilled on the opaque surface, so these are transparent regions with transmittance value 1 and phase 0. To improve the efficiency of the near focus we have considered a hybrid design in which the

innermost 3 opaque rings were replaced with transparent rings of thickness *h* equivalent to a phase change of π. So,

$$h = \frac{\lambda_0}{2\cdot\left(n_{CI} - n_c\right)}, \quad (1)$$

where λ_0 is the design wavelength, n_{CI} is the refractive index of the corneal inlay material, and n_c is the refractive index of the cornea. In this way, a half wave phase shift is provided between the holes and the transparent region at the central part of the inlay. The HDCI transmittance distribution is shown in Fig. 1b), where the transparent surface with π phase is represented in blue. As can be seen in this figure, the HDCI evaluated in this study consisted in a disk of 4.15 mm diameter with a central hole of 1.00 mm diameter surrounded by the 3 innermost transparent rings up to a radius of 1.133 mm and other 7 outermost opaque rings up the external radius of the inlay. In this way, the effect of the combination of phase and amplitude in the HDCI can be appreciated, even for the smallest pupil we considered in this work (see the green circle in Fig. 1b). Both ADCI and the HDCI have a total of 9640 holes of different size, being the smallest ones of 18 μm diameter. They were designed to provide a near diffractive focus corresponding to a nominal addition of +3.00 D for the design wavelength (550 nm).

By using Eq. 1 we have found that the structure of the inlay must have a thickness *h* = 4.91 μm. The same thickness was considered for the ADCI in the following analysis.

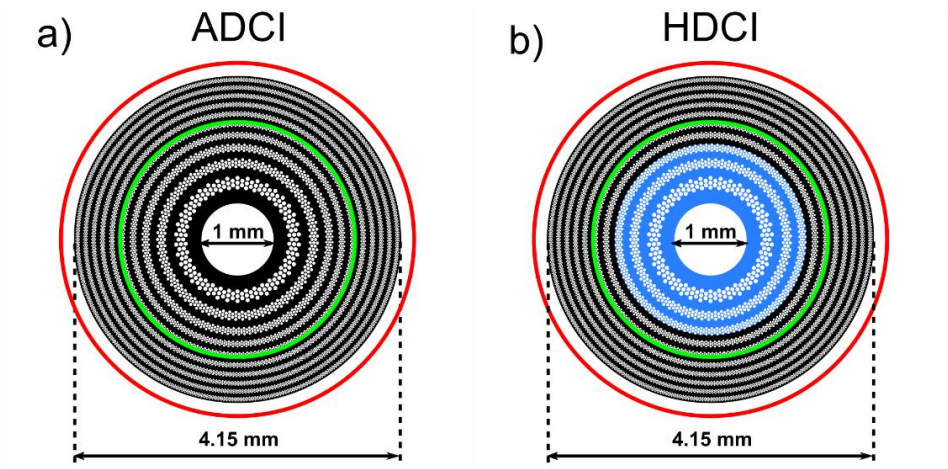

Figure 1: Structure of the corneal inlays evaluated in this study. The black regions are opaque. While the white and blue zones are transparent with a phase 0 and π phase, respectively. The green and red circles represent the pupils diameters considered in the numerical assessment of the inlays: 3.0 mm (green) and 4.5 mm (red).

Results

To validate the HDCI design the Zemax OpticStudio optical design software (http://www.zemax.com/os/opticstudio) was employed to simulate the theoretical model eye proposed by Liou and Brennan [Liou97]. This model eye is especially well adapted to investigate the optical properties of corneal inlays because it was designed using biometric data obtained from patients aged around 45 years (early presbyopes). Additionally, the Liou-Brennan model eye has an aspheric cornea, a decentered pupil (0.5 mm in the nasal direction), a lens with refractive index gradients in the axial and radial directions and a visual axis tilted 5° to the optical axis (kappa angle). The ADCI and the HDCI were sequentially positioned in this model eye at a depth of 0.20 mm from the anterior corneal surface according to the surgical procedure followed for other types of amplitude corneal inlays like Kamra [Arlt15]. Within this model the entrance and exit pupil were located at 3.1 mm, and at -26.3 in front of the cornea and the retina, respectively. Table 1 shows the data sheet used in the simulations. The ADCI was introduced as a *User Defined Aperture* (.uda file), since with this kind of files the locations of the holes in the inlay surface and their dimensions can be easily programmed. On the other hand, the HDCI was simulated by a *Grid Sag Surface* with the phase corresponding to the inner 3 rings superimposed to another .uda file similar to the one employed for the ADCI but with internal radius of 1.133 mm (see Fig.1). Two different pupil diameters were evaluated: 3.0 mm and 4.5 mm simulating photopic and mesopic conditions. Monochromatic light of 550 nm was considered in the analysis, coincident with the design wavelength of the inlays, which corresponds to the maximum sensitivity of the human eye in photopic conditions [Gross08].

Surface	Radius (mm)	Asphericity	Thickness (mm)	Refractive index
Anterior Cornea	7.77	-0.18	0.200	1.376
Anterior CI	7.77	-0.18	0.005	1.376
Posterior CI	7.77	-0.18	0.295	1.376
Posterior Cornea	6.40	-0.60	3.16	1.336
Iris	-	-	0.100	1.337
Anterior Lens	12.4	-0.94	1.59	1.368 + 0.049057 z − 0.015427 z2 − 0.001978 r2
Posterior Lens	Infinity	-	2.43	1.407 − 0.006605 z2 − 0.001978 r2
Retina	-8.10	0.96	16.26	1.336

Table 1: Liou-Brennan model eye Zemax data sheet (r and z are radial and axial coordinates in the crystalline lens)

2.5. Proposal of a new diffractive corneal inlay to improve near vision in a presbyopic eye

To evaluate the optical quality of the inlays shown in Fig.1, the MTFs were measured for objects at different vergences, in 0.1 D steps between +0.50 D and -3.50 D. Since the theoretical model eye is asymmetric, the ray tracing program calculates, the sagittal and tangential MTF and, therefore for each vergence, both MTFs were averaged to obtain the MTFs shown in the following results. Fig. 2 shows MTFs at far and near foci for both corneal inlays with both pupillary conditions. Note that, the MTFs for near vision are shown in logarithmic scale in order to better appreciate the differences between both designs. As can be noted in near vision for both pupils, the MTFs provided by the HDCI are better since the phase structure at the transparent area of the HDCI improves the diffraction efficiency, increasing the amount of light directed to the near focus. On the other hand, for distant vision the ADCI provides the best MTFs.

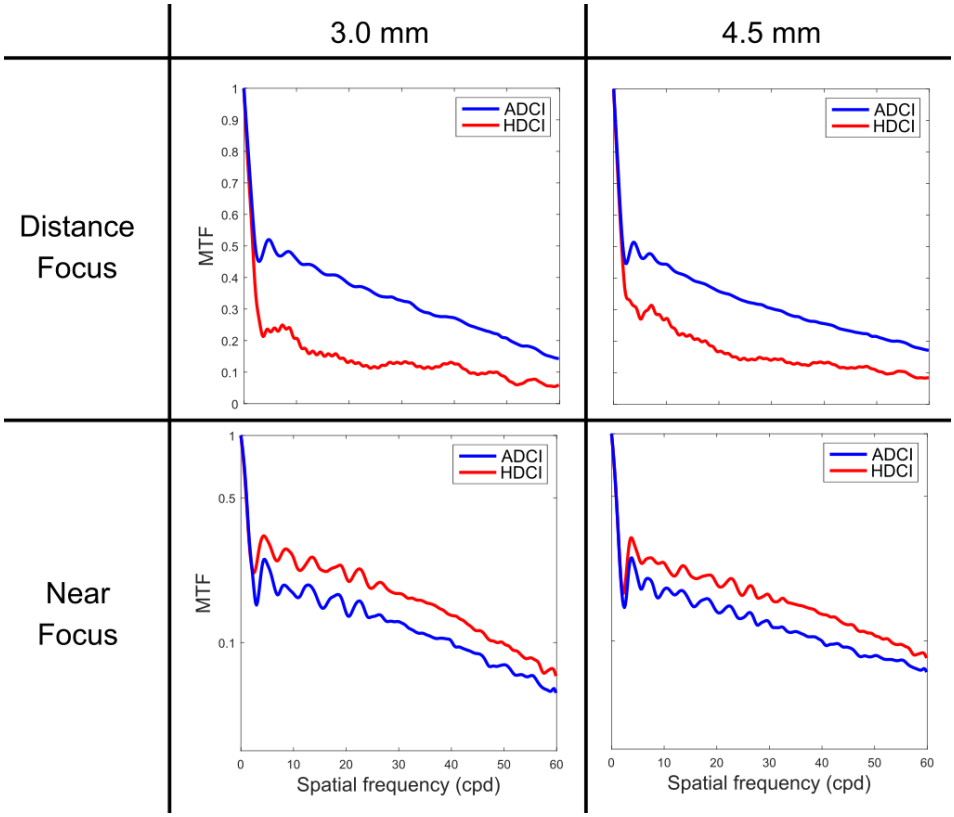

Figure 2: MTFs for distance and near foci provided by the ADCI (blue) and HDCI (red) with pupil diameters of 3.0 mm and 4.5 mm.

To give insight into how is the relative image quality for distance and near objects provided by both designs, the AMTF has been calculated. In fact, this metric showed a high correlation with the visual acuity [Alarcon16]. In our case we have selected the range of spatial frequencies between 9.5 cycles per degree and 30 cycles per degree, equivalent to visual acuities between 0.5 logMAR and 0.0

logMAR. Fig. 3 shows the AMTFs provided by the corneal inlays with different pupils. As can be seen, both designs have a bifocal profile but for both pupil diameters, the near focus the HDCI presents a higher value of the AMTF with an extended depth of focus, in comparison with the ADCI. On the other hand, as expected from the results shown in Fig. 2, the ADCI has a better performance for distance objects.

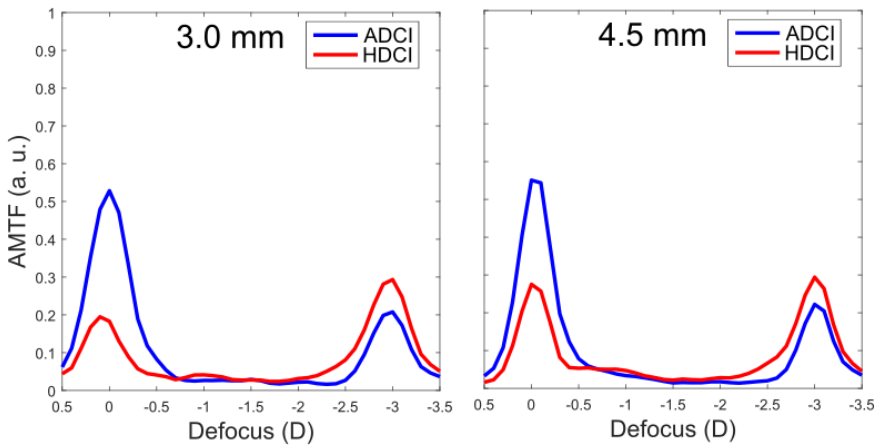

Figure 3: Through the focus AMTFs for both inlays: ADCI (blue) and HDCI (red)

To complete our analysis, the PSFs provided for the HDCI and the ADCI were also obtained at distance and near foci for both models. Additionally, simulated images of a tumbling *Es* optotype were obtained for two pupil diameters. The results are shown in Figs. 4 and 5. The optotype with letter sizes corresponding to visual acuities 0.4, 0.2 and 0 in the logMAR scale, has been convolved with the PSFs in order to obtain the image simulation using a custom Matlab code (Mathworks, Inc. R2018b). The PSFs provided by Zemax are shown in these figures and were normalized by the software to their respective maximum values. However, the PSF used in the convolution with the object were rescaled and normalized with respect to their total energy of the PSF to obtain images in which the contrast can be directly compared. These results also confirm the results obtained in Figs. 2 and 3; i.e. the images of near objects with the HDCI are better than those obtained with ADCI for both pupil diameters. In fact, in both cases the Weber contrast, defined as $C=(L_{max}-L_{min})/ L_{Background}$, where L_{max}, L_{min}, and $L_{Background}$ are luminance maximum, minimum, and background, respectively, improved by 3.5%. Finally, to show the extended depth of focus for near, images simulations were obtained at object vergence of 2.5 D. The results are shown in Fig. 6. The better performance at near of the HDCI can be clearly seen in this figure.

2.5. Proposal of a new diffractive corneal inlay to improve near vision in a presbyopic eye

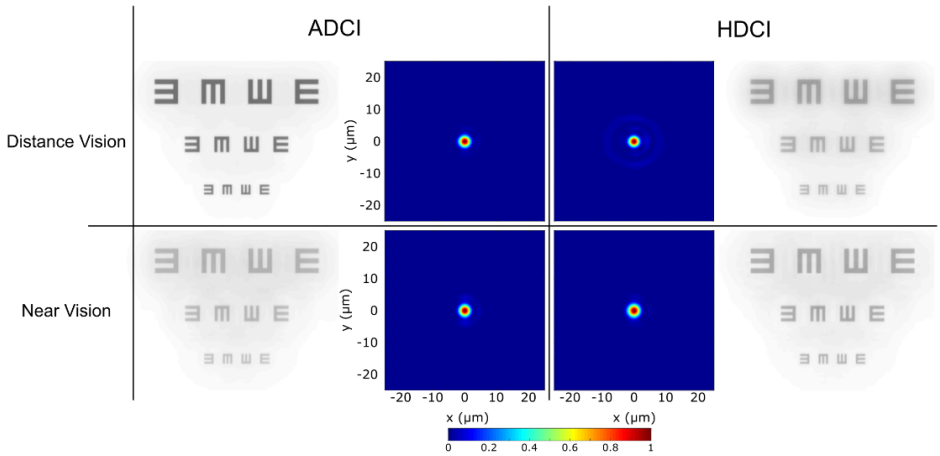

Figure 4: PSFs and image simulation of both corneal inlays in distance and near vision for 3.0 mm of pupil.

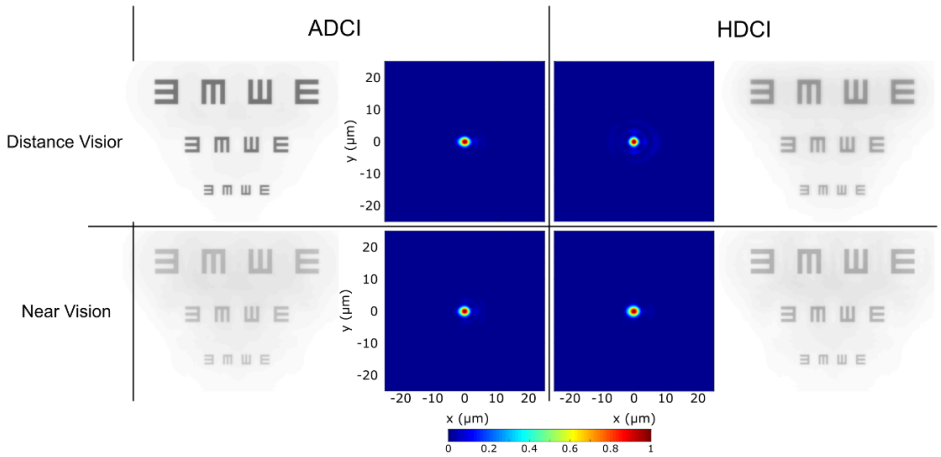

Figure 5: PSFs and image simulation of both corneal inlays in distance and near vision for 4.5 mm of pupil.

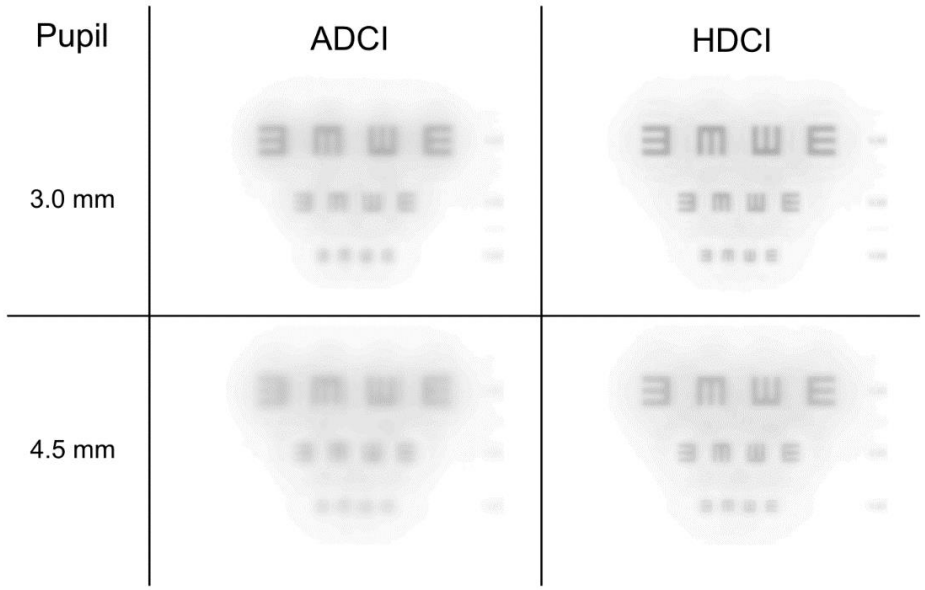

Figure 6: Image simulation of both corneal inlays at object vergence of 2.5 D.

Conclusions

Diffractive corneal inlays are the newest type of corneal implants designed for the treatment of presbyopia. Previous designs consisted on a pure amplitude models having different construction parameters (such as the central hole radius, the inlay diameter, addition, number and distribution of micro-holes), that provide different results, proving that diffractive corneal inlays could be customized to meet different patient's needs [Montagud-Martínez19b, Montagud-Martínez19c]. In this work we added a new variable to the design parameters of diffractive corneal inlays, which consists of introducing a transparent region on the diffractive surface to improve the diffraction efficiency of the near focus. The performance of the resulting model, HDCI, was compared with an equivalent amplitude model, ADCI, with the same number and distribution of micro-holes. With the new model we found an improvement of the near focus efficiency, and an extension of the depth of focus for near. However, this benefits were obtained at the cost of losing contrast for distance objects, and it seems that the previous design provides an overall better optical quality. Now, taking into account that normally, corneal inlays are implanted monocularly in the non-dominant eye [Arlt15], this fact is not necessarily a great disadvantage for distance vision, because the fellow eye could compensate for this.

Thus, in further studies the HDCI will be analyzed under different realistic variations that affect its optical properties, such as the influence of the inlay decentration and its behavior under polychromatic illumination. Moreover, both designs need to be tested subjectively to assess their performance.

Funding

Ministerio de Economía y Competitividad, Spain, (DPI2015–71256–R). Generalitat Valenciana (PROMETEO/2019/048), Spain.

Acknowledgments

D. Montagud-Martínez and V. Ferrando acknowledge the financial support from the Universitat Politècnica de València, Spain (fellowships FPI-2016 and PAID-10-18, respectively).

Disclosures

The authors declare no conflicts of interest.

References

[Alarcon16] Alarcon A, Canovas C, Rosen R, Weeber H, Tsai L, Hileman K, et al. Preclinical metrics to predict through-focus visual acuity for pseudophakic patients. Biomed Opt Express, BOE. 2016;7(5):1877–88.

[Arlt15] Arlt E, Krall E, Moussa S, Grabner G, Dexl A. Implantable inlay devices for presbyopia: the evidence to date. Clin Ophthalmol. 2015;9:129–37.

[Charman14] Charman WN. Developments in the correction of presbyopia II: surgical approaches. Ophthalmic Physiol Opt. 2014;34(4):397–426.

[Furlan17] Furlan WD, García-Delpech S, Udaondo P, Remón L, Ferrando V, Monsoriu JA. Diffractive corneal inlay for presbyopia. J Biophotonics. 2017;10(9):1110–4.

[Giménez06] Giménez F, Monsoriu JA, Furlan WD, Pons A. Fractal photon sieve. Opt Express, OE. 2006;14(25):11958–63.

[Gross08] Gross H, Blechinger F, Achtner B, Handbook of Optical Systems. Vol. 4, Survey of Optical Instruments, 2015, 1092 p.

[Kipp01] Kipp L, Skibowski M, Johnson RL, Berndt R, Adelung R, Harm S, et al. Sharper images by focusing soft X-rays with photon sieves. Nature. 2001;414(6860):184–8.

[Lindstrom13] Lindstrom RL, Macrae SM, Pepose JS, Hoopes PC. Corneal inlays for presbyopia correction. Curr Opin Ophthalmol. 2013;24(4):281–7.

[Liou97] Liou H-L, Brennan NA. Anatomically accurate, finite model eye for optical modeling. J Opt Soc Am A, JOSAA. 1997;14(8):1684–95.

[Montagud-Martínez19b] Montagud-Martínez D, Ferrando V, Machado F, Monsoriu JA, Furlan WD. Imaging Performance of a Diffractive Corneal Inlay for Presbyopia in a Model Eye. IEEE Access. 2019;7:163933–8

[Montagud-Martínez19c] Montagud-Martínez D, Ferrando V, Monsoriu JA, Furlan WD, Optical Evaluation of New Designs of Multifocal Diffractive Corneal Inlays, J Ophthalmol, 2019; vol. 2019 1-6

[Trindade15] Trindade C, Small aperture (pinhole) intraocular implant to increase depth of focus. U.S; 14/297, 447. 2015

2.6. A new trifocal corneal inlay for presbyopia

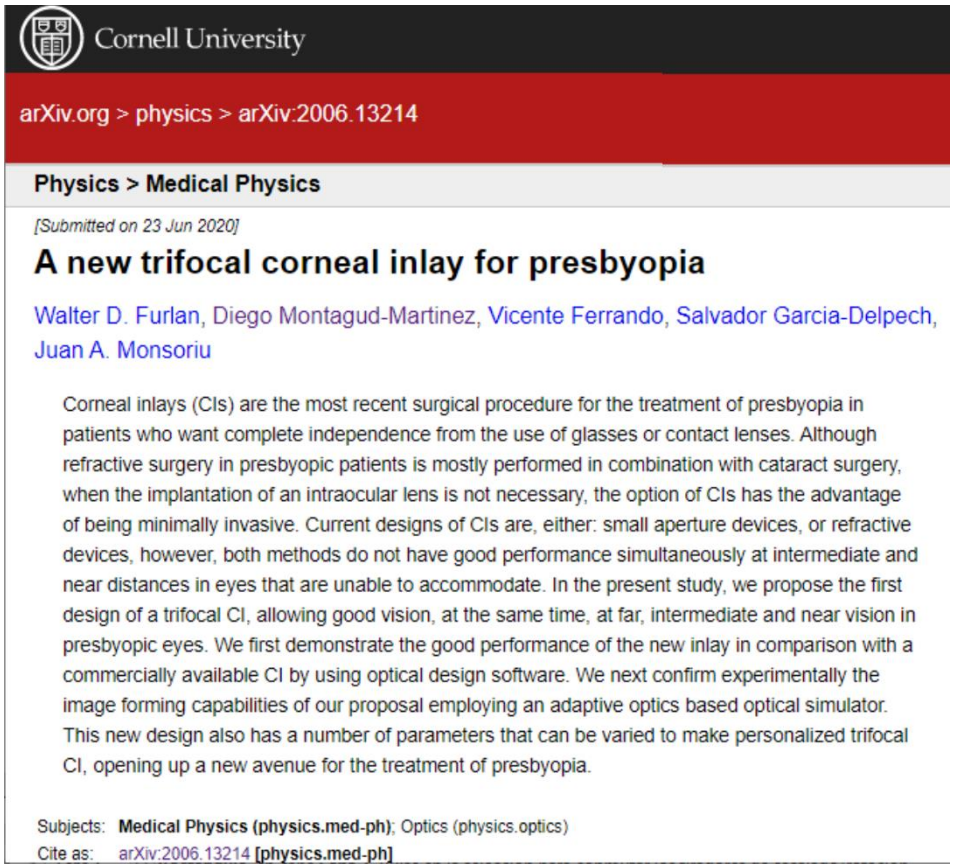

Cornell University

arXiv.org > physics > arXiv:2006.13214

Physics > Medical Physics

[Submitted on 23 Jun 2020]

A new trifocal corneal inlay for presbyopia

Walter D. Furlan, Diego Montagud-Martinez, Vicente Ferrando, Salvador Garcia-Delpech, Juan A. Monsoriu

Corneal inlays (CIs) are the most recent surgical procedure for the treatment of presbyopia in patients who want complete independence from the use of glasses or contact lenses. Although refractive surgery in presbyopic patients is mostly performed in combination with cataract surgery, when the implantation of an intraocular lens is not necessary, the option of CIs has the advantage of being minimally invasive. Current designs of CIs are, either: small aperture devices, or refractive devices, however, both methods do not have good performance simultaneously at intermediate and near distances in eyes that are unable to accommodate. In the present study, we propose the first design of a trifocal CI, allowing good vision, at the same time, at far, intermediate and near vision in presbyopic eyes. We first demonstrate the good performance of the new inlay in comparison with a commercially available CI by using optical design software. We next confirm experimentally the image forming capabilities of our proposal employing an adaptive optics based optical simulator. This new design also has a number of parameters that can be varied to make personalized trifocal CI, opening up a new avenue for the treatment of presbyopia.

Subjects: **Medical Physics (physics.med-ph)**; Optics (physics.optics)
Cite as: arXiv:2006.13214 **[physics.med-ph]**

2.6. A new trifocal corneal inlay for presbyopia

Walter D. Furlan[1*], Diego Montagud-Martínez[2], Vicente Ferrando[2] y Juan A. Monsoriu[2]

1 Departamento de Óptica y Optometría y Ciencias de la Visión, Universitat de València, 46100 Burjassot, Spain.

2 Centro de Tecnologías Físicas, Universitat Politècnica de València, 46022 Valencia, Spain.

* walter.furlan@uv.es

Abstract

Corneal inlays (CIs) are the most recent surgical procedure for the treatment of presbyopia in patients who want complete independence from the use of glasses or contact lenses. Although refractive surgery in presbyopic patients is mostly performed in combination with cataract surgery, when the implantation of an intraocular lens is not necessary, the option of CIs has the advantage of being minimally invasive. Current designs of CIs are, either: small aperture devices, or refractive devices, however, both methods do not have good performance simultaneously at intermediate and near distances in eyes that are unable to accommodate. In the present study, we propose the first design of a trifocal CI, allowing good vision, at the same time, at far, intermediate and near vision in presbyopic eyes. We first demonstrate the good performance of the new inlay in comparison with a commercially available CI by using optical design software. We next confirm experimentally the image forming capabilities of our proposal employing an adaptive optics based optical simulator. This new design also has a number of parameters that can be varied to make personalized trifocal CI, opening up a new avenue for the treatment of presbyopia.

Introduction

Presbyopia is the most common refractive defect in the population, affecting the quality of life of people over 45 years old, which nowadays exceeds two billion people worldwide. [Fricke18]. Its treatment, aimed to restore the ability to see clearly objects at near distances (depleted by the loss of accommodation) has multiple options, including multifocal spectacles, contact lenses and refractive surgery. Within this last option, the most recent approach is the implantation of CIs, entailing a minimally invasive and reversible surgery [Charman14, Moarefi17]. Currently, all CIs are implanted monocularly in the non-dominant eye, producing a variant of the monovision technique, that consists in using the dominant eye for distance vision and the non-dominant one for intermediate-near vision. CIs are small devices of a biocompatible material that are implanted into ‘pockets’ in the corneal stroma created by cavitation using femtosecond lasers.

Thus, special care must be taken in the design of these devices and/or in the choice of inlay material to avoid the interruption of the normal cell activity in the stroma around it.

Based on different physical principles, several types of CIs have been proposed, each one having its own strengths and weaknesses [Charman14, Moarefi17]. At present, the most successful, and widely studied, commercial CIs are the refractive Flexivue Microlens® (Presbia Cooperatief, UA, Irvine, CA, USA) [Beer20, Limnopoulou13, Garza13, Malandri15], and the small aperture KAMRA® inlay (Acufocus, Inc., Irvine, CA, USA) [Waring11, Vilupuru15, Vukich18].

Refractive Inlays (RI) act locally at central part of the cornea either, by modifying its curvature or by altering the refractive index to improve near vision. However, RIs produce a loss of uncorrected distance visual acuity (UDVA) and contrast sensitivity [Beer20, Limnopoulou13, Malandrini15]. Besides, an increase of higher order aberrations in the operated eye, especially spherical aberration has also been reported [Garza13, Beer17]. To avoid degenerative material deposition and inflammation, refractive non-porous inlays should be manufactured with materials that ensure that flux of metabolic species is not modified by the device [Pinsky14].

On the other hand, small aperture corneal inlays are simply opaque discs with a central hole that, acting as pinhole, produces an extended depth of focus at the cost of a loss of contrast sensitivity in the image. Thousands of micro-holes are randomly distributed on its surface to allow the passage of nutrients. The main shortcomings of small aperture inlays are associated with the intrinsic low light-throughput of the quasi-opaque ring. In fact, as the amount of light that reaches the retina of the fellow eye is significantly higher, the binocular distance visual performance, and the stereoacuity for near and intermediate distances are adversely affected [Gilchrist87, Plainis13, Castro18]. Moreover, the diffraction produced by these pores aggravates the loss of contrast sensitivity previously mentioned.

Diffractive corneal inlays (DCIs) are the latest reported phakic surgery for the presbyopia correction [Furlan17]. This proposal is still under development, but it was presented as a promising alternative to solve some of the abovementioned drawbacks of refractive and small aperture corneal inlays. As the name indicates, DCIs work under the physical principle of diffraction, and are based on the so-called “photon sieve” concept, which was first proposed by Kipp et al. [Kipp01] for focusing X-rays. In a photon sieve, the alternate transparent and opaque rings of an amplitude Fresnel zone plate (a binary diffractive lens) are replaced by an arrangement of non-overlapping micro-holes distributed in the corresponding transparent Fresnel zones. Several unique and interesting properties of photon sieves were exploited in different areas [Andersen05, Menon05, Giménez06]. Recently, our group proposed the first DCI as a combination of the photon sieve

and the small aperture corneal inlay concepts. A DCI is in practice an opaque ring with thousands of micro-holes in its surface that in addition to allow the flow of nutrients, are strategically allocated to produce a focal point meant to see at near distances, thus converting the cornea into a bifocal optical system [Montagud-Martínez19b]. Moreover, it has been proposed that by optimizing the size and spatial distribution of the micro-holes, different designs would be able to vary the addition and the intensity ratio of different focal spots can be controlled through adjusting the proportion of the area of the DCI central hole and the surrounding structure [Montagud-Martínez19c]. The performance of our bifocal diffractive inlay has been verified by numerical simulation and optical bench experiments [Furlan17, Montagud-Martínez19b, Montagud-Martínez19c, Montagud-Martínez20]. In spite of their improved light transmission efficiency with respect to the small aperture corneal inlays, previous models of DCIs have still a low light throughput due to the high proportion of opaque area.

On the other side, contrary to (premium) trifocal intraocular lenses, which are nowadays a very well established alternative to bifocal and monofocal lenses in cataract surgery, CIs have not yet passed yet the bifocal era. Indeed, patients implanted with CIs frequently still need spectacles for near or intermediate clear vision.

In this paper we propose the first trifocal corneal inlay for the treatment of presbyopia, which additionally is a pure phase diffractive device that, opposite to previous amplitude diffractive proposals, is fully transparent to improve light efficiency. We assessed the image quality and optical properties of this device, named Phase Diffractive Corneal Inlay (PDCI), in comparison with those of a commercially available refractive CI. To this end, Zemax OpticStudio design software (version 18.7, LLC, Kirkland, WA, USA) was employed to simulate the effects of both inlays in the Liou-Brennan model eye [Liou97]. In the analysis, we used the modulation transfer function (MTF), the area under the MTF (AMTF), as merit functions; and a visual optical simulator has been employed to obtain the images provided by both inlays of objects at different vergences.

Methods

Lens design and characteristics

The PDCI is the evolution of previous deigns of DCIs proposed by our group [Montagud-Martínez19b, Montagud-Martínez19c, Montagud-Martínez20] in which we have combined two physical principles: the extended depth of focus provided by a mask with a small aperture (pin-hole), and the photon sieve. Therefore, previous DCIs designs are essentially opaque disks with a central hole and thousands of micro-holes distributed into annular zones that coincide with those of a Fresnel zone plate. By properly positioning and sizing of these micro-holes, only the zeroth and first positive and negative diffraction orders foci are present, and the high orders of the underlying conventional Fresnel zone plate

are almost suppressed. It is very well known that the low diffraction efficiency of amplitude Fresnel zone plates can be improved up to a factor of 4, by replacing the opaque areas of the plate by a transparent phase-type material having the appropriate thickness to introduce a π phase shift between alternate zones [Kirz74]. This is the main idea behind the new design of DCI here presented. Complementary to this, several parameters can regulate the focusing performance of a PDCI. A typical example is shown in Fig. 1. First, as our aim is to obtain a trifocal device, we need to partially restore the 0th diffraction order to use it as the focus for the intermediate distances. This can be achieved simply by modifying the diameter of the central hole *H*. The micro-holes in the periphery (odd rings of the zone plate) produce two main additional foci, the negative and positive and 1st diffraction orders, which are intended to far and near distance vision, respectively. In general terms, the number *N* of micro-holes on each ring and the diameter (*d)*, of the holes in the i^{th} ring determine the total PDCI patterned area and therefore the PDCI diffraction efficiency. The diameters of the holes in a conventional photon sieve are usually expressed as a function of the ring width *w*, as *d=Kw*, where *K* is a constant. So, there is a compromise between *N* and *d* in order to avoid overlapping between holes, preserving in this way the PDCI in a single structure.

The refractive index of the material chosen for the construction of the PDCI, n_I regulates the exact thickness of the inlay *h* for the design wavelength λ_0:

$$h = \frac{\lambda_0}{2\cdot\left(n_I - n_c\right)} \quad (2)$$

The PDCI under test shown in Fig. 1 was designed to provide a near diffractive focus corresponding to a nominal addition (near focus) of +3 D, to compare its performance with the commercial RCI Flexivue Microlens (Presbia, Irvine, CA, USA). Hence, in our simulations the material selected for the PDCI was an hydrogel with a refractive index of index $n_I = 1.458$. We assumed the refractive index of the corneal stroma is $n_C = 1.376$ corresponding to one employed in the Liou-Brennan eye model ($\lambda_0 = 555$ nm), Using Eq. (1) the thickness of the inlay results: *h*=3.5 microns.

In our case the diffractive structure was a disk of 4.2 mm diameter with a central hole of 0.7 mm diameter, surrounded by 5 rings conformed by a total of 253 holes of different size d obtained with *K*=1.62, being the smallest ones of 75 □m. The optical characterization of the PDCI was initially performed using Zemax OpticStudio design software (v. 18.7, LLC, Kirkland, WA, USA) in comparison with the abovementioned Flexivue Microlens. This RCI is a transparent, hydrogel-based, concave–convex disc made out of hydroxyethyl methacrylate and methyl methacrylate with a 3.2 mm diameter and ~15–20 μm thickness [Fricke18] The central 1.6 mm diameter is plano, and the annular peripheral zone in our

simulations had an add power of +3.0 D. At the center of the disc, a 0.51 mm hole facilitates the transfer of nutrients into the cornea through the lens. [Malandrini15]

Table 1 shows the parameters of Liou-Brennan's theoretical model eye, which reflects average biometrical data from a large group of individuals; incorporating a grin based model crystalline lens and the corresponding inlay in each case. The insertion of the CIs, in the model eye, was introduced as a "Grid Sag Surface", both at the same depth, 0.3 mm, from the anterior surface of the cornea.

The AMTFs of the two CIs were calculated for frequencies between 0 and 50 cycles/degree. These spatial frequencies that correspond to decimal visual acuities up to 1.6, were employed to calculate the average of sagittal and tangential MTFs at different vergences: from +0.50 D to -3.50 D in 0.10 D steps, and with two different pupil diameters: 3.0 and 4.5 mm, emulating photopic and mesopic conditions. In the simulations, we employed two different settings for the illumination: monochromatic light, matching the design wavelength (555 nm) and polychromatic light using the *photopic bright* setting of Zemax which uses five weighted wavelengths. The optimum target for the far distance focus was obtained independently for each device taking the best AMTF value as a quality criterion. In the calculations the ideal eye’s pre-surgical refractive state for the PDCI resulted +1.75D while for the RI was emmetropia. This is equivalent to assuming that the inlay surgery was performed simultaneously with LASIK or PRK in patients who are not already at an optimal preoperative refraction, which is a common and safe clinical procedure with commercial corneal inlays [Moshirfar18].

Surface	Radius (mm)	Asphericity	Thickness (mm)	Refractive index
Anterior Cornea	7.77	-0.18	0.200	1.376
Anterior CI	7.77	-0.18	0.005	1.376
Posterior CI	7.77	-0.18	0.295	1.376
Posterior Cornea	6.40	-0.60	3.16	1.336
Iris	-	-	0.100	1.337
Anterior Lens	12.4	-0.94	1.59	1.368 + 0.049057 z − 0.015427 z2 − 0.001978 r2
Posterior Lens	Infinity	-	2.43	1.407 − 0.006605 z2 − 0.001978 r2
Retina	-8.10	0.96	16.26	1.336

Table 1: Liou-brennan model eye zemax data sheet (r and z are radial and axial coordinates in the crystalline lens)

Adaptive Optics Visual Simulator

The experimental measurements in this work were taken using the VAO adaptive optics visual simulator (Voptica S.L., Murcia, Spain). This clinical instrument allows to place optical stimuli different vergences through a micro display and to show to the patient its image through any optical phase profile [Manzanera07, Hervella20]. The stimulus was an optotype with three high-contrast letters (tumbling Es) of different sizes corresponding to visual acuities of 0.4; 0.2 and 0.0 logMAR units. In our case, we have incorporated the phase of both inlays into the system following the indications of the manufacturer as CSV files with 846x846 values covering a pupil of 4.5 mm diameter. In this study, through-focus images provided by the corneal inlays in the VAO system were recorded in the range 0.0D - 3.0 D in 0.25 D steps using a 8 bits CCD camera (Edmund-Optics with model EO-10012C Lite Edition) with a resolution of 3840 x 2748 pixels and CCD dimensions of 6.41 x 4.59 (mm). The focusing lens was an achromatic doublet with 30 mm focal (AC254-030-A-ML, Thorlabs Inc. Newton, NJ, USA). Therefore, by recording images the visual stimuli through the VAO system, with a CCD camera replacing the eye, our aim was to found an agreement with the numerical simulations of the through the focus performance of both inlays. This was done despite that the real size of the projected phase CIs could not be measured experimentally because according to the manufacturer a real image of them is projected into the pupil plane of the observer's eye, but the exact location of this plane is not specified. Consequently, although the instrument works with a single pupil diameter of 4,5 mm its projection over the artificial eye could have a magnification slightly different than 1.

Results

The PDCI here presented is a diffractive lens constructed by micro-holes drilled in a single sheet of a pure phase biocompatible material, which as shown in Fig. 1, is intended to be implanted in the cornea of a presbyopic eye. The optical quality of the PDCI was evaluated comparatively with a commercially available Refractive Corneal Inlay (RCI); fist, numerically by using Zemax software, and later, experimentally with an adaptive optics visual simulator with an artificial eye.

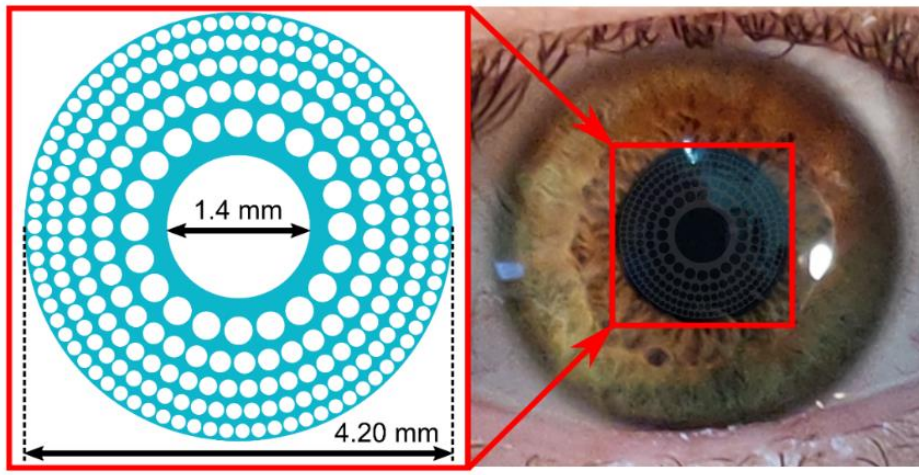

Figure 1: PDCI design. The blue areas in the left figure represent a biocompatible (transparent), hydrogel-based, material of refractive index of 1.458 (see Methods section for details). The image on the right is a simulation of the appearance of the PDCI (in stark contrast) on a real eye.

Numerical results

Figure 2a shows the trough-the-focus AMTFs, computed under polychromatic light, for both CIs in the Liu-Brennan model eye with 3.0 mm and 4.5 mm pupil diameters. The best far-distance focus was obtained for each device independently.

Continuous lines are the results obtained with the inlays centered on the visual axis. As can be seen, the PDCI presents a clear trifocal profile, with an intermediate focus at 1.75 D and a near focus at 3.0 D, which are maintained with both pupil diameters. On the contrary, as can be seen in the same figure the behavior of the RCI is very much pupil dependent. In fact, for a 3.0 mm pupil diameter, the RCI is clearly monofocal (near vision), but for 4.5 mm pupil it turns into a bifocal device with a higher value of the AMTF at the far focus.

To consider the influence of the CIs centration in the expected outcomes of the surgery, we have computed the AMTFs for the same pupil diameters but with the inlays decentered 1.0 mm towards the temporal direction in the model eye. Dotted

lines in Fig. 2a show the results. As can be seen, the larger diameter of the PDCI, which is feasible because its high porosity that does not interfere with the passage of nutrients, is beneficial in making this device less sensitive to decentering than the RCI. Indeed, for a 3.0 mm diameter pupil, a decentering of 1.0 mm is already sufficient for some of the light to pass outside the RCI, which results in a very noticeable change between the centered and decentered AMTFs (see the blue lines in Figs. 2a).

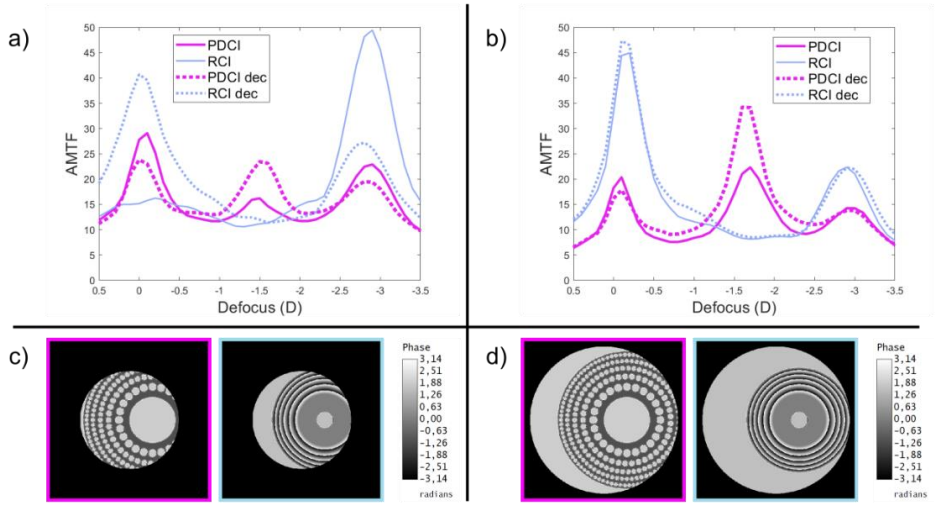

Figure 2: AMTFs of PDCI (magenta) and RCI (blue) for 3.0 mm (a), and 4.5 mm pupil (b). Dotted lines correspond to the AMTFs with the optical inlays decentered 1.0 mm with respect to the pupil center as shown in the phase maps shown with the corresponding color frames in (c) for 3.0 mm and (d) for 4.5 mm pupil diameters.

As, it has been recently shown that visual acuity (VA) defocus curves can be approximately predicted using a semiempirical non-linear function of the monochromatic (green light) AMTF [Vega18], we have employed the mathematical expression reported in that work i.e.:

$$\mathrm{VA} = 5.06 \exp\left(\frac{\mathrm{AMTFg}}{3.03}\right) \quad (1)$$

to obtain the VA in logMAR units. In this expression the AMTFg is the monochromatic AMTF obtained for the wavelength reported in Ref. [Vega18] (530 nm). The result for the 4.5 mm pupil diameter is shown in Fig. 3. Our aim was to compare this numerical result with the experimental results obtained with the adaptive optics visual simulator as will be shown in the next subsection.

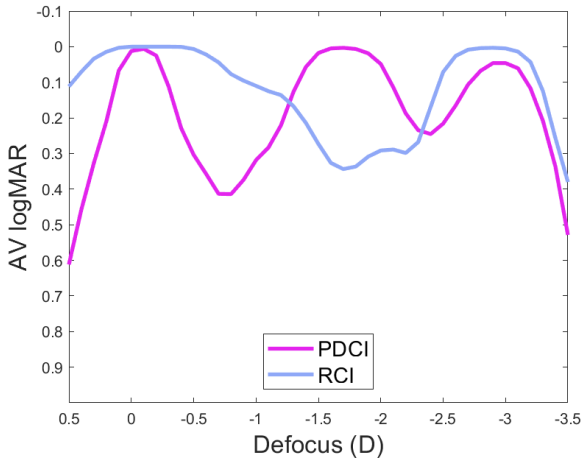

Figure 3: Through-focus VA curves for the PDCI (magenta), and RCI (blue) obtained from the AMTFs using Eq. (1). The pupil size is 4.5 mm and the abscissa axis has the origin (0.0 D defocus) at the distance focus of each lens.

Experimental results

An adaptive optics-based visual simulator (VAO system, VOptica, Murcia, Spain) was employed to get experimental images provided by the PDCI in comparison with those obtained with the RCI. This system allows simulating vision with any phase device virtually implanted in the tested eye with a pupil diameter of 4.5 mm and has been measured with different ophthalmic elements. The test object for the experiment was a tumbling E optotype with three different letter sizes corresponding to logMAR visual acuities of 0.4, 0.2 and 0.0. The recorded images of the optotytpe by a CCD camera (acting as an artificial eye) at different vergences are shown in Fig. 4. These images were taken using the green channel of the VAO system in order to correlate the results with the numerical simulations shown in Fig. 3. As can be seen, the VA images are in agreement with the theoretical predictions. In particular, for the PDCI images note the asymmetry in the depth of focus of the near and far foci. In fact, the curve in the Fig. 3 predicts a better image for -2.5 D than for -0.5D (despite both are 0.5 D apart from the near and far focus respectively). Interestingly, just the opposite happens for the RCI, i.e.; the image at -0.5D is better than the image at -2.5 D, which is in accordance with the blue curve in Fig. 3. Moreover, the absence of intermediate focus for the RCI and the lower contrast of the images, at far and near distances, obtained with the PDCI shown in Fig. 4 were also predicted in Fig 3.

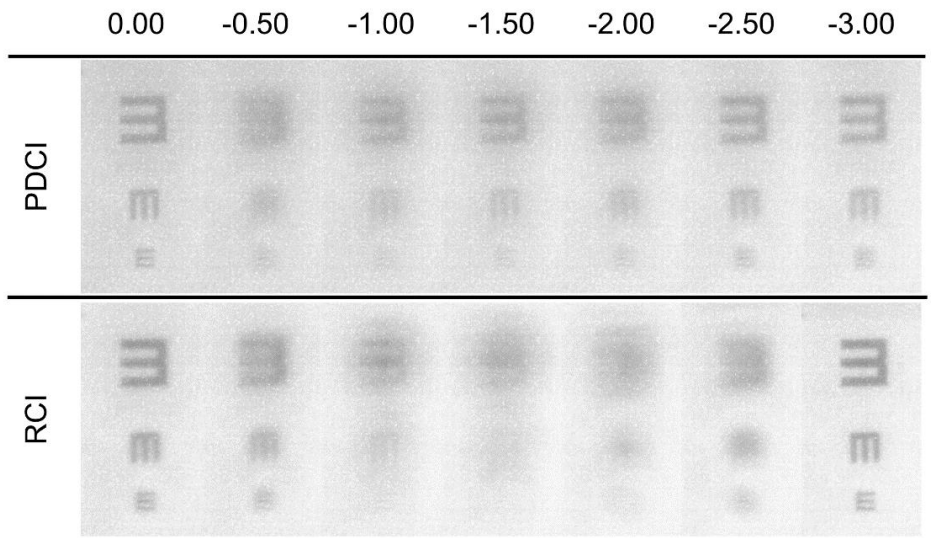

Figure 4: Images of a tumbling E optotype corresponding to 0.4 ,0,2 and 0 logMAR VA obtained the VAO system simulating the PDCI and RCI with the object at different vergences from 0.0 D to -3.0 D.

Discussion and Conclusions

In this work, we have presented the design and optical properties of the first fully-transparent trifocal corneal inlay. This new device (PDCI) represents a considerable potential advantages over previous models of diffractive inlays [Montagud-Martínez19b, Montagud-Martínez19c, Montagud-Martínez20], which on the one hand, are simply bifocals, and, on the other hand, have a lower luminous efficiency because they are partially opaque. We have demonstrated theoretically and experimentally that the PDCI presents good visual performance at intermediate distances while, at far and near distances the results are comparable to those obtained with a commercial RCI (Flexivue) under the same pupillary conditions. Prior to this, several studies have shown that such an inlay is clinically effective for the treatment of presbyopia [Limnopoulou13, Malandrini15, Beer17]. However, it was found that the gain in near visual acuity in the operated eye is always accompanied by a loss of distance visual acuity, thus monovision is mandatory with this inlay model to preserve good binocular distance visual acuity with some independence on pupil size. In this sense, another result of this work was the assessment of the influence of different pupil diameters on the vision of objects at different distances for the virtually operated eye with both inlays [Fig.2]. It is important to mention here that clinical studies of Flexivue, reported VA outcomes but do not mention the pupillary conditions under which they were measured. Another essential point to be considered in the outcomes of CI surgery is the centering of the implant [Beer17, Han19]. However, for RCIs there are no quantitative results to justify this hypothesis. Currently only two studies [Beer20, Beer17] describe only qualitatively what could happen with

a Flexivue decentering. In this work the offset of the inlays was numerically evaluated and it is proven that it is critical for RCI in small pupils (See Fig. 2a.). Thus, the results here presented provide additional information about the RCIs not reported previously, and highlight the importance of both, pupil size and centering. Importantly, we have predicted that our proposal is more robust than the RCI in both aspects.

As a common feature with other corneal surgeries, our proposal could be practiced concurrently or independently with LASIK or PRK in myopic or hyperopic eyes [Steinert17]. However, just as the optimum candidates for small aperture corneal inlays, are slightly myopic eyes [Tabernero12], in our case this optimum condition would be obtained for slightly hyperopic eyes to take advantage of the virtual focus for its use as a far distance focus. Related to this previous refractive condition, as the kappa angle depends on the axial length, with hyperopic eyes tending to have a larger angle kappa than myopic eyes [Tabernero12], the robustness against decentering can be considered another important property of the PDCI. Complimentary to this, and advantage in our case is that there is a certain degree of freedom to design the implant so that the value of the near (and intermediate) addition could be varied. Moreover, for a given value of the addition, the spatial distribution and diameters of micro-holes in each zone can also be modified to obtain an optimized relative intensity between the near and far foci. Even more, further improvements in customized PDCIs models could are feasible considering that the micro-holes density along the radial and azimuthal coordinates can be varied to achieve sphero-cylindrical PDCI for astigmatism and/or high order ocular aberrations.

Finally, it is important to note that the photon sieve concept applied to CI designs opens other interesting options to be explored in the future —some of which are already under way. These include the use of other multifocal diffractive structures (fractal [Monsoriu04], Fibonacci [Monsoriu13], Thue-Morse [Ferrando15], etc.); and, remarkably, taking into account that the flux of metabolic species is affected by any inlay (especially those made of non-porous materials) the effect of the inlay on the long-term health of the cornea is of primary importance. In this sense, our design is fully compatible with the recent advances reported in 3D bioprinting of corneal stroma equivalents with highly transparent, biocompatible, and stable materials. [Bektas20].

In conclusion, in this study, we have demonstrated the feasibility of the first trifocal corneal inlay for the presbyopia treatment. Our proposal was numerically and experimentally, evaluated in comparison with a commercially available refractive corneal inlay. Trifocality, and robustness against decentration are benefits not previously reported simultaneously by any other CI. Thus, the implantation of PDCI seems to be an interesting alternative to be explored for phakic presbyopic patients who desire spectacle independence, and would be fully compatible with

(previous or in combination) laser refractive procedure in myopic and hyperopic patients; and also, with cataract surgery afterwards.

Funding

Ministerio de Economía y Competitividad, Spain, (DPI2015–71256–R). Generalitat Valenciana (PROMETEO/2019/048), Spain.

Acknowledgments

D. Montagud-Martínez and V. Ferrando acknowledge the financial support from the Universitat Politècnica de València, Spain (fellowships FPI-2016 and PAID-10-18, respectively).

Disclosures

The authors declare no conflicts of interest.

Competing interests

The authors declare no competing interests.

References

[Andersen05] Andersen G. Large optical photon sieve. Opt Lett, OL. 2005;30(22):2976–8.

[Beer17] Beer SMC, Santos R, Nakano EM, Hirai F, Nitschke EJ, Francesconi C, et al. One-Year Clinical Outcomes of a Corneal Inlay for Presbyopia. Cornea. 2017;36(7):816–20

[Beer20] Beer SMC, Werner L, Nakano EM, Santos RT, Hirai F, Nitschke EJ, et al. A 3-year follow-up study of a new corneal inlay: clinical results and outcomes. Br J Ophthalmol. 2020;104(5):723–8.

[Bektas20] Bektas CK, Hasirci V. Cell loaded 3D bioprinted GelMA hydrogels for corneal stroma engineering. Biomater Sci. 2019;8(1):438–49.

[Castro18] Castro JJ, Ortiz C, Jiménez JR, Ortiz-Peregrina S, Casares-López M. Stereopsis Simulating Small-Aperture Corneal Inlay and Monovision Conditions. J Refract Surg. 2018;34(7):482–8.

[Charman14] Charman WN. Developments in the correction of presbyopia II: surgical approaches. Ophthalmic Physiol Opt. 2014;34(4):397–426.

[Ferrando15] Ferrando V, Giménez F, Furlan WD, Monsoriu JA. Bifractal focusing and imaging properties of Thue Morse Zone Plates. Opt Express, OE. 2015;23(15):19846–53.

[Fricke18] Fricke TR, Tahhan N, Resnikoff S, Papas E, Burnett A, Ho SM, et al. Global Prevalence of Presbyopia and Vision Impairment from Uncorrected Presbyopia: Systematic Review, Meta-analysis, and Modelling. Ophthalmology. 2018;125(10):1492–9.

[Furlan17] Furlan WD, García-Delpech S, Udaondo P, Remón L, Ferrando V, Monsoriu JA. Diffractive corneal inlay for presbyopia. J Biophotonics. 2017;10(9):1110–4.

[Garza13] Garza EB, Gomez S, Chayet A, Dishler J. One-year safety and efficacy results of a hydrogel inlay to improve near vision in patients with emmetropic presbyopia. J Refract Surg. 2013;29(3):166–72.

[Gilchrist87] Gilchrist J, Pardhan S. Binocular Contrast Detection with Unequal Monocular Illuminance*. Ophthalmic and Physiological Optics. 1987;7(4):373–7.

[Giménez06] Giménez F, Monsoriu JA, Furlan WD, Pons A. Fractal photon sieve. Opt Express, OE. 2006;14(25):11958–63.

[Han19] Han G, Lim DH, Yang CM, Park GH, Park D-Y, Moon HS, et al. Refractive corneal inlay for presbyopia in emmetropic patients in Asia: 6-month clinical outcomes. BMC Ophthalmology. 2019;19(1):66.

[Hervella20] Hervella L, Villegas EA, Robles C, Artal P. Spherical Aberration Customization to Extend the Depth of Focus With a Clinical Adaptive Optics Visual Simulator. J Refract Surg. 2020;36(4):223–9.

[Kipp01] Kipp L, Skibowski M, Johnson RL, Berndt R, Adelung R, Harm S, et al. Sharper images by focusing soft X-rays with photon sieves. Nature. 2001;414(6860):184–8.

[Kirz74] Kirz J. Phase zone plates for x rays and the extreme uv. J Opt Soc Am, JOSA. 1974;64(3):301–9.

[Limnopoulou13] Limnopoulou AN, Bouzoukis DI, Kymionis GD, Panagopoulou SI, Plainis S, Pallikaris AI, et al. Visual outcomes and safety of a refractive corneal inlay for presbyopia using femtosecond laser. J Refract Surg. 2013;29(1):12–8.

[Liou97] Liou H-L, Brennan NA. Anatomically accurate, finite model eye for optical modeling. J Opt Soc Am A, JOSAA. 1997;14(8):1684–95.

[Malandrini15] Malandrini A, Martone G, Menabuoni L, Catanese AM, Tosi GM, Balestrazzi A, et al. Bifocal refractive corneal inlay implantation to improve near

vision in emmetropic presbyopic patients. J Cataract Refract Surg. 2015;41(9):1962–72.

[Manzanera07] Manzanera S, Prieto PM, Ayala DB, Lindacher JM, Artal P. Liquid crystal Adaptive Optics Visual Simulator: Application to testing and design of ophthalmic optical elements. Opt Express, OE. 2007;15(24):16177–88.

[Menon05] Menon R, Gil D, Barbastathis G, Smith HI. Photon-sieve lithography. J Opt Soc Am A, JOSAA. 2005;22(2):342–5.

[Moarefi17] Moarefi MA, Bafna S, Wiley W. A Review of Presbyopia Treatment with Corneal Inlays. Ophthalmol Ther. 2017;6(1):55–65.

[Monsoriu04] Monsoriu JA, Saavedra G, Furlan WD. Fractal zone plates with variable lacunarity. Opt Express, OE. 2004;12(18):4227–34.

[Monsoriu13] Monsoriu Serra JA, Calatayud Calatayud A, Remón Martín L, Furlan WD, Saavedra G, Andrés Bou P. Bifocal Fibonacci Diffractive Lenses. In: IEEE Photonics Journal 2013;5:3400106-3400106.

[Montagud-Martínez19b] Montagud-Martínez D, Ferrando V, Machado F, Monsoriu JA, Furlan WD. Imaging Performance of a Diffractive Corneal Inlay for Presbyopia in a Model Eye. IEEE Access. 2019;7:163933–8

[Montagud-Martínez19c] Montagud-Martínez D, Ferrando V, Monsoriu JA, Furlan WD, Optical Evaluation of New Designs of Multifocal Diffractive Corneal Inlays, J Ophthalmol, 2019; vol. 2019 1-6

[Montagud-Martínez20] Montagud-Martínez D, Ferrando V, Monsoriu JA, Furlan WD. Proposal of a new diffractive corneal inlay to improve near vision in a presbyopic eye. Appl Opt, AO. 2020;59(13):D54–8.

[Moshirfar18] Moshirfar M, Bean AE, Albarracin JC, Rebenitsch RL, Wallace RT, Birdsong OC. Retrospective Comparison of Visual Outcomes After KAMRA Corneal Inlay Implantation With Simultaneous PRK or LASIK. J Refract Surg. 2018;34(5):310–5.

[Pinsky14] Pinsky PM. Three-dimensional modeling of metabolic species transport in the cornea with a hydrogel intrastromal inlay. Invest Ophthalmol Vis Sci. 2014;55(5):3093–106.

[Plainis13] Plainis S, Petratou D, Giannakopoulou T, Radhakrishnan H, Pallikaris IG, Charman WN. Small-aperture monovision and the Pulfrich experience: absence of neural adaptation effects. PLoS ONE. 2013;8(10):e75987.

[Steinert17] Steinert RF, Koch DD, Cochener B, Lang A, Barragán-Garza E, Chayet A, et al. Corneal remodeling after implantation of a shape-changing inlay

concurrent with myopic or hyperopic laser in situ keratomileusis. J Cataract Refract Surg. 2017;43(11):1443–9.

[Tabernero12] Tabernero J, Artal P. Optical modeling of a corneal inlay in real eyes to increase depth of focus: optimum centration and residual defocus. J Cataract Refract Surg. 2012;38(2):270–7.

[Vega18] Vega F, Millán MS, Garzón N, Altemir I, Poyales F, Larrosa JM. Visual acuity of pseudophakic patients predicted from in-vitro measurements of intraocular lenses with different design. Biomed Opt Express. 2018 ;9(10):4893–906.

[Vilupuru15] Vilupuru S, Lin L, Pepose JS. Comparison of Contrast Sensitivity and Through Focus in Small-Aperture Inlay, Accommodating Intraocular Lens, or Multifocal Intraocular Lens Subjects. Am J Ophthalmol. 2015;160(1):150-162.e1.

[Vukich18] Vukich JA, Durrie DS, Pepose JS, Thompson V, van de Pol C, Lin L. Evaluation of the small-aperture intracorneal inlay: Three-year results from the cohort of the U.S. Food and Drug Administration clinical trial. J Cataract Refract Surg. 2018;44(5):541–56.

[Waring11] Waring GO. Correction of presbyopia with a small aperture corneal inlay. J Refract Surg. 2011;27(11):842–5.

Capítulo 3
Discusión general

En este capítulo de la Tesis se resumen los resultados obtenidos en las publicaciones anteriormente presentadas.

Como se ha comprobado a lo largo de los capítulos previos, esta Tesis Doctoral profundiza en el estudio de los implantes intracorneales difractivos multifocales para la corrección de la presbicia y tiene como objetivo principal mejorar el diseño original previamente publicado [Furlan17], generando nuevos diseños optimizados de implantes intracorneales difractivos multifocales [Furlan20, Montagud-Martínez19a, Montagud-Martínez19b, Montagud-Martínez19c, Montagud-Martínez20].

Para optimizar y calcular las propiedades ópticas del diseño original, en primer lugar, se utilizó un programa de trazado de rayos, el cual permite introducir cualquier superficie óptica (en nuestro caso el DCI) y evaluar sus propiedades.

Las características físicas del DCI se pueden medir en el programa de trazado de rayos utilizando una superficie única, en el interior de una cubeta, o en un modelo de ojo teórico, entre otras opciones. Debido a que los modelos de ojo teórico se aproximan más a la realidad clínica, todos los estudios mostrados en la Tesis se han valido de dichos modelos para medir las propiedades ópticas de los diferentes CIs que se han presentado.

Por esta razón, primero se debe seleccionar un modelo de ojo teórico acorde a las características clínicas. Cabe recordar que la cirugía de estos implantes tiene como objetivos présbitas jóvenes con edades comprendidas entre 45 y 50 años.

En la **primera publicación** se evaluó una IOL en tres modelos de ojo teórico [Atchison06, Escudero-Sanz99, Liou97], todos ellos ampliamente utilizados en la bibliografía. Cada modelo de ojo teórico presenta unas características similares, siendo los modelos de Atchison y Navarrro los más parecidos, mientras que el modelo de Liou-Brennan es más complejo pues tiene en cuenta otros parámetros tales como son el ángulo kappa o el descentramiento pupilar. Los tres modelos mostraron resultados similares, si bien es cierto el modelo de Liou-Brennan, a pesar de obtener resultados peores, tanto para la MTF como la AMTF, la pérdida de calidad óptica de la FIOL con respecto a la monofocal fue inferior a la de los otros modelos de ojo teórico. Además, la influencia de la aberración esférica fue crucial y afectó de la misma manera, pero en cuantía diferente a cada modelo de ojo teórico debido a que cada modelo presenta una aberración esférica global diferente.

El propio software de trazado de rayos presenta un modelo de ojo teórico propio, por tanto, además de estudiar los modelos de ojo teóricos más comunes, se evaluó el modelo del software en la **segunda publicación**. En este trabajo, ya se emplearon los CIs, tanto el KAMRA inlay comercial como dos diseños propios de DCIs. Ambos diseños se diferenciaban en el tamaño del agujero central (DCI #1: 1.0 mm y DCI#2: 1.6 mm respectivamente). El modelo de ojo teórico de

Zemax es un modelo simple y simétrico. En este estudio se evaluaron las propiedades ópticas (MTF, AMTF y PSF) de los tres CIs y se comprobó cómo ambos diseños de DCIs presentaban una ligera disminución de la MTF de lejos con respecto al CI comercial, mientras que en la MTF de cerca se generaba un foco. Por consiguiente, teniendo en cuenta que los CIs se implantan en el ojo no dominante para que el ojo dominante pueda ver de lejos, esto supone una mejora de ambos DCIs con respecto al CI comercial. Debido al propio diseño de ambos DCIs, el DCI #1, de menor agujero central y con más micro-agujeros que favorecen la difracción, debía mostrar una peor MTF en lejos y una mejor MTF en cerca con respecto al DCI #2. Este hecho se comprobó al realizar la simulación numérica. Por consiguiente, los dos diseños de DCIs mejoraron las prestaciones visuales en cerca en comparación con el CI comercial.

En la **tercera publicación**, se compararon los mismos diseños de DCIs (DCI #1 o DCI 1.0, DCI #2 o DCI 1.6) con el mismo CI comercial pero esta vez se evaluó el modelo de ojo teórico del software y el de Liou-Brennam, el cual se aproxima más a los pacientes reales, y se añadieron métricas nuevas (además de la MTF, se midió las AMTFs en un rango de frecuencias espaciales diferentes, las PSFs se recalcularon utilizando un script propio y se convolucionaron con un optotipo de C's de Landolt para obtener las imágenes simuladas finales). Para una pupila de 3.0 mm los resultados obtenidos en ambos modelos de ojos fueron prácticamente iguales. Las discrepancias menores se observaron en la pupila de 4.5 mm debido al efecto de la aberración esférica, la cual es diferente para cada modelo de ojo teórico. Sin embargo, este efecto provoca un desplazamiento de los focos en la AMTF de un modelo con respecto a otro. Además, se observó la simulación de las imágenes mostrando cómo cada modelo de ojo resolvería un optotipo de C's de Landolt. Mientras que ambos DCIs permitieron resolver las C's, el CI comercial no fue capaz de resolver nada en visión próxima.

Por las razones expuestas anteriormente, y debido a que el modelo de Liou-Brennan no sólo es uno de los modelos más extendidos entre la comunidad científica, sino que sus parámetros están seleccionados a partir de datos biométricos de pacientes de una edad entorno a los 45 años, los siguientes trabajos y publicaciones se realizaron utilizando dicho modelo de ojo teórico.

Una vez se optimizaron los parámetros del DCI (eligiendo el DCI #1 frente al DCI #2) y se compararon sus propiedades ópticas y clínicas con el CI comercial. En la **cuarta publicación** se evaluó además de diferentes propiedades ópticas, una característica clínica fundamental en los implantes corneales, la sensibilidad al descentramiento. Dicha propiedad es sumamente importante, debido a que cuanto más sensible sea el CI al descentramiento, mayor centrado necesitará para obtener un buen rendimiento visual. En dicho trabajo se comparó el diseño del DCI #1 con el CI comercial y se midieron sus propiedades ópticas centrando y descentrando ambos implantes 0.8 mm en dirección temporal. Se obtuvo que

mientras que el CI comercial perdía su extensión de foco en pupila de 3.0 mm, el DCI mostró una robustez al descentramiento mucho mayor.

Tras optimizar el diseño del DCI, con unas propiedades ópticas y clínicas mejores al CI comercial, se modificaron los parámetros para mejorar el foco en visión de cerca. Para ello, se partió del diseño del DCI óptimo (con radio interno de 1.0 mm) y se transformaron los anillos internos opacos, en anillos transparentes con un desfase de π respecto a los micro-agujeros del DCI. Se comparó el nuevo diseño híbrido (HDCI) con el DCI #1 en el ojo de Liou-Brennan y se midieron las propiedades ópticas. Como se puede observar en la **quinta publicación** se consiguió el objetivo de mejorar el foco de cerca, pero la pérdida en lejos fue mayor que la mejora en cerca. Sin embargo, como ya se ha dicho anteriormente, a pesar de esa pérdida, debido a que los CIs se insertan en el ojo no dominante dejando el ojo dominante para visión lejana, esta desventaja no tiene por qué ser significativa. Además, el nuevo diseño (HDCI) presenta menos zonas opacas y por tanto deja pasar más luz a la retina.

Por último, se transformó el diseño original del DCI (zonas opacas y micro-agujeros) por un diseño de fase completo (zonas transparentes con un desfase de π con respeto a los micro-agujeros). Dicho DCI (PDCI) también fue optimizado, y a diferencia del DCI mostrado en las **publicaciones 2, 3 y 4**, se obtuvo un agujero central de 1.4 mm y un diámetro total de 4,15 mm. El nuevo diseño presentó tres focos, el orden 0 y a ambos lados los órdenes difractivos -1 y +1. Por tanto, se comparó el PDCI, trifocal añadiendo una base, con un CI comercial refractivo de características similares. También se midió la sensibilidad al descentramiento de ambos, descentrando 1.0 mm en la dirección temporal. En el **sexto artículo** se puede comprobar como PDCI presentó tres focos similares en magnitud de AMTF para visión de lejos, intermedia y cerca tanto en pupila de 3.0 mm como 4.5 mm mientras que el CI comercial mostró un perfil monofocal en cerca para pupila pequeña y un perfil bifocal para pupila grande. En cuanto a la sensibilidad al descentramiento, ambos CIs se vieron afectados, si bien hay que resaltar que mientras que el PDCI mantuvo su trifocalidad, el CI comercial para pupila de 3.0 mm pasó a mostrar un perfil bifocal. Además de los resultados numéricos obtenidos con el programa de trazado de rayos, se utilizó un simulador visual de óptica adaptativa y se compararon ambos implantes en dicho dispositivo con un ojo artificial présbita. Los resultados obtenidos con el simulador visual y con la simulación numérica tuvieron una alta correlación y se confirmó el perfil trifocal de PDCI para pupila de 4.5 mm. Por tanto, en este artículo el PDCI se presentó como el primer CI trifocal, capaz de cubrir las distancias intermedias, y obtuvo buena robustez al descentramiento.

Capítulo 4
Conclusiones

En este capítulo se analizan los objetivos de la investigación planteados en el Capítulo 1 y las principales conclusiones de cada publicación. También se exponen cuáles son las aportaciones más relevantes de la Tesis y se proponen futuras líneas de investigación.

4.1. Cumplimiento de los objetivos

El primer objetivo, "*Selección, comparación y evaluación de un dispositivo óptico en diferentes modelos de ojo teórico"* se completó en las **tres primeras publicaciones** seleccionando el modelo de ojo teórico de Liou-Brennan como el más adecuado y comparándolo con los modelos de Navarro, Atchison y el del propio software.

El segundo objetivo, "*Optimizar los parámetros del DCI original de amplitud y medir las propiedades ópticas del implante dentro de modelos de ojo teórico"* fue resuelto en las **publicaciones 2 y 3**, haciendo hincapié en que DCI presenta una gran cantidad de parámetros a modificar, como el tamaño del agujero central, la distribución de micro-agujeros alrededor de cada zona o la separación entre ellos. En las publicaciones presentadas en la Tesis, sólo se optimizan dos parámetros: el tamaño del agujero central y la opacidad o transparencia del DCI (si este es de amplitud, híbrido o fase). Sin embargo, se realizaron estudios previos para determinar el número de micro-agujeros por zona o la distancia entre ellos.

La **publicación 4** se centró en el objetivo de "*Comparar las propiedades ópticas y características clínicas entre el diseño optimizado del DCI y un CI comercial"*. No solo se compararon dichas características, sino que además el nuevo diseño de DCI obtuvo un rendimiento mejor en visión cercana y una menor sensibilidad al descentramiento que el CI comercial.

El cuarto objetivo "*Modificar los parámetros de diseño del DCI para mejorar las propiedades ópticas en visión cercana*", se llevó a cabo en la **5ª publicación**. Se diseñó un nuevo DCI híbrido, con una parte interna transparente de fase y una externa de amplitud. También se mejoró el rendimiento visual en visión próxima

Por último, el objetivo de "*Obtener un nuevo diseño con perfil trifocal y compararlo con un CI comercial de características similares"* se cumplió con el último apartado del capítulo 2. No solo se mostraron las propiedades trifocales del nuevo diseño PDCI, sino que también se comprobó su mayor rendimiento visual frente a las actuales alternativas comerciales.

4.2. Aportaciones realizadas

Tras comprobar el cumplimiento de todos los objetivos propuestos al comenzar la Tesis, se van a resumir las aportaciones realizadas.

En primer lugar, a partir del diseño original del DCI, el cual sólo se midió en banco óptico, se ha optimizado y logrado obtener dos nuevos diseños, DCI #1 y DCI #2, que mejoran numéricamente las prestaciones del CI comercial más utilizado.

En segundo lugar, se diseñó un nuevo modelo de DCI (HDCI), híbrido en fase y amplitud, el cual mejoró el rendimiento visual en visión cercana con respecto al DCI #1.

En tercer lugar, se logró un diseño puramente de fase (PDCI), obteniendo además un perfil trifocal y un mayor paso de luz hacia el ojo, pues no presenta zonas opacas. Dicho diseño no sólo se evaluó numéricamente, sino que se midió experimentalmente en un simulador visual de óptica adaptativa.

Aparte de mostrar cuatro diseños de DCI, cada uno de ellos con propiedades únicas respecto a los otros, y compararlos siempre con implantes comerciales de referencia, esta Tesis demuestra la gran utilidad de las simulaciones numéricas para el diseño de nuevos elementos ópticos y su alta correlación con medidas experimentales en banco óptico y simuladores visuales de óptica adaptativa.

4.3 Futuras líneas de investigación

El siguiente paso, una vez diseñado, optimizado y evaluado los implantes intracorneales con mejores prestaciones consistiría en fabricar dichos implantes en lentes de contacto y evaluar su rendimiento visual clínicamente con pacientes reales cuyo perfil sea similar a los pacientes que se operan quirúrgicamente con los CIs comerciales. Además de utilizar lentes de contacto, que sería una aproximación no invasiva a llevar el implante, se podría utilizar el simulador visual de óptica adaptativa. Sin embargo, como el simulador visual trabaja únicamente en fase, solamente el PDCI podría ser estudiado por este método.

Si los resultados clínicos concordaran con los resultados numéricos y experimentales, presentados en esta Tesis, el último paso sería introducir quirúrgicamente los diseños más óptimos y realizar un ensayo clínico comparando los diferentes implantes corneales.

Capítulo 5
Bibliografía General

[Alarcon16] Alarcon A, Canovas C, Rosen R, Weeber H, Tsai L, Hileman K, et al. Preclinical metrics to predict through-focus visual acuity for pseudophakic patients. Biomed Opt Express, BOE. 2016;7(5):1877–88.

[Andersen05] Andersen G. Large optical photon sieve. Opt Lett, OL. 2005;30(22):2976–8.

[Arlt15] Arlt E, Krall E, Moussa S, Grabner G, Dexl A. Implantable inlay devices for presbyopia: the evidence to date. Clin Ophthalmol. 2015;9:129–37.

[Artal17] Artal P. Handbook of Visual Optics, Two-Volume Set. Boca Ratón: CRC Press Taylor & Francis Group; 2017. 856 p.

[Atchison06] Atchison DA. Optical models for human myopic eyes. Vision Research. 2006;46(14):2236–50.

[Atchison16] Atchison DA, Blazaki S, Suheimat M, Plainis S, Charman WN. Do small-aperture presbyopic corrections influence the visual field? Ophthalmic Physiol Opt. 2016;36(1):51–9.

[Atchison17] Atchison DA, Schematic eyes, 1st ed. Taylor & Francis, Boca Raton, 2017.

[Bakaraju08] Bakaraju RC, Ehrmann K, Papas E, Ho A. Finite schematic eye models and their accuracy to in-vivo data. Vision Res. 2008;48(16):1681–94.

[Beer17] Beer SMC, Santos R, Nakano EM, Hirai F, Nitschke EJ, Francesconi C, et al. One-Year Clinical Outcomes of a Corneal Inlay for Presbyopia. Cornea. 2017;36(7):816–20.

[Beer20] Beer SMC, Werner L, Nakano EM, Santos RT, Hirai F, Nitschke EJ, et al. A 3-year follow-up study of a new corneal inlay: clinical results and outcomes. Br J Ophthalmol. 2020;104(5):723–8.

[Bektas20] Bektas CK, Hasirci V. Cell loaded 3D bioprinted GelMA hydrogels for corneal stroma engineering. Biomater Sci. 2019;8(1):438–49.

[Calatayud13] Calatayud A, Remón L, Martos J, Furlan WD, Monsoriu JA. Imaging quality of multifocal intraocular lenses: automated assessment setup. Ophthalmic and Physiological Optics. 2013;33(4):420–6.

[Castro16] Castro JJ, Soler M, Ortiz C, Jiménez JR, Anera RG. Binocular summation and visual function with induced anisocoria and monovision. Biomed Opt Express. 2016;7(10):4250–62.

[Castro18] Castro JJ, Ortiz C, Jiménez JR, Ortiz-Peregrina S, Casares-López M. Stereopsis Simulating Small-Aperture Corneal Inlay and Monovision Conditions. J Refract Surg. 2018;34(7):482–8.

[Charman14] Charman WN. Developments in the correction of presbyopia II: surgical approaches. Ophthalmic Physiol Opt. 2014;34(4):397–426.

[Charman19] Charman WN, Liu Y, Atchison DA. Small-aperture optics for the presbyope: do comparable designs of corneal inlays and intraocular lenses provide similar transmittances to the retina? J Opt Soc Am A Opt Image Sci Vis. 2019;36(4):B7–14.

[Escudero-Sanz99] Escudero-Sanz I, Navarro R. Off-axis aberrations of a wide-angle schematic eye model. J Opt Soc Am A, JOSAA. 1999;16(8):1881–91.

[Ferrando15] Ferrando V, Giménez F, Furlan WD, Monsoriu JA. Bifractal focusing and imaging properties of Thue Morse Zone Plates. Opt Express, OE. 2015;23(15):19846–53.

[Fricke18] Fricke TR, Tahhan N, Resnikoff S, Papas E, Burnett A, Ho SM, et al. Global Prevalence of Presbyopia and Vision Impairment from Uncorrected Presbyopia: Systematic Review, Meta-analysis, and Modelling. Ophthalmology. 2018;125(10):1492–9.

[Furlan16] Furlan WD, Remón L, Llorens C, Rodriguez-Vallejo M, Monsoriu JA. Comparison of two different devices to assess intraocular lenses. Optik. 2016;127(20):10108–14.

[Furlan17] Furlan WD, García-Delpech S, Udaondo P, Remón L, Ferrando V, Monsoriu JA. Diffractive corneal inlay for presbyopia. J Biophotonics. 2017;10(9):1110–4.

[Furlan20] Furlan WD, Montagud-Martínez D, Ferrando V, Monsoriu JA. A new trifocal corneal inlay for presbyopia. Enviado.

[Garcia-Delpech18] Garcia-Delpech S, Udaondo P, Furlan WD, Monsoriu JA, Montagud-Martínez D. Lentes de contacto multifocales y de foco extendido. Ribeiro F, Presbiopia, 1ed, Lisboa: Sociedade Portuguesa de Oftalmologia; 2018. 260 p.

[Garza13] Garza EB, Gomez S, Chayet A, Dishler J. One-year safety and efficacy results of a hydrogel inlay to improve near vision in patients with emmetropic presbyopia. J Refract Surg. 2013;29(3):166–72.

[Gilchrist87] Gilchrist J, Pardhan S. Binocular Contrast Detection with Unequal Monocular Illuminance*. Ophthalmic and Physiological Optics. 1987;7(4):373–7.

[Giménez06] Giménez F, Monsoriu JA, Furlan WD, Pons A. Fractal photon sieve. Opt Express, OE. 2006;14(25):11958–63.

[Gross08] Gross H, Blechinger F, Achtner B, Handbook of Optical Systems. Vol. 4, Survey of Optical Instruments, 2015, 1092 p.

[Han19] Han G, Lim DH, Yang CM, Park GH, Park D-Y, Moon HS, et al. Refractive corneal inlay for presbyopia in emmetropic patients in Asia: 6-month clinical outcomes. BMC Ophthalmology. 2019;19(1):66.

[Hayasi09] Hayashi K, Manabe S, Hayashi H. Visual acuity from far to near and contrast sensitivity in eyes with a diffractive multifocal intraocular lens with a low addition power. Journal of Cataract & Refractive Surgery. 2009;35(12):2070–6.

[Hervella20] Hervella L, Villegas EA, Robles C, Artal P. Spherical Aberration Customization to Extend the Depth of Focus With a Clinical Adaptive Optics Visual Simulator. J Refract Surg. 2020;36(4):223–9.

[Internet19a] KAMRA Inlay Restores Reading Vision [Internet]. [cited 2019 Aug 14]. Available from: https://kamra.com/

[Internet 19b] Zemax OpticStudio Knowledgebase—Zemax [Internet]. [cited 2019 Aug 14]. Available from: https://customers.zemax.com/os/resources/learn/knowledgebase/zemax-models-of-the-human-eye.

[ISO14] ISO 11979-2:2014. Ophthalmic implants — Intraocular lenses — Part 2: Optical properties and test methods.

[Kipp01] Kipp L, Skibowski M, Johnson RL, Berndt R, Adelung R, Harm S, et al. Sharper images by focusing soft X-rays with photon sieves. Nature. 2001;414(6860):184–8.

[Kirz74] Kirz J. Phase zone plates for x rays and the extreme uv. J Opt Soc Am, JOSA. 1974;64(3):301–9.

[Limnopoulou13] Limnopoulou AN, Bouzoukis DI, Kymionis GD, Panagopoulou SI, Plainis S, Pallikaris AI, et al. Visual outcomes and safety of a refractive corneal inlay for presbyopia using femtosecond laser. J Refract Surg. 2013;29(1):12–8.

[Lindstrom13] Lindstrom RL, Macrae SM, Pepose JS, Hoopes PC. Corneal inlays for presbyopia correction. Curr Opin Ophthalmol. 2013;24(4):281–7.

[Liou97] Liou H-L, Brennan NA. Anatomically accurate, finite model eye for optical modeling. J Opt Soc Am A, JOSAA. 1997;14(8):1684–95.

[Liu19] Liu J, Dong Y, Wang Y. Efficacy and safety of extended depth of focus intraocular lenses in cataract surgery: a systematic review and meta-analysis. BMC Ophthalmol. 2019;19(1):198.

[Machado17] Machado FJ, Monsoriu JA, Furlan WD. Fractal light vortices. In: Chapter from the Book Vortex Dynamics and Optical Vortices. 1st ed. Intech; 2017. 257 p.

[Malandrini15] Malandrini A, Martone G, Menabuoni L, Catanese AM, Tosi GM, Balestrazzi A, et al. Bifocal refractive corneal inlay implantation to improve near vision in emmetropic presbyopic patients. J Cataract Refract Surg. 2015;41(9):1962–72.

[Manzanera07] Manzanera S, Prieto PM, Ayala DB, Lindacher JM, Artal P. Liquid crystal Adaptive Optics Visual Simulator: Application to testing and design of ophthalmic optical elements. Opt Express, OE. 2007;15(24):16177–88.

[Menon05] Menon R, Gil D, Barbastathis G, Smith HI. Photon-sieve lithography. J Opt Soc Am A, JOSAA. 2005;22(2):342–5.

[Moarefi17] Moarefi MA, Bafna S, Wiley W. A Review of Presbyopia Treatment with Corneal Inlays. Ophthalmol Ther. 2017;6(1):55–65.

[Monsoriu04] Monsoriu JA, Saavedra G, Furlan WD. Fractal zone plates with variable lacunarity. Opt Express, OE. 2004;12(18):4227–34.

[Monsoriu13] Monsoriu Serra JA, Calatayud Calatayud A, Remón Martín L, Furlan WD, Saavedra G, Andrés Bou P. Bifocal Fibonacci Diffractive Lenses. In: IEEE Photonics Journal 2013;5:3400106-3400106.

[Montagud-Martínez19a] Montagud-Martínez D, Ferrando V, Garcia-Delpech S, Monsoriu JA, Furlan WD. Diffractive Corneal Inlays: A New Concept for Correction of Presbyopia. Chapter from the Book Visual Impairment and Blindness - What We Know and What We Have to Know. Intech Open

[Montagud-Martínez19b] Montagud-Martínez D, Ferrando V, Machado F, Monsoriu JA, Furlan WD. Imaging Performance of a Diffractive Corneal Inlay for Presbyopia in a Model Eye. IEEE Access. 2019;7:163933–8.

[Montagud-Martínez19c] Montagud-Martínez D, Ferrando V, Monsoriu JA, Furlan WD, Optical Evaluation of New Designs of Multifocal Diffractive Corneal Inlays, J Ophthalmol, 2019; vol. 2019 1-6.

[Montagud-Martínez19d] Montagud-Martínez D, Ferrando V, Monsoriu JA, Furlan WD, Influencia del modelo de ojo teórico en la evaluación numérica de lentes intraoculares fractales (aceptado) Suplemento de la Revista Mexicana de Física.

[Montagud-Martínez19e] Montagud-Martínez D, Ferrando V, Monsoriu JA, Furlan WD, Influencia del modelo de ojo teórico en la evaluación numérica de lentes intraoculares fractales. “Encuentro Iberoamericano de Óptica” Cancún (2019).

[Montagud-Martínez20] Montagud-Martínez D, Ferrando V, Monsoriu JA, Furlan WD. Proposal of a new diffractive corneal inlay to improve near vision in a presbyopic eye. Appl Opt, AO. 2020;59(13):D54–8.

[Moshirfar18] Moshirfar M, Bean AE, Albarracin JC, Rebenitsch RL, Wallace RT, Birdsong OC. Retrospective Comparison of Visual Outcomes After KAMRA Corneal Inlay Implantation With Simultaneous PRK or LASIK. J Refract Surg. 2018;34(5):310–5.

[Pinsky14] Pinsky PM. Three-dimensional modeling of metabolic species transport in the cornea with a hydrogel intrastromal inlay. Invest Ophthalmol Vis Sci. 2014;55(5):3093–106.

[Plainis13] Plainis S, Petratou D, Giannakopoulou T, Radhakrishnan H, Pallikaris IG, Charman WN. Small-aperture monovision and the Pulfrich experience: absence of neural adaptation effects. PLoS ONE. 2013;8(10):e75987.

[Remón18] Remón L, García-Delpech S, Udaondo P, Ferrando V, Monsoriu JA, Furlan WD. Fractal-structured multifocal intraocular lens. PLoS ONE. 2018;13(7):e0200197.

[Saavedra03] Saavedra G, Furlan WD, Monsoriu JA. Fractal zone plates. Opt Lett, OL. 2003;28(12):971–3.

[Schwarz14] Schwarz C, Manzanera S, Prieto PM, Fernández EJ, Artal P. Comparison of binocular through-focus visual acuity with monovision and a small aperture inlay. Biomed Opt Express. 2014;5(10):3355–66.

[Schwiegerling13] Schwiegerling JT. Eye Axes and Their Relevance to Alignment of Corneal Refractive Procedures. J Refract Surg. 2013;29(8):515–6.

[Seyeddain13] Seyeddain O, Bachernegg A, Riha W, Rückl T, Reitsamer H, Grabner G, et al. Femtosecond laser-assisted small-aperture corneal inlay implantation for corneal compensation of presbyopia: two-year follow-up. J Cataract Refract Surg. 2013;39(2):234–41.

[Steinert17] Steinert RF, Koch DD, Cochener B, Lang A, Barragán-Garza E, Chayet A, et al. Corneal remodeling after implantation of a shape-changing inlay concurrent with myopic or hyperopic laser in situ keratomileusis. J Cataract Refract Surg. 2017;43(11):1443–9.

[Tabernero11] Tabernero J, Schwarz C, Fernández EJ, Artal P. Binocular Visual Simulation of a Corneal Inlay to Increase Depth of Focus. Invest Ophthalmol Vis Sci. 2011;52(8):5273–7.

[Tabernero12] Tabernero J, Artal P. Optical modeling of a corneal inlay in real eyes to increase depth of focus: optimum centration and residual defocus. J Cataract Refract Surg. 2012;38(2):270–7.

[Trindade15] Trindade C, Small aperture (pinhole) intraocular implant to increase depth of focus. U.S; 14/297, 447. 2015

[Vega18] Vega F, Millán MS, Garzón N, Altemir I, Poyales F, Larrosa JM. Visual acuity of pseudophakic patients predicted from in-vitro measurements of intraocular lenses with different design. Biomed Opt Express. 2018 ;9(10):4893–906.

[Vilupuru15] Vilupuru S, Lin L, Pepose JS. Comparison of Contrast Sensitivity and Through Focus in Small-Aperture Inlay, Accommodating Intraocular Lens, or Multifocal Intraocular Lens Subjects. Am J Ophthalmol. 2015;160(1):150-162.e1.

[Vukich18] Vukich JA, Durrie DS, Pepose JS, Thompson V, van de Pol C, Lin L. Evaluation of the small-aperture intracorneal inlay: Three-year results from the cohort of the U.S. Food and Drug Administration clinical trial. J Cataract Refract Surg. 2018;44(5):541–56.

[Wang18] Wang MX,Swartz TS, Rock N, Surgical Correction of Presbyopia: The Fifth Wave, Thorofare, NJ: SLACK Incorporated; 2018. 164 p.

[Waring11] Waring GO. Correction of presbyopia with a small aperture corneal inlay. J Refract Surg. 2011;27(11):842–5.

[Yilmaz08] Yilmaz OF, Bayraktar S, Agca A, Yilmaz B, McDonald MB, van de Pol C. Intracorneal inlay for the surgical correction of presbyopia. J Cataract Refract Surg. 2008;34(11):1921–7.

[Yilmaz11] Yılmaz OF, Alagöz N, Pekel G, Azman E, Aksoy EF, Cakır H, et al. Intracorneal inlay to correct presbyopia: Long-term results. J Cataract Refract Surg. 2011;37(7):1275–81.